Institute of
GEOLOGICAL
& NUCLEAR
SCIENCES
Limited

Whakatane Microzoning Study
Volume 2 - Appendices

Confidential

By R Beetham, G Dellow, J Cousins, V Mouslopoulou, J Hoverd, M Gerstenberger, B Stephenson, P Davenport & P Barker

Client Report
2004/18
February 2004

Institute of
GEOLOGICAL
& NUCLEAR
SCIENCES
Limited

Whakatane Microzoning Study
Volume 2 — Appendices

by R. Beetham, G. Dellow, J. Cousins, V. Mouslopoulou, J. Hoverd,
M. Gerstenberger, B. Stephenson, P. Davenport & P. Barker

Prepared for

Environment Bay of Plenty

CONFIDENTIAL

Institute of Geological & Nuclear Sciences client report 2004/18
Project Number: 430W1029

**The data presented in this Report are
available to GNS for other use from**
March 2004

Gracefield Research Centre, 69 Gracefield Road, PO Box 30368, Lower Hutt, New Zealand, Telephone: +64-4-5701444, Facsimile: +64-4-5704600
A Crown Research Institute

This volume contains the appendices that accompany the Main Report (Volume 1 of Client Report CR 2004-18 Whakatane Microzoning Study)

APPENDICES

Appendix 1:	NIWA Report
Appendix 2:	Nakamura Data
Appendix 3:	SCPT Data
Appendix 4:	MM Intensity descriptions

CONTENTS

APPENDIX 1

NIWA Report

Location of Active Faults in the Urban Whakatane Coastal Zone, Using Marine Geophysical Data

NIWA Client Report: WLG2003-82
October 2003

NIWA Project: GNS04301

Location of Active Faults in the Urban Whakatane Coastal Zone, Using Marine Geophysical Data

Authors
Geoffroy Lamarche

Prepared for

Institute of Geological and Nuclear Sciences

NIWA Client Report: WLG2003-82
October 2003

NIWA Project: GNS04301

National Institute of Water & Atmospheric Research Ltd
301 Evans Bay Parade, Greta Point, Wellington
Private Bag 14901, Kilbirnie, Wellington, New Zealand
Phone +64-4-386 0300, Fax +64-4-386 0574
www.niwa.co.nz

Contents

Reviewed by:

Dr Philip Barnes

Approved for release by:

Dr Andrew Laing

Formatting checked

Executive Summary

Seismic reflection profiles acquired within 10 km of the coast, offshore of urban Whakatane, provide a cross section across three large offset faults in the upper 1500 m below the seafloor. The data indicate clear late Pleistocene – Holocene activity. The faults are the previously recognised White Island Fault to the west and the newly named Keepa and Kohi faults to the east.

High-resolution seismic reflection data were acquired using boomer, CHIRP and 3.5 kHZ seismic sources. The high-resolution seismic profiles provide a resolution of 20 to 50 cm within the first 40-80 meters beneath the seafloor. The post-last glacial erosional surface was identified on most high-resolution seismic profiles, and has an inferred age of 9.3 ± 1.8 kyrs BP in the coastal zone. Numerous offsets of this surface demonstrate intense Holocene activity in the region.

The White Island Fault extends from the coast to more than 25 km to the north. Its Holocene activity within 10 km of the coast is often masked by recent river sediment cover, but one 7.6 ± 1.5 m vertical displacement approximately 10 m beneath the seafloor yields a vertical slip rate of 0.8 ± 0.33 mm/yr.

The Keepa Fault displays the largest offset of the post-last glacial surface. At present, the Keepa Fault accommodates the most strain of the three interpreted faults in the coastal zone, with an observed 21.1± 4.2 m vertical offset yielding a 2.3 ± 0.9 mm/yr slip rate. To the north, the fault merges with the White Island Fault, and extends to the south toward the Whakatane Fault, onshore. The Keepa Fault may therefore, represent the direct extension of the Whakatane Fault or a more recent relay linking the Whakatane Fault to the south with White Island Fault to the North.

The Kohi Fault displays large vertical displacement at depth, but only minor offsets on the 9.3 kyrs reflector suggesting little Holocene activity. The Kohi Fault projects towards the mouth of the Whakatane River, and may extend onshore along this trend towards the Whakatane Fault.

On the basis of this study, we recommend additional high-resolution seismic reflection data be acquired within 5 km of the coast in order to better constrain the geometry and timing of faulting, and in particular to constrain the relationship between the White Island and Keepa faults and identify their precise location at the coast.

Introduction

This report was commissioned by the Institute of Geological and Nuclear Sciences as part of an earthquake microzoning study of urban Whakatane for Environment Bay of Plenty (EBoP). To this end, NIWA was contracted to provide a review on information available on the offshore extension of the Whakatane Fault.

This report provides an overview of marine seismic reflection profiles, of varying resolution and penetration, that were used to identified active fault traces beneath the seafloor within 10 km offshore of Whakatane city. Where possible, the report provides an estimate of the late Pleistocene to Holocene vertical displacements and vertical slip-rates.

Three SW-trending faults are imaged on seismic reflection profiles in the area immediately north of urban Whakatane, clearly displacing the **Post-last Glacial erosional Surface** (PGS). These faults are the already identified **White Island Fault,** and the newly recognised **Keepa Fault** and **Kohi Fault. All are considered active geological structures**.

Limits of the present study

The present report is limited to data available within approximately 10 km offshore, north of urban Whakatane so as to cover the likely offshore extension of the Whakatane Fault and its merging with the major regional White Island Fault to the north (fig. 1 2 & 3). The report extends approximately 10 km either side of the mouth of the Whakatane River, hence covering the offshore extension of the Waimana and Waikaremoana faults to the east, and the coastal part of the White Island Fault to the west.

Geological Background

Back-arc extension associated with the Hikurangi subduction system is recognized along a narrow northeast-trending normal fault system, which marks the eastern boundary of the Quaternary Taupo Volcanic Zone of central North Island. Extension has resulted in the formation of the 18-km-wide Whakatane Graben, which spans the Bay of Plenty coastline and extends north-eastward for about 50 km across the continental shelf. Morphologically, the graben is characterised by a subdued bathymetric trough bounded by the Motuhora scarp to the east and Rurima Ridge to the west (Fig. 1). Subsidence within the offshore Whakatane graben is estimated to average 2–2.5 mm/yr over the last 100 kyrs, while extension is at least 3.5 mm/yr,

accounting for half of the 7 mm/yr extension across the 40-km-wide TVZ [Wright, 1990, 1992].

Seismic reflection data show that the Whakatane Graben is characterised by a 15–20 km wide zone of active normal faulting with seafloor and sub-seafloor expressions of some 50 faults indicating repeated movement over at least the last 50 kyr [Lamarche 2000; Wright, 1990]. The graben is filled by approximately 3 km of sediments lying over an irregular basement of Mesozoic greywacke with volcanic intrusions (Davey et al. 1997). Structurally the graben is limited to the east by the west-dipping White Island Fault and to the west by a diffuse zone of intense faulting on the crest of Rurima Ridge. The White Island Fault has a conspicuous seabed expression along the Motuhora scarp, which reaches 80 m in height, and along the White Island canyon. Davey et al. (1995), on the basis of a single long multichannel seismic (MCS) profile postulate that the locus of active deformation has moved eastwards with time and that the most recent fault to be formed is the White Island Fault. Onshore, a recent example of violent fault displacement within the Whakatane Graben occurred during the 1987 Edgecumbe earthquake, Magnitude 6.3 [Beanland et al. 1989], which resulted in major infrastructure damage costing over 300 million dollars.

East of the Motuhora scarp, a series of N0°E to N25°E faults trend obliquely to the White Island Fault, which they intersect to the north. Southwards, these faults connect with the North Island Dextral Fault Belt (NIDFB, Beanland, 1995; Wright, 1992; Fig. 1). The NIDFB is an active transcurrent fault system that traverses the North Island of New Zealand from Wellington to the Bay of Plenty. The Whakatane Fault is part of the NIDBF. The strike-slip rate at the Bay of Plenty coast is poorly constrained and estimated to be about 1 mm/yr (Beanland, 1995).

Data Sources

Four marine geophysical surveys were undertaken in the Bay of Plenty by NIWA as part of its Public Good Science Funded research programme since 1988 (Fig. 2). The geophysical data acquired essentially consist of seismic reflection profiles with penetrations and resolutions varying depending on the equipment used (see Table 1). All surveys, except Kah0102, included 3.5 kHz seismic profiling, which provided an excellent indicator of seafloor and immediate sub-seafloor (<40 m) fault rupture. Signal penetration and resolution heavily depended on sea conditions, water depth and sea-floor substrate. For instance, gas-rich or hard bottom seafloor within the coastal zone usually resulted in drastically reduced penetration and resolution.

Table 1: Seismic reflection data acquired in the coastal zone of urban Whakatane. MCS: Multi-channel Seismic Reflection; SCS: Single Channel Seismic Reflection. Approximate maximum penetration and resolution were calculated using sediment velocity of 1600 m/s for SCS, 3.5 kHz, boomer and CHIRP data, and 1800 m/s for MCS data (Taylor, et al., in press).

Voyage name	Year	Equipment used	Approx. max. Resolution	Approx. max. Penetration
Cr2017	1988	3.5 kHz	40 cm	30 m
		SCS	1 m	300 m
Cr2043	1990	3.5 kHz	40 cm	30 m
		SCS	1 m	300 m
Tan9914	1999	3.5 kHz	40 cm	40 m
		MCS	5-20 m	1800 m
Kah0102	2001	Boomer	50 cm	120 m
		CHIRP	20 cm	40 m

We used the data acquired during four geophysical surveys in order to identify active faulting in the coastal zone of urban Whakatane (Table 1, and Fig. 1).

- Surveys Cr2017 (1988) and CR2043 (1990, example in Fig. 7) included SCS and 3.5 kHz seismic reflection data [Wright, 1990, 1992]. The 3.5 kHz profiles are of good quality and provide valuable information on the recent fault activity. However, the poor navigation system often resulted in approximate location of the fault. In the coastal zone, penetration of the SCS data was limited by shallow water depth and gas-rich sub-seafloor, so that no information were provided below ca. 300 m beneath the seafloor.

- TAN9914 survey is undoubtedly the largest and most comprehensive one in the central and eastern Bay of Plenty region. The 25-day survey was undertaken in November 1999 by NIWA aboard RV *Tangaroa*. The data acquired included 2200 km of MCS and high-resolution (3.5 kHz) seismic reflection data, along with refraction profiles for accurate sediment velocity analysis, magnetic and gravity measurements, sidescan sonographs, and core samples. Across the Whakatane Graben, the seismic profile spacing is less than 1 km normal to the graben axis, and the southernmost shore-parallel profile is approximately 2 km from the coast at Whakatane. The resolution and penetration of the 3.5 kHz are approximately 40 cm and 40 m, respectively. The resolution of the MCS varies greatly with depth, and is estimated at 3–5 m in the near surface (<~200 m). The penetration of MCS ranges from 1 to 2 km. Both resolution and penetration weaken in the coastal zone because of shallow water and presence of unconsolidated gas-rich mud in the upper surface.

- Survey KAH0102 was undertaken in January 2001 onboard RV *Kaharoa* to acquire high and very-high resolution seismic reflection data using a boomer source from NIWA, and a CHIRP source from the Southampton Oceanographic Centre (Bull et al. 2001). The optimal resolution of the boomer and CHIRP are approximately 20 and 50 cm respectively with a maximum penetration of 50 and 120 m, respectively.

Late Pleistocene-Holocene sediments and erosional surface

Wright (1990) documents in detail the seismic sequence imaged in 3.5 kHz profiles in the Bay of Plenty, and provides evidence for interpreting the near-surface (5–60 m) stratigraphic sequence as representing sediments deposited since the last glacial transgression. The post glacial transgressive marine ravinement surface is clearly recognised regionally across the whole survey area, and has been correlated over the whole Whakatane Graben and east of the White Island Fault with confidence. It therefore provides a marker that can be utilised to quantify vertical slip rates across the faults. To best estimate the age of the **Post-last Glacial erosional Surface (PGS)** in the coastal zone offshore of urban Whakatane, we considered its diachroneity, the history of sea level rise (Carter et al. 1986), and the possible post-glacial tectonic subsidence rate.

PGS formed during the last sea-level rise as the zone of marine abrasion rolled up from its lowest position (-120 m) at 18 kyr BP to its present position ca. 6.5 kyr ago. Considering the present water depth of 10 to 50 m, and the sea-level curve of Carter et al. (1986), we interpret that PGS close to the present shoreline developed about 7.5 to 11.1 kyr ago. Subsidence in this area, east of White Island Fault is not well constrained, but is less than 1 mm/yr, and its influence on the inferred age of PGS is minimal. We therefore assigned an age of 9.3±1.8 kyr to PGS reflector. We use this age to derive vertical slip rates from PGS reflector offsets (Table 2).

Active Faults in Urban Whakatane Coastal Zone

MCS profiles T23 (Fig. 4) and T8 (Fig. 5, location on Fig. 3) reveal three, well identified, large offset faults and numerous small structures in the near coastal zone of urban Whakatane. The three large faults were correlated on all SCS and MCS reflection profiles with confidence, and are named, from west to east, the White Island, Keepa and Kohi faults. Because uncertainties in onshore-offshore fault correlations, we do not use the name "Whakatane Fault" offshore. Possible correlations are discussed later in this report. The large faults correlate on high resolution seismic profiles (CHIRP, Boomer and 3.5 kHz) with multiple reflector offsets, as best exemplified on lines K15 and K16 (Fig. 6). This is coherent with upward splaying of faults in the near surface. In some cases, however, there were no

satisfactory correlations across seismic lines. This is particularly noticeable on CHIRP and Boomer profiles K16 (Fig. 6) and K15.

White Island Fault

The westernmost fault in the study area is the White Island Fault, a major feature that extends at least 40 to 50 km northwards. This fault is well expressed on all MCS profiles. The fault surface expression corresponds to the Motuhora Scarp north of 37°52'S (latitude of Motuhora Island), which demonstrates its recent activity. South of 37°52'S, the surface expression of White Island Fault diminishes, and Motuhora scarp disappears beneath a thick recent sediment cover originating from the Whakatane and Rangitaiki rivers. However, the fault remains well expressed beneath this sedimentary layer in the Pleistocene-Holocene sequence on MCS lines T23 and T8 (Fig. 5). On line T23 (Fig. 4), located 4 km from the coast, a vertical displacement greater than 50 ms twt (i.e. ca 40 m) is measurable across the White Island Fault on a high amplitude horizon within the first 100 ms of penetration. This indicates that the fault has had Quaternary activity within 4 km of the coast.

Offsets of the PGS reflector on lines K16 (Fig. 6) and K17 range 6 to 7.6 m (Table 2) at ~ 25 m (30 ms) beneath seafloor. Reflector offsets are clearly visible above the PGS, up to 10 m (13 ms) beneath the seafloor. A broad flexure of the seafloor across the fault on line K15, attests of the recent activity of this fault close to the coast. The flexure has total relief of up to 6.1± 0.4 m. The PGS reflector is not identified beneath the flexure, but younger horizons (age unknown) are offset and may provide a minimum displacement value for PGS (see Table 2). Approximately 1 km to the east, an offset of 6-7.8 m is measured on PGS (Fig. 3, Table 2). Although there is no fault identified immediately to the north on line T14b that we can correlate this fault expression with, we believe it represents an active strand of White Island Fault with which it may connect around line T23 (Fig. 3).

The data clearly suggests that the White Island Fault reaches the coast of the Bay of Plenty. The main strand trends N44°E, and projects on the coastline at 176°56.5'E. The eastern strand, as identified by offset reflectors on line K15, projects into the coast at 176°57.5'E.

West of White Island Fault, numerous sub-surface faults are observed on high resolution and MCS data. In particular, south of Motuhora Island (37°51'S), two faults trending N55°E and N62°E clearly offset reflectors above the PGS reflector (Fig. 3), indicating Holocene activity.

Keepa Fault

The Keepa Fault (new name) is a N24°E-striking fault splaying off southward from White Island Fault at approximately 37°51'S. The fault is well identified on MCS profiles T8 (Fig. 5), T7 and T23 (Fig. 4), SCS profile W5 (Fig. 7) and very-high resolution profile K16 (Fig. 6), and has a minimum length of 7 km, from line T154 to line T49 (Fig. 3). The fault is best expressed at depth on line T8 (Fig. 5) as two sub-parallel splays merging at depth. There is a clear horizon offset within the first 100 ms of penetration that indicates Quaternary activity. The fault is identified on MCS line T23 (Fig. 4) by a truncated high amplitude horizon at 0.7 s twt.

Recent activity is indicated by offset of the PGS reflector (Table 2). Measured vertical offsets are indicated on Fig. 3 and Table 2. Most interestingly, Keepa Fault appears on boomer line K16 (Fig. 6), as a series of 4, and possibly 6, small displacement faults accommodating 14-21 m of vertical offset (Table 2). This pattern of upward splaying is only visible on the high-resolution seismic profiles and suggests that these superficial faults merge at depth to a single fault strand. Hence, the displacement at depth along the single fault strand may be equal to the cumulative offsets measured on high-resolution seismic profiles. A similar pattern is observed on the southernmost profile (K15), where 6 fault traces are observed immediately beneath PGS. The pre-PGS cumulative offset over the 6 fault traces is 16 ± 3.6 m while cumulative offset of PGS is 3.4–4.7 m. Less than one kilometre to the west along K15, a single fault offset of 9.6–12.4 m of PGS indicates an important active fault. There is no observed reflector offset on the 3.5 kHz lines to the north (T14b) and south (T49) with which to correlate this fault expression, nor is there any MCS data available at that latitude, that would help demonstrate that this fault strand merges at depth with either Keepa Fault or White Island Fault. However, because of the proximity of Keepa Fault we favour an interpretation of this superficial fault offset as representing an active strand of Keepa Fault.

The main continuous strand of Keepa Fault, as interpreted from line T14b northward, projects onto the coastline at 176°58.5'E, while the fault zone defined on line K15, only 2 km from the coast, projects onto the coastline between 176°58'E and 176°59.1'E.

Kohi Fault

The Kohi Fault (new name) is revealed by the conspicuous eastern truncation of east dipping reflectors on line T23 (Fig. 4). There is up to 1 s twt (~800–1000 m) vertical offset of the high amplitude reflector imaged on MCS profile T23 at ca. 1 s twt on the western side of the fault. The offset across Kohi Fault diminishes northwards as shown by the smaller displacement visible on MCS line T8 (Fig. 5). Although late Pleistocene activity is clearly indicated from interpretation of lines T23 and SCS line

W5 (Fig. 7), we were only able to identify offsets of the PGS reflector on lines K15, T6 and T8 (Fig. 5, Table 2). These measurements are small compared with those along Keepa fault (around 1 m on line T6 and K15). Close to shore, on line K15, there is a broad flexure at the seafloor across Kohi Fault, with relief of 1.2 m which may indicate recent activity.

The Kohi Fault correlates well across all seismic lines to form a 10–16 km-long segment from line K15, only ~1 km north of Kohi Point, to north of line T12 (outside the area of Fig. 3). The fault projects towards the mouth of the Whakatane River, and may extend onshore along this trend towards the Whakatane Fault.

Other active faults in the vicinity

Two other faults of regional importance were identified east of the Kohi Fault, namely the Waimana and Waikaremoana fault zones (Fig. 1, 3 and 8). Both fault zones clearly have a long history of activity as indicated by the large displacements visible on MCS profiles (Fig. 8). Recent activity is indicated by clear displacement of the PGS reflector. These faults extend northwards for at least 30 km where they are truncated by the northern segment of the White Island Fault (Lamarche, 1999). Southward, both faults almost certainly extend onshore into the Ohiwa Harbour (Fig. 1), and southward along the onshore faults with the same names.

Further study of both the offshore segments of the Waimana and Waikaremaoa faults would be beneficial to the overall evaluation of seismic risk in the region.

Vertical Slip Rates

We derived vertical slip rates for White Island, Keepa and Kohi faults in the region restricted between 37°51'S (latitude of Motuhora Is.) and the coast. Because the lateral component of displacement on the faults has not been determined, the rates are minimum values. We used the inferred age of 9.3 ± 1.8 kyrs for the PGS. The maximum vertical slip rates for White Island, Keepa and Kohi faults in this area are respectively 0.8 ± 0.32 mm/yr, 2.3 ± 0.91 mm/yr and 0.3 ± 0.11 mm/yr (Table 2). The large PGS offset observed on line K15 between White Island and Keepa faults yields a maximum slip rate of 1.3 ± 0.53 mm/yr. These values are derived from a limited number of measurements and should be treated with care, but clearly show that Keepa Fault is the most active structure in the coastal zone of Whakatane.

Extension of the Whakatane Fault

Both the Keepa and Kohi faults trend toward urban Whakatane within 3 km of the coast. It is likely that both faults extend onshore and one or both could represent extensions of the Whakatane Fault.

The Kohi Fault has had a long history with large total displacements extending well into the Pleistocene. Line T23 (Fig. 4) indicates that the fault separates a sedimentary half-graben to the west from a seismically incoherent body to the east, that we infer to be greywacke basement. Onshore, the topography suggests a structural control on the location of the Whakatane River mouth, and southwards along the well marked topographic scarp immediately east of Whakatane city, close to the known location of the Whakatane Fault. This suggests that the Kohi Fault extends onshore to the south and merges with the Whakatane Fault. Although Kohi Fault appears to be an important, large displacement structure, the minor offsets on the PGS reflector indicate little Holocene activity along this fault.

Table 2. Vertical separation and estimated vertical slip rate for the Post-last Glacial erosional Surface (PGS).

Line	source	Horizon	Displ (m)	SR (mm/yr)	Error (40%)	comments
White Island Fault				**0.8**	**± 0.33**	
Kah15	Boomer	PGS	1.6 ± 0.3	0.2	± 0.07	
Kah15	Boomer	s/f				flexure, no age
Kah16	Boomer	PGS	7.6 ± 1.5	0.8	± 0.33	
Kah17	CHIRP	PGS	5.9 ± 1.2	0.6	± 0.25	
Kah12	CHIRP	PGS	5.3 ± 1.3	0.6	± 0.23	
Between Keepa Fault and WIF *(from east to west)*				**1.3**	**± 0.53**	
Kah15	Boomer	PGS	9.6 ± 1.9	1.0	± 0.41	min
Kah15	Boomer	PGS	12.4 ± 2.5	1.3	± 0.53	max
Kah15	Boomer	PGS	6.0 ± 1.2	0.6	± 0.26	min
Kah15	Boomer	PGS	7.8 ± 1.5	0.8	± 0.34	max
Keepa Fault				**2.3**	**± 0.91**	
Kah15	Boomer	Pre PGS	16.4 ± 3.3			age unknown
Kah15	Boomer	PGS	3.4 ± 0.7	0.4	± 0.15	min
Kah15	Boomer	PGS	4.7 ± 0.9	0.5	± 0.20	max
Tan48	3.5 kHz	PGS	1.6 ± 0.3	0.2	± 0.07	min (very faint)
Tan48	3.5 kHz	PGS	4.7 ± 0.9	0.5	± 0.20	max (very faint)
Tan6	3.5 kHz	post PGS	1.1 ± 0.2			age unknown
Kah17	CHIRP	post PGS	4.2 ± 0.8			age unknown
Kah16	Boomer	PGS	13.9 ± 2.8	1.5	± 0.60	min
Kah16	Boomer	PGS	21.1 ± 4.2	2.3	± 0.91	max
Kah12	CHIRP	PGS	3.7 ± 0.7	0.4	± 0.16	
Tan8	3.5 kHz	PGS	1.6 ± 0.3	0.2	± 0.07	
T154	3.5 kHz	PGS	2.9 ± 0.6	0.3	± 0.12	
Tan154	3.5 kHz	PGS	8.9 ± 1.8	1.0	± 0.38	

Table 2. (*continued*)

Kohi Fault			**0.3**	**± 0.11**	
Kah15	s/f	1.2 ±0.2			flexure
Kah15	PGS	1.1 ±0.2	0.1	± 0.05	max
Tan6	PGS	1.1 ±0.2	0.1	± 0.05	
Tan8	PGS	2.5 ±0.5	0.3	± 0.11	

Displacements were calculated using a 1600 m/s velocity in the upper sedimentary layer (Taylor, 2003). Error on vertical displacement is estimated at 0.3 m, which correspond to a 0.5 mm error in the measurement on the seismic profile, unless a range is given with minimum (min) and maximum (max) measurements, when ambiguous interpretations occur due to gas, poor resolution or penetration. Slip rates were derived using an age of 9.3±1.8 kyrs ascribed to Post-last Glacial erosional Surface (**PGS**) (see text). A 40% error on the slip rate is derived from the summation of the 20% errors on both age and measured displacements. Vertical displacements for horizons immediately beneath and above PGS are indicated but no inference is made on slip rate. Measurements are listed northward for each individual fault. **WIF**. White Island Fault; **s/f** : Seafloor; **Displ;** Vertical displacement; **SR:** Vertical Slip Rate

Near sea-floor and seafloor displacements along Keepa Fault clearly indicate its recent tectonic activity. It is unclear whether the fault represents the direct offshore Whakatane Fault or not, but it is currently accommodating greater strain than the active Kohi Fault. It is possible that Keepa Fault is a direct extension of Whakatane Fault or that it represents a more recent relay linking the Whakatane Fault to the south with White Island Fault to the North. This latter hypothesis remains to be validated but may have important consequences for interpretation of fault kinematics and for assessing fault lengths. It may also have important implications for the tectonic history of the region.

Recommendations

Fault locations and measurements of fault offsets were made on a limited number of seismic profiles, but provided compelling evidence that seismic data obtained from Boomer and CHIRP sources are ideally suited to study recent tectonic activity in the coastal zone. However only three Boomer and CHIRP profiles are available in the coastal zone of urban Whakatane.

We recommend, therefore, additional high-resolution seismic reflection data be acquired within 5 km of the coast in order to better constrain the geometry of the faulting. In particular, additional data would help to map the relationship between White Island Fault and Keepa Fault, constrain their short term activity, and identify their precise connection to the coast. Such profiles should to be acquired parallel to the coast in a area spanning from White Island to Kohi faults with one or two profiles perpendicular to tie the interpretation. Such a survey is logistically feasible from a small boat, would require one or two days of operation depending on the extent of the survey, is cost effective and provides rapid result.

Should new high-resolution data be acquired, we strongly recommend that a swell filter be applied either during or after acquisition, as well as a frequency filter. Such processing is routine in high-resolution seismic data survey and greatly improves the quality of the final profiles.

NIWA has the capability to acquired and process high resolution seismic data in the coastal zone using its boomer source and the Globe Claritas® seismic processing software.

Conclusions

The available MCS and high-resolution seismic reflection data acquired in the coastal zone of urban Whakatane provide compelling evidence for Holocene fault ruptures within 5 km of the mouth of the Whakatane River. There are three large faults capable of generating potentially damaging earthquakes in this area: the White Island Fault, and the two newly named Keepa Fault and Kohi Fault. Both the Keepa and Kohi Fault may connect southward with the Whakatane Fault. The Keepa Fault presently shows more activity with larger vertical displacement of Holocene markers (<10,000 yrs), and may represent the active extension of the Whakatane Fault. The Kohi and White Island faults have larger total displacements but lesser activity since 9300 yrs BP. All faults may project onto the coast.

Scientific References

Beanland, S., Blick, G. H., Darby, D. J. (1995). Normal faulting in a back-arc basin: Geological and geodetic characteristics of the 1987 Edgecumbe, earthquake, New Zealand. Journal of Geophysical Research 95(B4): 4693–4708.

Bull, J.; Dix, J.; Lamarche, G.; Taylor, S.; Wiles, P. (2001). Cruise report – KAH0102 – Active faulting in the southern Whakatane Graben – application of high resolution reflection seismology.

Davey, F.J.; Henrys, S.; Lodolo, E. (1997). A seismic crustal section across the East Cape convergent margin, New Zealand. Tectonophysics 269(3–4): 199–215.

Davey, F.J.; Henrys, S.A.; Lodolo, E. (1995). Asymmetric rifting in a continental back-arc environment, North Island, New Zealand. Journal of Volcanology and Geothermal Research 68(1/3): 209–238.

Carter, R.M.; Carter, L.; Johnson, D. (1986). Sedimentary effects of episodic post-glacial transgression, in New Zealand and Australia, with comments on global correlation of submergent shorelines. Sedimentology 33: 629–649.

Lamarche, G.; Barnes, P.; Bull, J.; Wilcox, S.; Mitchell, J.; Garlick, R.; Hill, A.; Taylor, S.; Horgan, H. (1999). Research Voyage TAN99–14 Report. Bay of Plenty Neotectonics – Whakatane Graben Extension, 10 November to 4th December 1999.

Lamarche, G.; Bull, J.M.; Barnes, P.M.; Taylor, S.K.; Horgan, H.J. (2000). Constraining fault growth rates and fault evolution in the Bay of Plenty, New Zealand. EOS Transactions 81(42): 481–486.

Taylor, S.K.; Bull, J.M.; Lamarche, G.; Barnes, P.M. (2003). Normal Fault Growth and Linkage during the last 1.5 Million Years: An Example from the Whakatane Graben, New Zealand. Journal of Geophysical Research – Solid Earth (in press).

Wright, I.C. (1990). Late Quaternary faulting of the offshore Whakatane Graben, Taupo Volcanic Zone, New Zealand. New Zealand Journal of Geology and Geophysics 33(2): 245–256.

Wright, I.C. (1992). Shallow structure and active tectonism of an offshore continental back-arc spreading system: the Taupo Volcanic Zone, New Zealand. Marine Geology 103: 287–309.

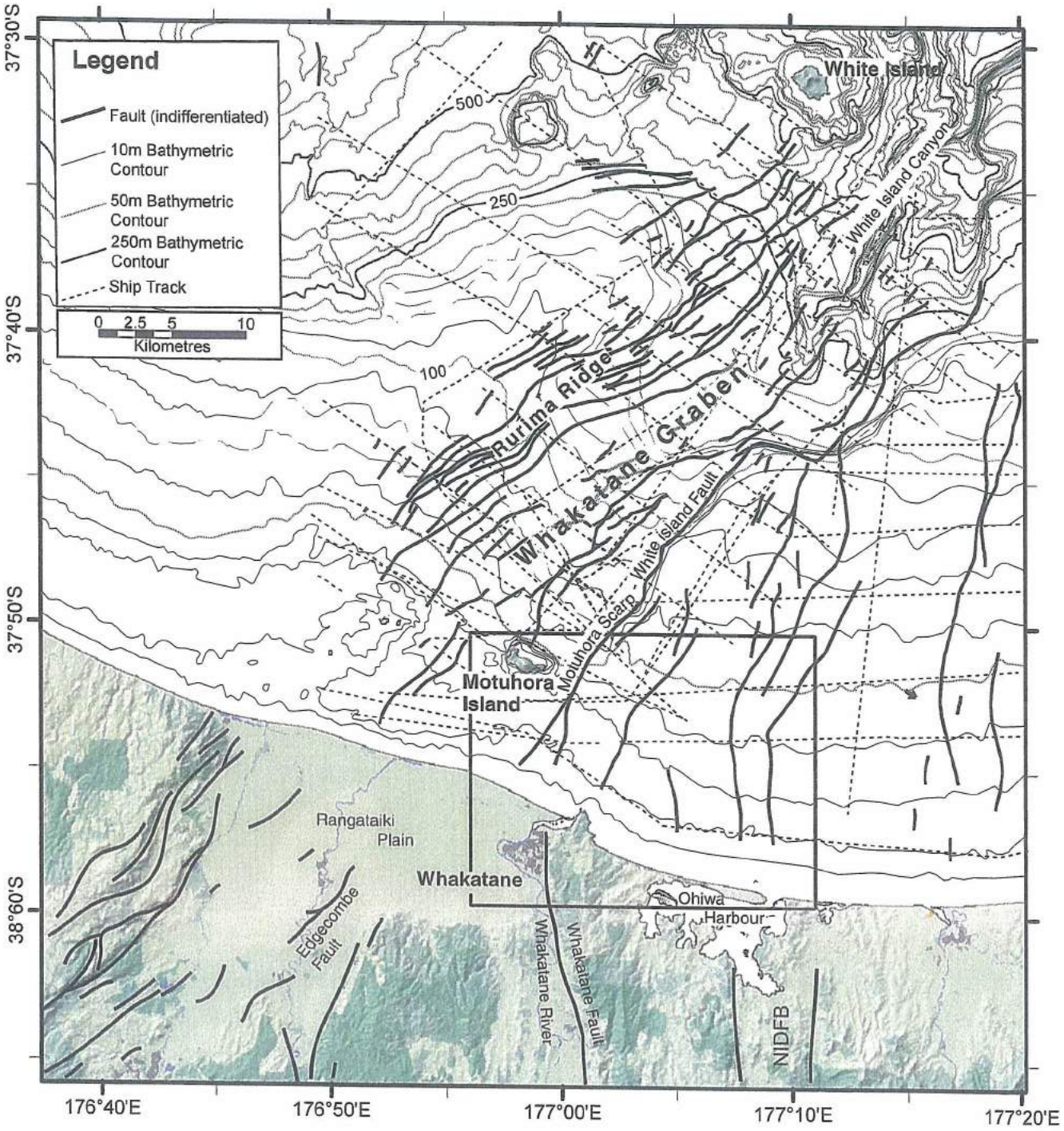

Figure 1 - Location of the survey area and simplified fault map of the Eastern Bay of Plenty (Whakatane Graben and to the east of it) from Lamarche et al., 2000. Onshore faults are provided by the Institute of Geological and Nuclear Sciences. Frame indicates position of Fig. 2 and 3. NIDFB: North Island Dextral Fault Belt. After Taylor et al., 2002.

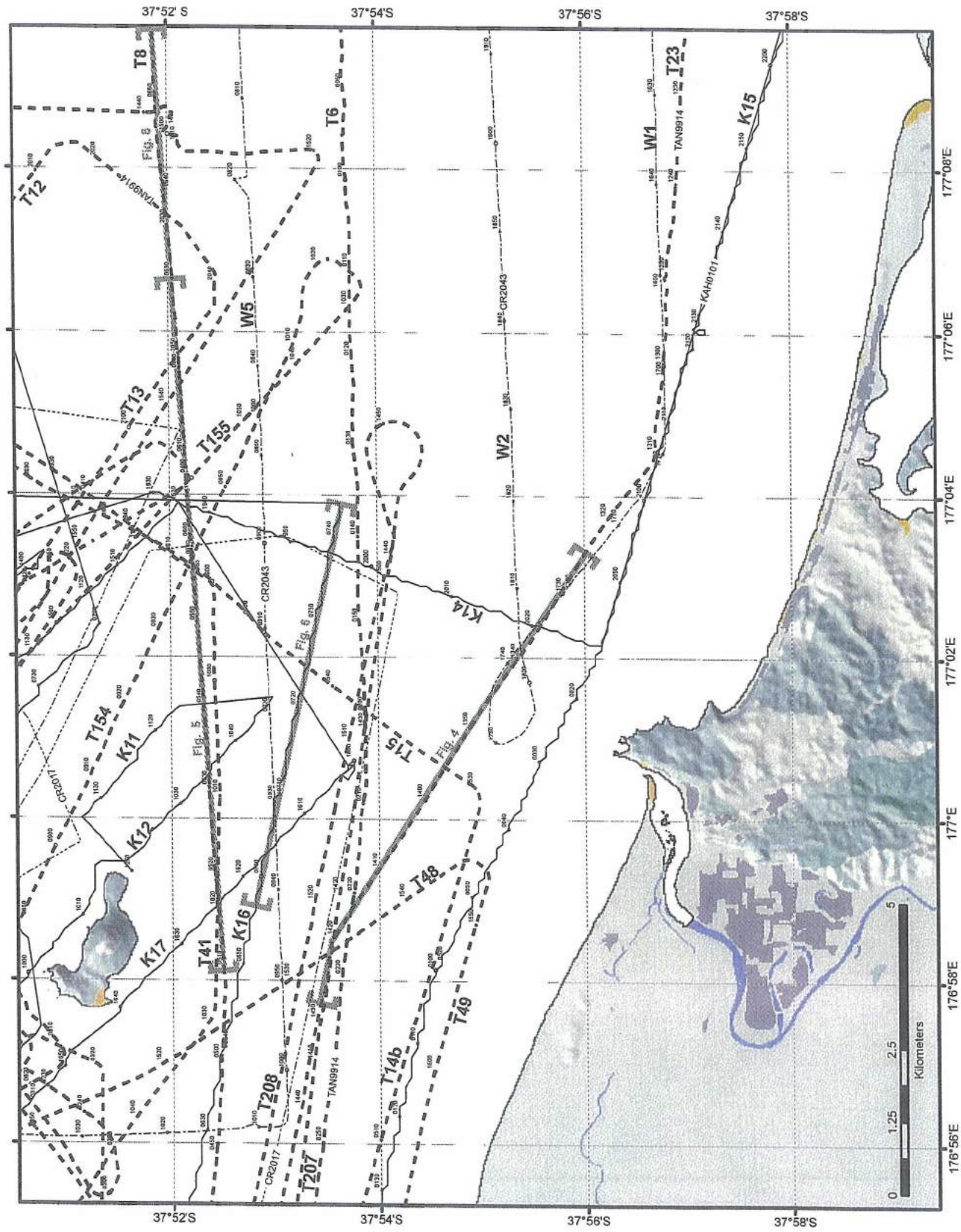

Figure 2 : Ship tracks of all geophysical surveys undertaken in the near coastal zone of urban Whakatane. Profile number indicated in bold font. Location of seismic profiles shown in figure 3 to 6 are indicated in thick grey line.

NIWA
Taihoro Nukurangi

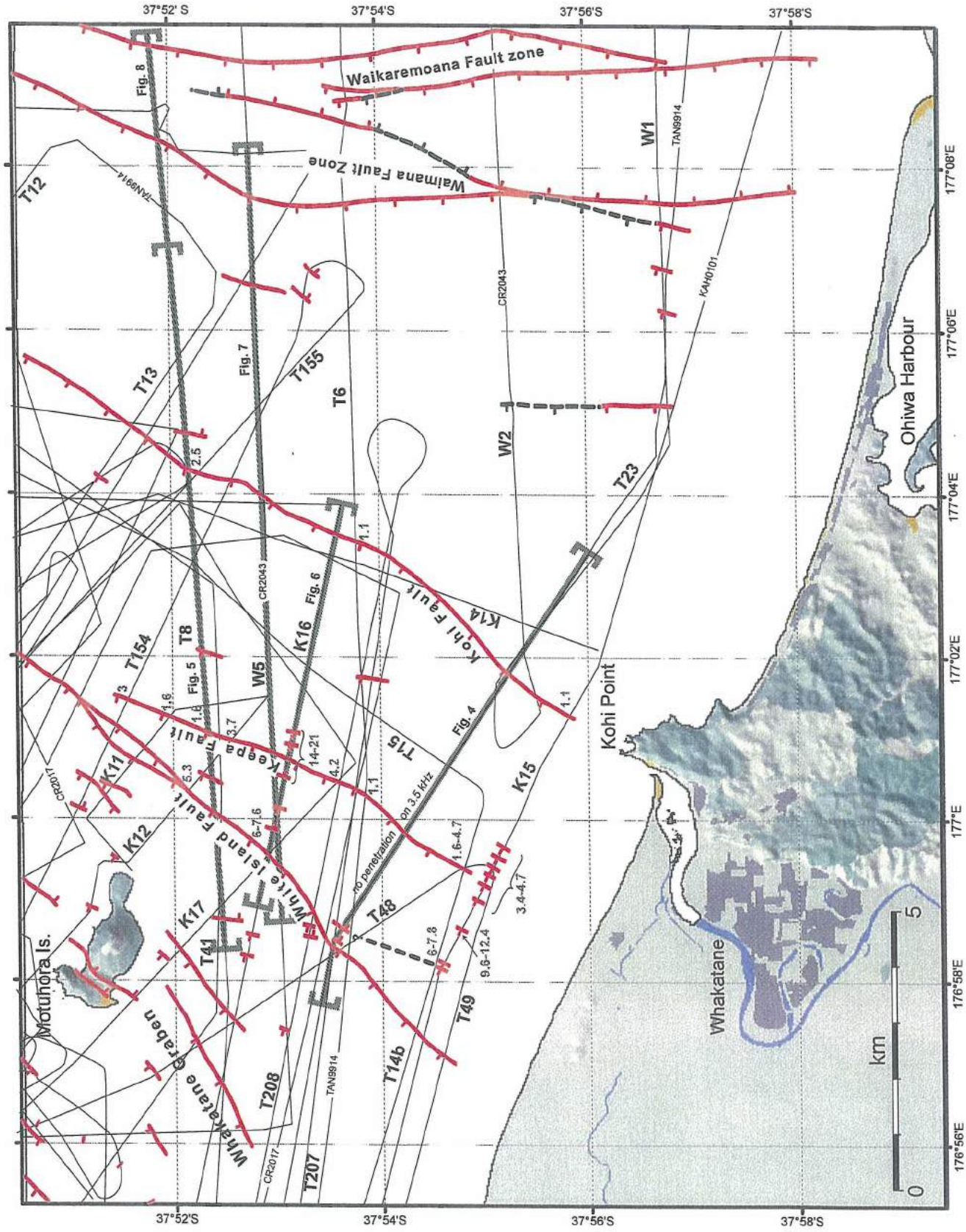

Figure 3 : Fault interpreted from MCS and high-resolution seismic reflection profiles. All seismic profiles are indicated with a thin black line without time stamps for clarity. Black dash are inferred faults. Tick indicate down-throw. Number in blue indicate vertical displacement (in meters) of the last-post glacial erosional surface (9.3 ± 1.8yrs BP).

NIWA
Taihoro Nukurangi

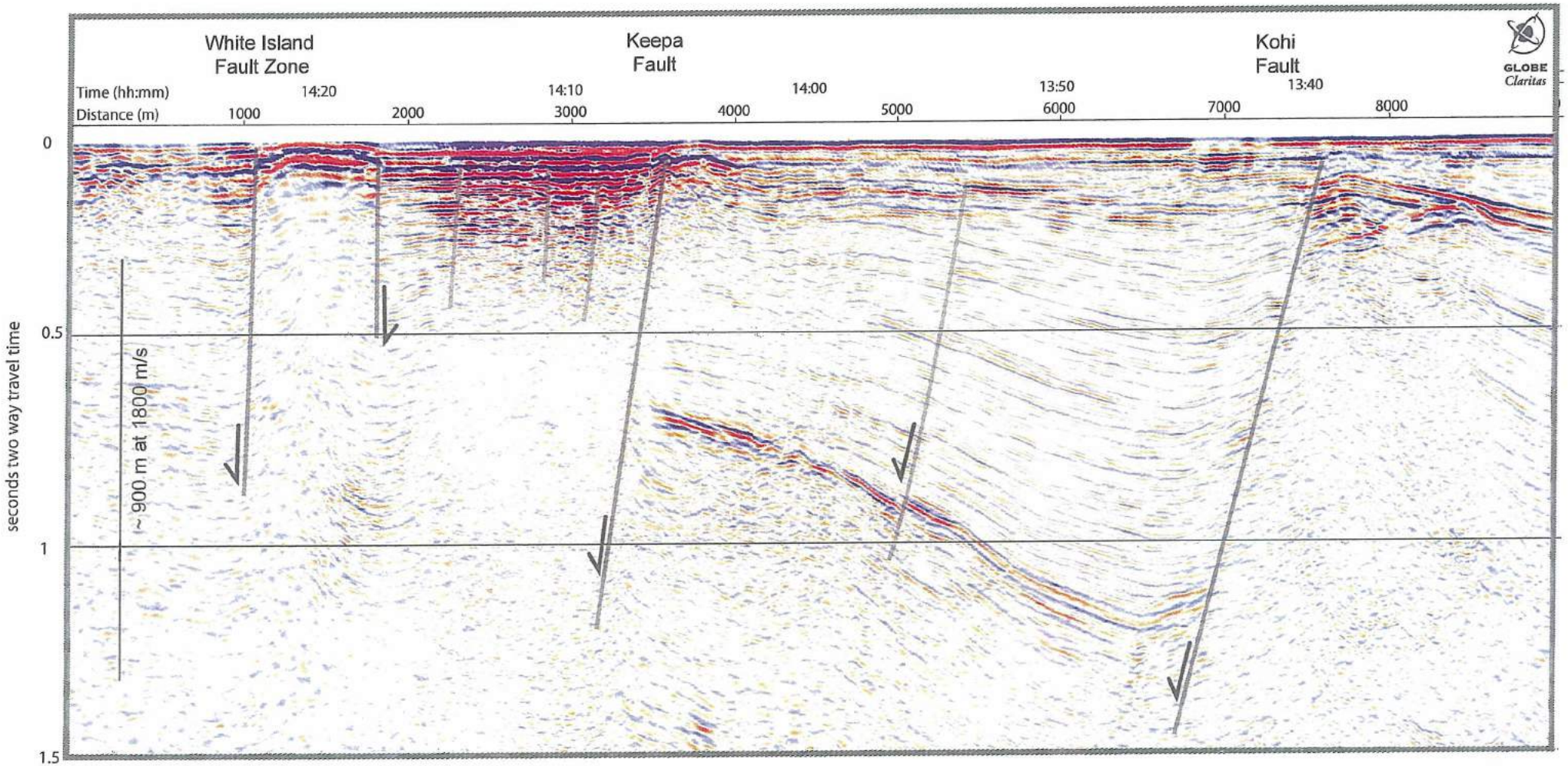

Figure 4 : Multi-channel seismic reflection profile T23 across the White Island, Keepa and Kohi faults in the coastal zone of urban Whakatane. This is the most inland seismic line acquired during Tan99-14 voyage. Metric scale is plotted on top of profile. Active (inactive) faults in dark (light) gray.

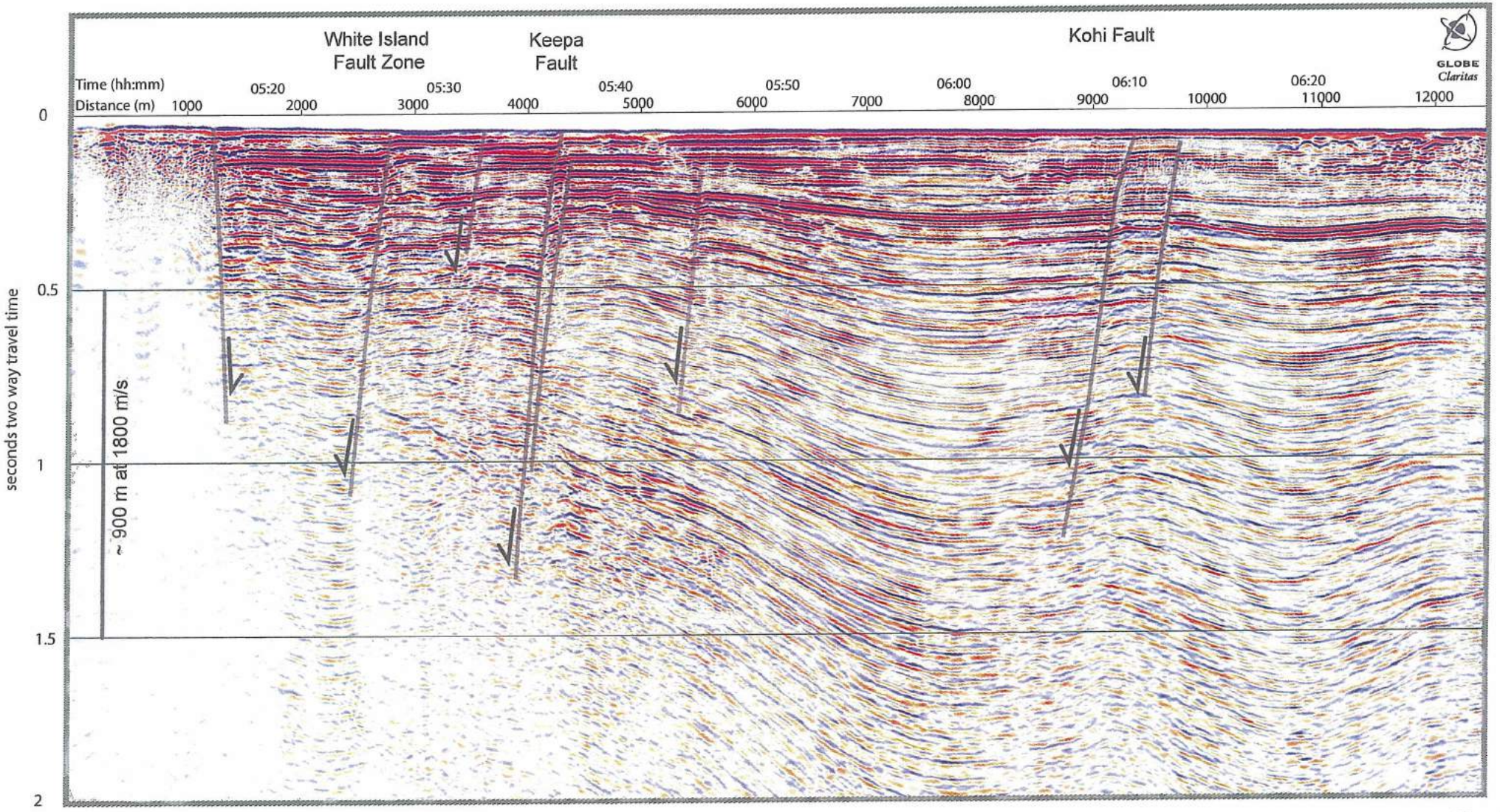

Figure 5 : Multi-channel seismic reflection profile T8 across the White Island, Keepa and Kohi faults in the coastal zone of urban Whakatane. Metric scale is plotted on top of profile. Active (inactive) faults in dark (light) gray.

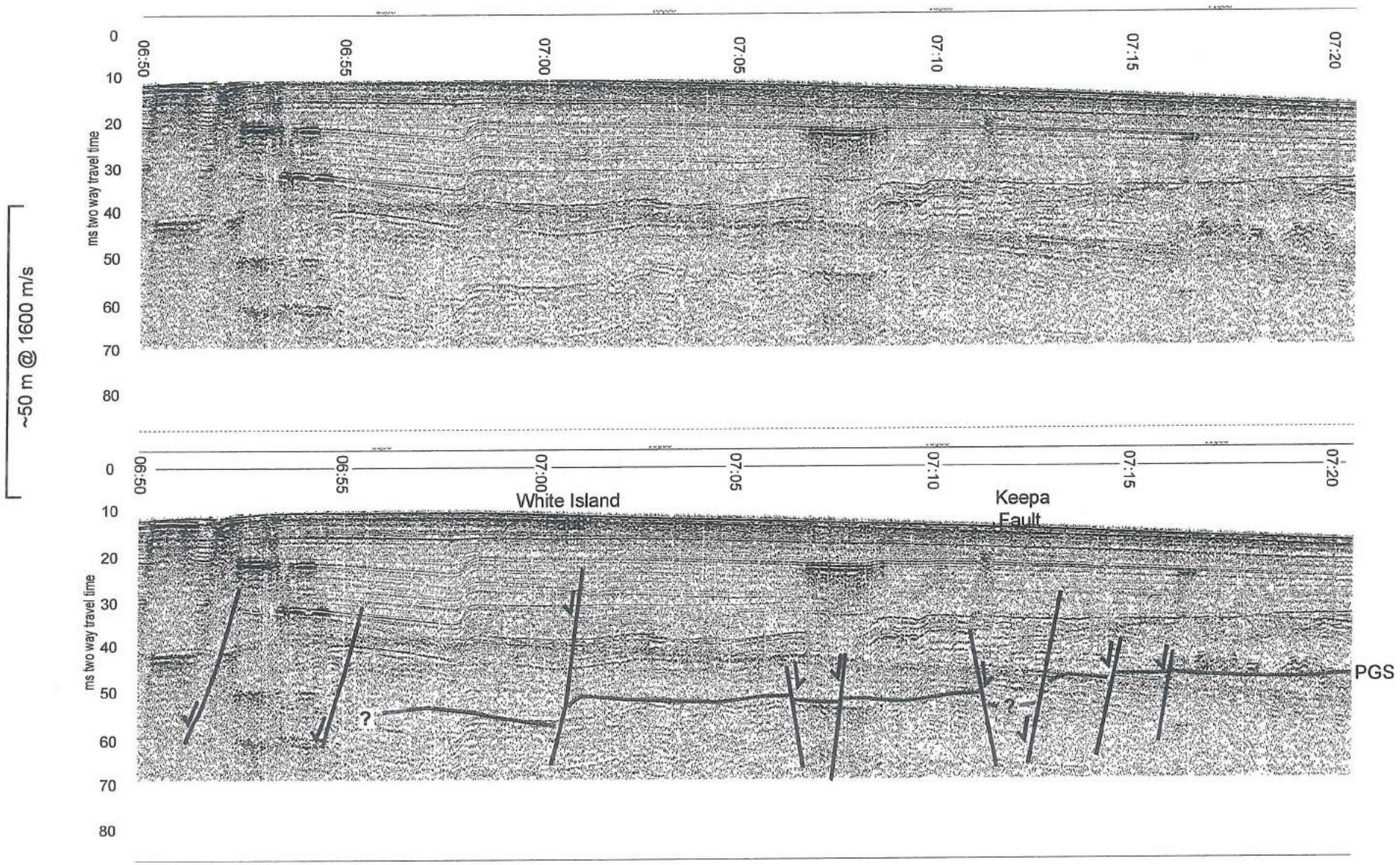

Figure 6 - Very-high-resolution (Boomer source) seismic reflection profile K16 across the White Island, Keepa and Kohi faults in the coastal zone of urban Whakatane. Post-last glacial erosional surface (PGS) is indicated.

NIWA
Taihoro Nukurangi

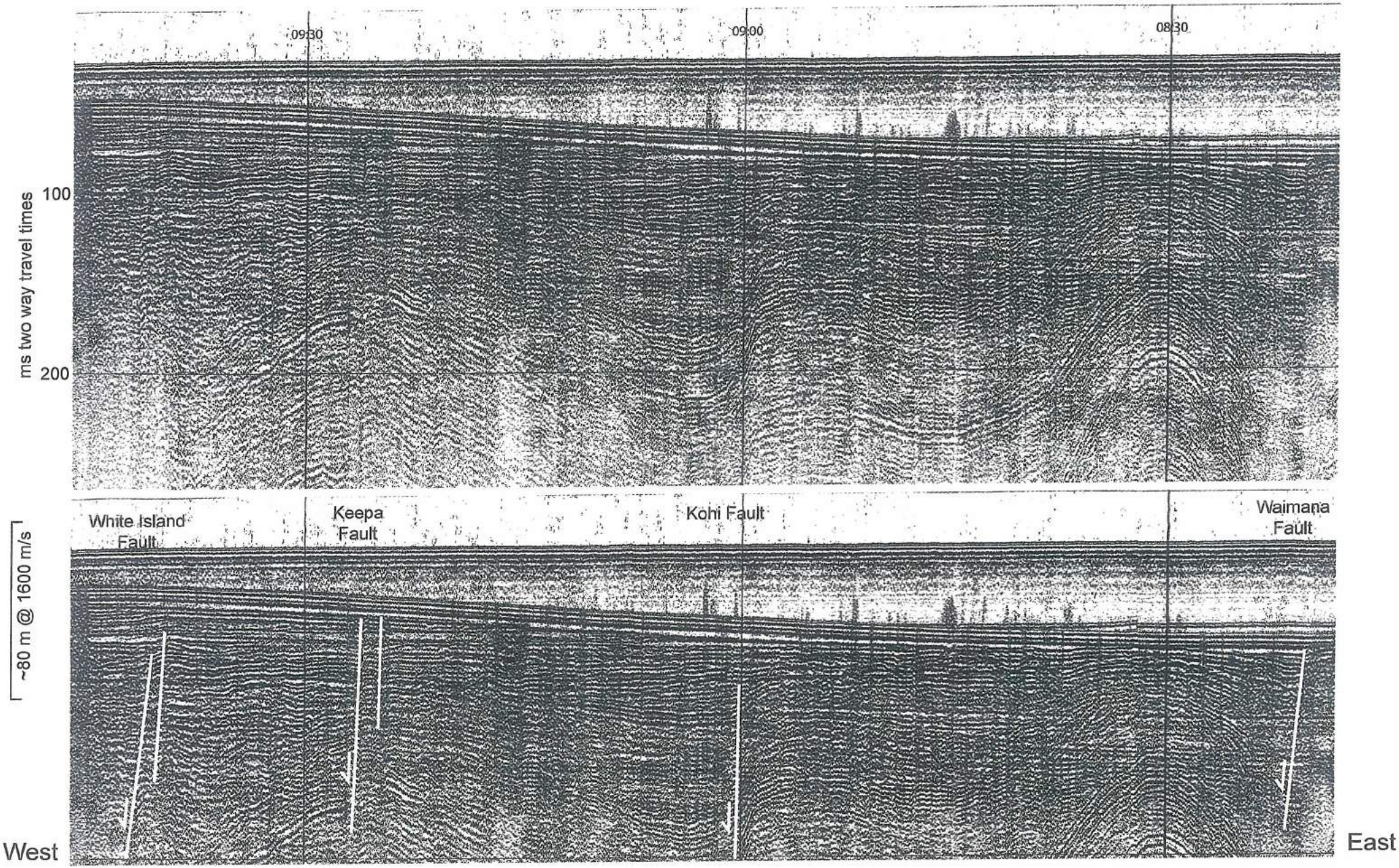

Figure 7 : Single-channel air gun seismic reflection profile W5 (voyage cr2043) across the White Island, Keepa and Kohi faults in the coastal zone of urban Whakatane.

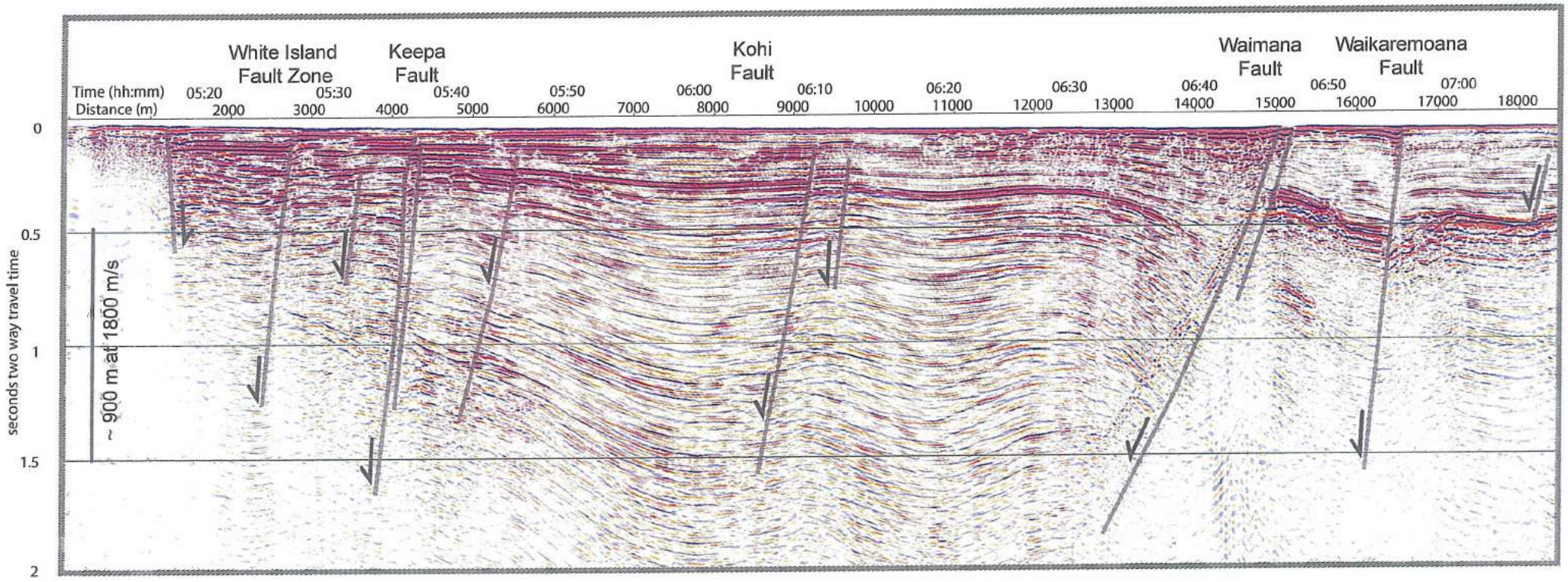

Figure 8 : Multi-channel seismic reflection profile T8 (voyage Tan99-14) extended to the east across Waimana and Waikaremoana faults in the coastal zone of urban Whakatane.

NIWA
Taihoro Nukurangi

APPENDIX 2

Nakamura Data

Nakamura Results from the Whakatane Urban Area

CONTENTS

Table A2-1: Summary of resonant frequencies at sites in Whakatane determined using the Nakamura method.

Figure A2-1: Nakamura results grouped according to ground shaking amplification potential.

Figure A2-2: Nakamura results grouped according to dominant site period (seconds).

Nakamura plots for sites W01-W53 (six to a page)

- Natural scale

- Log-log scale

1.0 SUMMARY

This appendix describes the methodology used in the acquisition of micro-tremor data and the results of processing the micro-tremor data using the Nakamura method (Nakamura, 1989). Ambient, or background ground vibrations are recorded on a portable seismograph. This data is then processed using the Nakamura method. This enables the potential resonance at a site to be evaluated. The value of the Nakamura technique is that data on site response (micro-tremor data) can be quickly gathered in the field, and analyzed to assess the resonant characteristics of a number of sites. The flexibility of the technique allows it to be used as a screening technique to identify which areas may or may not be susceptible to the amplification of strong ground shaking. The Nakamura method provides a reasonable estimate of the natural frequency of a resonant site, and a rough estimate of the amplification, provided that the local geology is simple. The Nakamura method will confidently locate highly resonant areas where a widespread uniform soft or weak layer has an abrupt interface with firmer material.

The quality of the data is good and allows the frequency/period of peak ground shaking for Whakatane to be contoured with some confidence (Figure A2-2). The first contour line is placed at a period of 0.6 seconds as this is a boundary condition for differentiating between ground class C (shallow "stiff" soils) and ground class D (deep or "soft" soils). Thereafter contours are at intervals of one second (i.e. at periods of 1, 2, and 3 seconds). The ground class as determined by Nakamura method is essentially in agreement with the ground class determined using seismic cone penetrometer data (see Appendix 3). The increase in site period from east to west across Whakatane is likely to reflect an increase in the total depth of soil.

2.0 THE NAKAMURA METHOD

In brief, the Nakamura method (Nakamura, 1989) considers waves trapped in a uniform surface layer. Multiple reflections of these waves between the top and bottom of the layer give rise to resonances. Vertical resonant motion at the surface is due to trapped p-waves, while horizontal resonant motion at the surface is due to trapped s-waves. P-waves travel much faster than s-waves in recent sediments and they will not be resonantly amplified at the s-wave natural frequency of a layer, so can be taken as a proxy for non-amplified s-waves. It follows that the ratio of the s-wave spectrum to the p-wave spectrum will have a character that shows the natural frequency and amplification factor of the site, and that the ratio of the spectrum of horizontal motion to the spectrum of vertical motion will behave in the same way. This latter ratio has been named the quasi-spectral ratio (sometimes referred to as the Nakamura ratio).

The method has been tested both by field measurements in known situations, and by computer modelling. The outcome of this testing is that for micro-tremor motions the method gives an accurate value of the dominant period of motion, and a rough estimate of the amplification factor applicable for low to moderate strength seismic input, provided site conditions are simple.

The technique has been applied in several areas around the world. Perhaps the most relevant work is that of Ohmachi et al, (1991), in which the Nakamura method was applied to micro-tremors recorded in the Marina district of San Francisco, the area which was severely damaged during the 1989 Loma Prieta earthquake. By using the Nakamura technique to analyze micro-tremors it was possible to show a strong correlation between the highly resonant sites identified using the Nakamura technique and the areas most heavily damaged during the earthquake.

3.0 THE NAKAMURA METHOD IN NEW ZEALAND

Nakamura's method has been applied by GNS to a number of sites in New Zealand (Alfredton, Timberlea, Miramar, Porirua and Parkway). Our experience with the applicability of the Nakamura Method agrees with those of other investigators in that, if the site is resonant, the frequency of resonance can be predicted, but that the amount of amplification is difficult to predict. In the case of Alfredton, the micro-tremor derived quasi-spectral ratio indicated moderate broad-band amplification; stronger than was seen in recordings of earthquakes.

In the cases of Timberlea and Miramar complex multiple resonances were indicated, and in Parkway (Wainuiomata) moderate resonant amplification was expected, but high amplifications were observed during earthquakes. This was in contrast with the main Wainuiomata valley where the quasi spectral ratio correctly predicted the extremely high amplifications which were observed. It appears that the results from the Wainuiomata main valley were accurate because the site approximates an extended soft layer over rock, whereas the Parkway gully is narrow and depth-varying. In the latter case, the quasi spectral ratio may reflect a very local geometry whereas earthquakes would excite the basin as a whole resulting in a different resonant character.

Results from Porirua emphasise the care which should be taken when considering quasi-spectral-ratios which are unsupported by other data. On the basis of Nakamura's method by itself, because the quasi-spectral ratio for Porirua was much the same as for Alfredton, the earthquake responses of the two sites could be expected to be similar. However, both these sites have been examined in great detail, and their soil-to-rock spectral ratios in small earthquakes are well known, as are the shear wave velocity profiles below both sites. The Porirua site in fact has much the same small earthquake amplification Wainuiomata

(extremely high amplification), albeit at a different frequency, and the Porirua amplification factor and frequency were both accurately predicted beforehand by Stephenson et al (1990) on the basis of geotechnical measurements.

The technique does appear to have limitations where the stratigraphy of a site lacks a clear interface between the soft and firm layers, especially in the case of a shear wave velocity profile which increases gradually with depth. The micro-tremors recorded at Alfredton, where there is such a shear wave profile yield a very broad-band quasi-spectral ratio. This does not mean that amplification is not expected. As energy propagates from the stiffer to the less stiff material the wave amplitude should increase, and such an increase occurs in Alfredton, as shown by the slightly greater amplitudes of motion seen on soil compared with rock during earthquakes. Further work should show whether broad band resonances are associated with velocities steadily increasing with depth.

Another possible limitation to the Nakamura technique is that structures other than basins can be expected to resonate with a natural frequency for horizontal motion which is quite different from the natural frequency for vertical motion. Examples are buildings, ridges and embankments. In such cases, the quasi-spectral ratio can reveal the resonant character of the relevant object, though the identity and extent of the object may not be obvious. Furthermore, such a resonant object could radiate seismic waves, which in turn could have a dominant horizontal component so that the resonant character of a building for instance, could emerge in micro-tremor records made close to it. This effect, if not recognized, can lead to ambiguous interpretations of micro-tremor recordings.

In general, we consider that the Nakamura method provides a reasonable estimate of the natural frequency of a resonant site, and a rough estimate of the amplification, provided that the local geology is simple. We can add, however, that we are confident that the method will locate highly resonant areas where a widespread uniform soft layer has an abrupt interface with firmer material.

4.0 DATA COLLECTION IN WHAKATANE

Micro-tremors (ambient ground vibrations) were recorded at 53 locations in Whakatane (Table A2-1, Figure A2-1 - following text). The survey was carried out by Peter Davenport in September 2003. The criterion employed for the detailed selection of a site for the first survey was quick and easy vehicular access, as anything else would extend the required 10 minute recording time. The measurement locations were selected on the basis of the geological mapping described in the main text, with the intention of assessing the resonance of each significant geological unit.

Recordings were made for a minimum of ten minutes at each location. In this process, a seismometer (Kinemetrics model L4C-3D) senses the ground velocity along each of three axes, producing voltages which are recorded by an EARSS seismograph (Gledhill, 1991) at a rate of 100 samples per second. The seismometer used has a nominal natural frequency of 1 Hz, and a nominal damping of 67% of critical.

Table A2-1 shows the assessed amplification and its resonant frequency.

Table A2-1: Summary of resonant frequencies at sites in Whakatane determined using the Nakamura method. Locations of other geotechnical investigations included for reference. It should be noted that the sites where geotechnical information is available, while often in the same general area, are not necessarily at exactly the same site. This is important when comparing results from the different investigations as the local geology can vary laterally.

5.0 RESULTS FOR WHAKATANE

The results of the Nakamura method applied to the collected micro-tremor data for Whakatane all show resonance to some degree with several sites showing complex multiple resonant peaks. The results are shown graphically in the plots that follow Figure A2-2.

The Nakamura data has been grouped in two ways to extract information. The first grouping is based on analysis of the form of the HVSR (horizontal to vertical spectral ratios) plots and consists of five classes:

1. HVSR ratio <0.7 Hz at high frequencies (will amplify);
2. HVSR ratio moderately low (>0.7 Hz) at high frequencies with peak and trough (will amplify);
3. HVSR ratio moderately low at high frequencies (>0.7 Hz) with peak and possible trough (most likely amplify);
4. Resonant peak at sufficiently high frequency (>3.7 Hz) that trough cannot be seen (probably amplify); and
5. Un-interpretable sites

When the HVSR data is plotted using the low frequency peak data (Figure A2-1) the most noticeable trend is that all the sites with a resonant peak at frequencies greater than 3.7 Hz are within 500 metres of the former coastal cliffs cut in greywacke. Among the sites that are given a "will amplify" class two locations stand out, the reclaimed land under the central business district and the area around Lake Sullivan, an old channel of the Whakatane River, in the last 2-300 years.

The second grouping uses the presence or absence of a peak at low frequencies. To assign ground class to a site, one of the parameters that can be used is the site period. To this end each of the Nakamura peak frequencies (Hz) has been converted to the reciprocal ground period (sec) for mapping purposes (Table A2-1).

However, when the data is plotted showing the presence or absence of a peak at low frequencies a clear pattern is discernable (Figure A2-2). All the sites that do not have low frequency peak plot within 6-800 metres of the former coastal cliffs. If the frequencies are converted to period all sites within this zone have a natural site period of less than 0.6 seconds. The sites with a peak at low frequency (<1.5 Hz) are all over 500 metres from the former coastal cliffs. All the sites that have a secondary peak are also within this zone.

The quality of the data is good and allows the frequency/period of amplified ground shaking for Whakatane to be contoured with some confidence (Figure A2-2). The first contour line is placed at a period of 0.6 seconds as this is a boundary condition for differentiating between ground class C (shallow "stiff" soils) and ground class D (deep or "soft" soils). Thereafter contours are at intervals of one second (i.e. at periods of 1, 2, and 3 seconds). The ground class as determined by Nakamura methods is essentially in agreement with the ground class determined using seismic cone penetrometer data (see below). The increase in site period across Whakatane is likely to reflect an increase in the total depth of soil from the cliffs towards the river channel.

5.1 The inferred location of the Whakatane Fault

Direct evidence for locating the position of the Whakatane Fault has not been identified in the data from these groupings. However, the increase in the period of the low frequency peaks in the west may indicate an increase in the thickness of the soft near-surface layer on the downthrown side of the Whakatane Fault.

6.0 REFERENCES

Gledhill, K.R., 1991: EARSS Users' Manual; Technica/ Report No 109, Geophysics Division, DSIR.

Nakamura, Y., 1989: A method for dynamic characteristics estimation of subsurface using micro-tremor on the ground surface. Quarterly Report of Railways Technical Research Institute, Vol 30(1), February, 1989.

Ohmachi, T., Nakamura, Y., and Toshinawa, T., 1991: Ground motion characteristics of the San Francisco Bay area detected by micro-tremor measurements. Proceedings: Second International Conference on Recent Advances in Geotechnical Earthquake Engineering and Soil Dynamics, March 11-15, 1991, St Louis, Missouri, Paper No LP08,

Stephenson, W.R., Barker, P.R., and Mew, G., 1990: Report on resonant alluvium conditions for part of Porirua basin, Contract 9A9101 between DSIR Division of Land and Soil Sciences and Wellington Regional Council.

Site No.	Primary peak (Hz)	Second peak (Hz)	HVSR form grouping	Primary peak (sec)	Second peak (sec)	Definite LFP (sec)	Possible LFP (sec)	No LFP (sec)
1	4		1	0.25				0.25
2			5					
3	3.4		3	0.29				0.29
4	3.4		1	0.29				0.29
5	2.2		1	0.45				0.45
6	5.6		4	0.18				0.18
7	7		4	0.14				0.14
8	4.7		2	0.21				0.21
9	3.7		1	0.27				0.27
10	4.6		4	0.22				0.22
11	5.2		4	0.19				0.19
12	3.9		1	0.26				0.26
13			1					
14	0.7	2.2	1	1.43	0.45	1.43		
15	0.46	2.2	3	2.17	0.45	2.17		
16	0.46	1.6	3	2.17	0.63	2.17		
17	0.54		3	1.85		1.85		
18	1.1		3	0.91		0.91		
19	0.62		2	1.61		1.61		
20	3.7		3	0.27				0.27
21	5.2		4	0.19				0.19
22	4		2	0.25			0.25	
23	0.75	0.95	1	1.33	1.05	1.33		
24	2.9		1	0.34			0.34	
25	1.4		3	0.71				0.71
26	0.5		3	2.00		2.00		
27	0.4		3	2.50		2.50		
28	0.45		3	2.22		2.22		
29	0.76		3	1.32		1.32		
30	0.31		3	3.23		3.23		
31	0.28	1.4	3	3.57	0.71	3.57		
32	0.3	1.4	3	3.33	0.71	3.33		
33	0.31	1	1	3.23	1.00	3.23		
34	0.36	1.2	3	2.78	0.83	2.78		
35	0.38	1	3	2.63	1.00	2.63		
36	0.4	1.1	3	2.50	0.91	2.50		
37	0.46	1.4	3	2.17	0.71		2.17	
38	2		1	0.50				0.50
39	5		4	0.20				0.20
40	3		1	0.33				0.33
41	3.7		4	0.27				0.27
42	0.9		3	1.11				1.11
43	1.1		3	0.91		0.91		
44	1		3	1.00		1.00		
45	1.2		2	0.83				0.83
46	0.7	2.4	3	1.43	0.42	1.43		
47	0.72	2.5	3	1.39	0.40	1.39		
48	0.72	3	1	1.39	0.33		1.39	
49	2.6		3	0.38				0.38
50	3.5		3	0.29				0.29
51	4.6		2	0.22				0.22
52	2.7		3	0.37				0.37
53	0.9		3	1.11		1.11		

Table A2-1: Summary of micro-tremor data processed using the Nakamura technique. The definitions of the categories used for grouping the data are given in the text. The initial values are given in terms of the frequency of the peak in hertz (Hz), but for the analysis of the low frequency peaks (LFP) the data is converted to period (seconds). The site No. locations are shown on Figure A2-1 and the contoured site period bands on Figure A2-2.

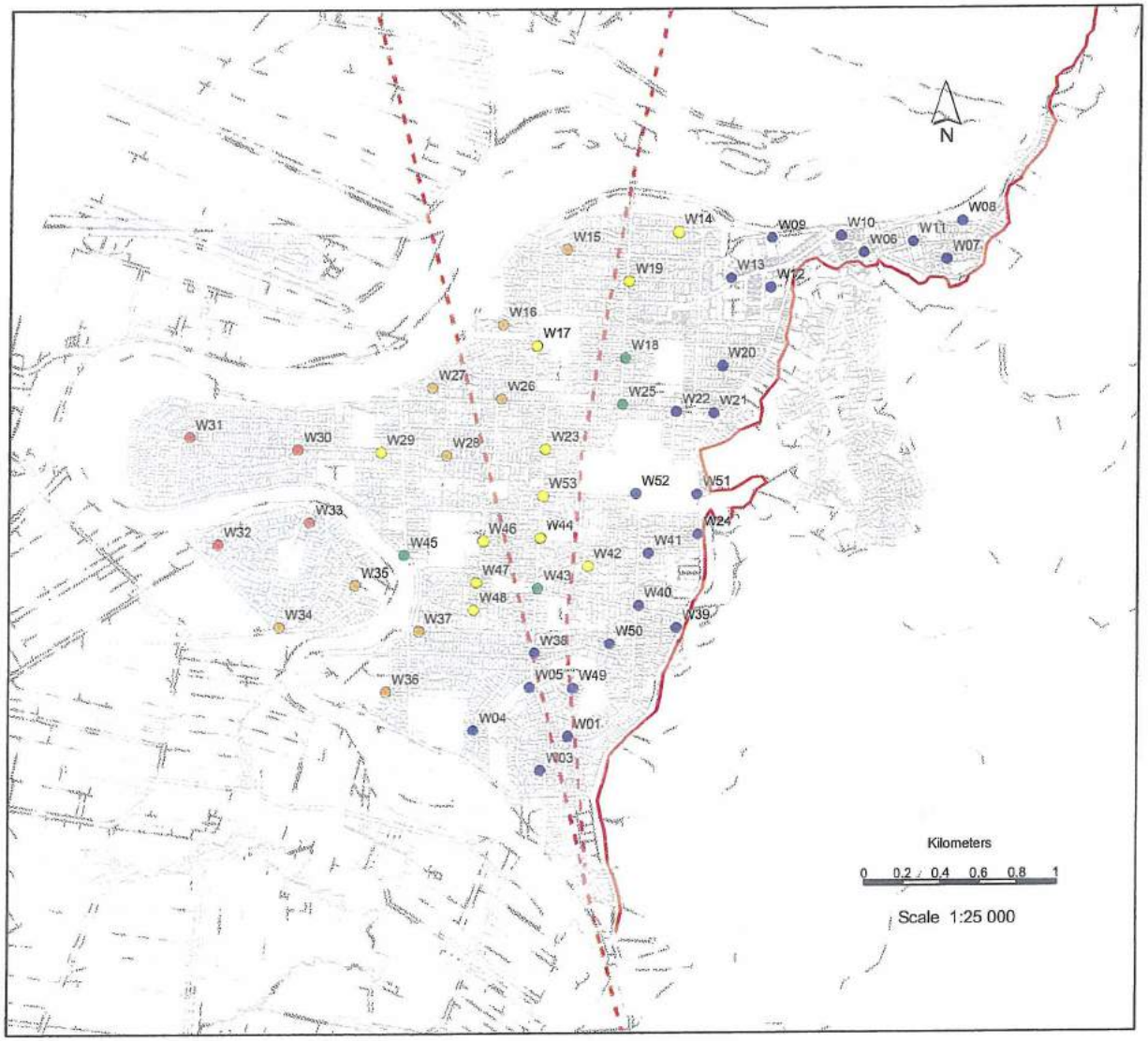

FIGURE:	A2 - 2
PROJECT:	Whakatane Microzoning
TITLE:	Nakamura results in Whakatane grouped according to dominant site period.
DATE:	January 2004
DRAFTED BY:	J. Hoverd
PROJECT NO.:	430W1029
CR:	
EXPLANATION:	Dominant site period measured in seconds. Base Map: Whakatane District cadastral data
LEGEND	Site period groups Site period > 3.0 s Site period 2.0 - 3.0 Site period 1.0 - 2.0 s Site period 0.6 - 1.0 s Site period 0.0 - 0.6 s Base of former coastal cliff Estimated fault location

Whakatane Quasi-Spectral Ratios

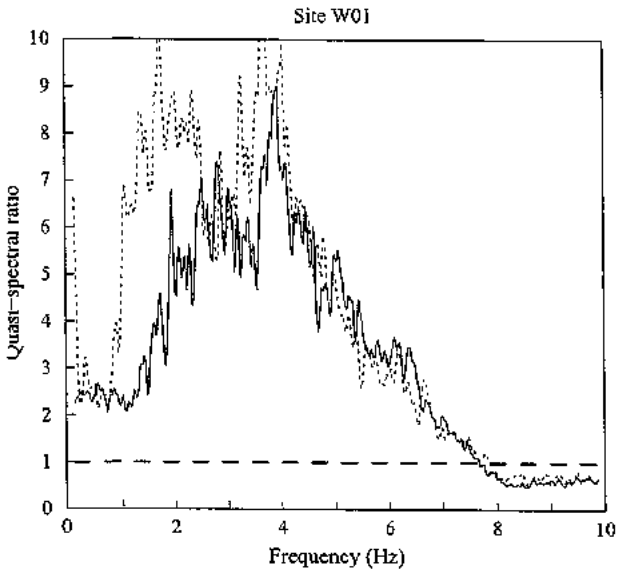

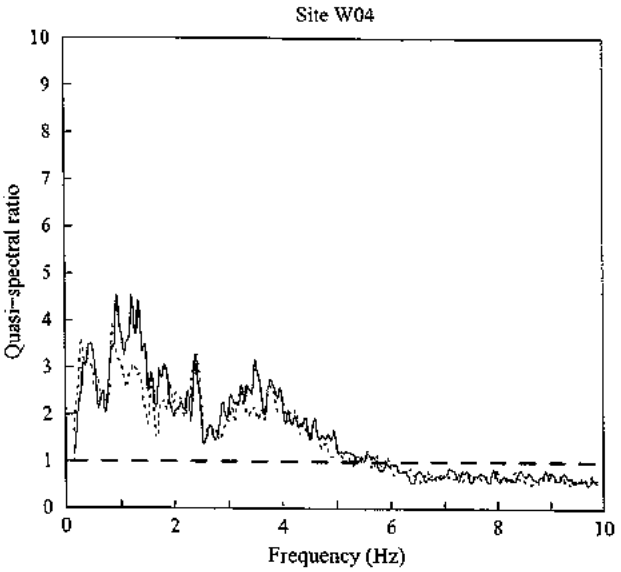

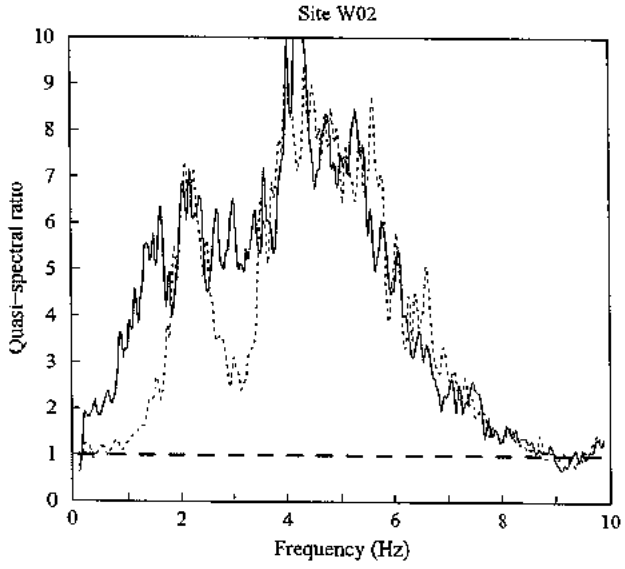

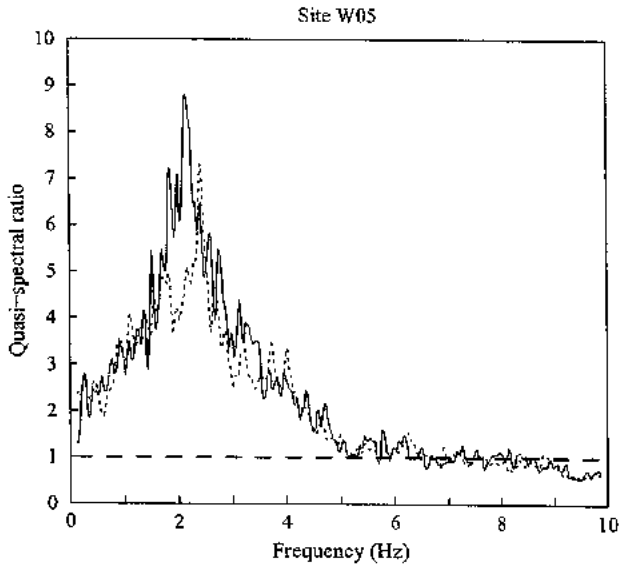

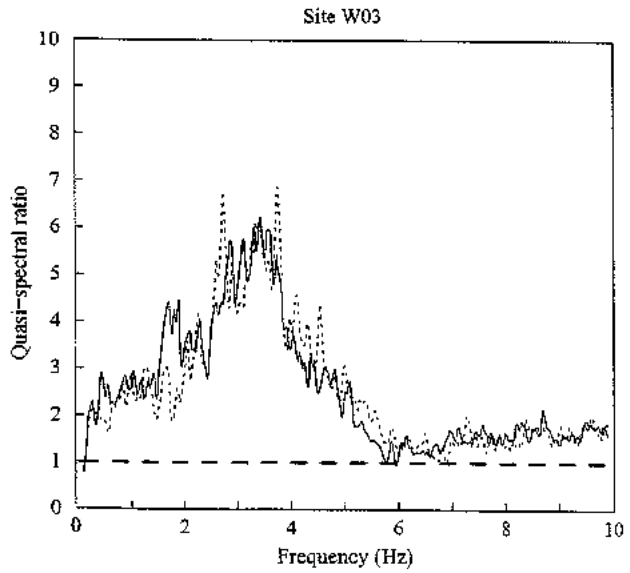

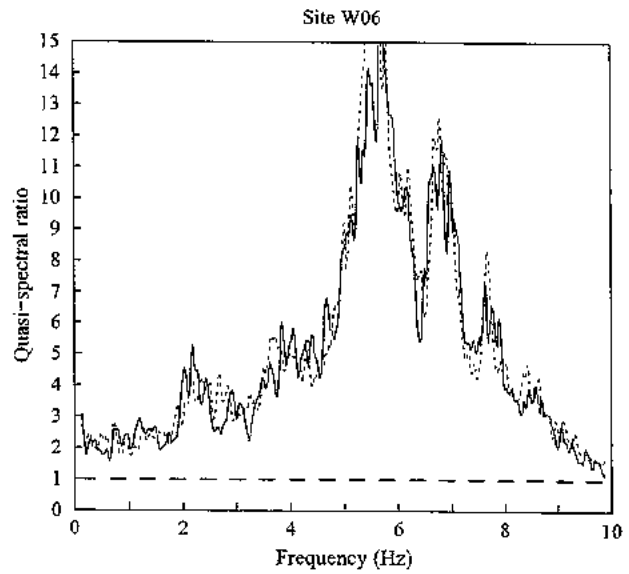

Whakatane Quasi–Spectral Ratios

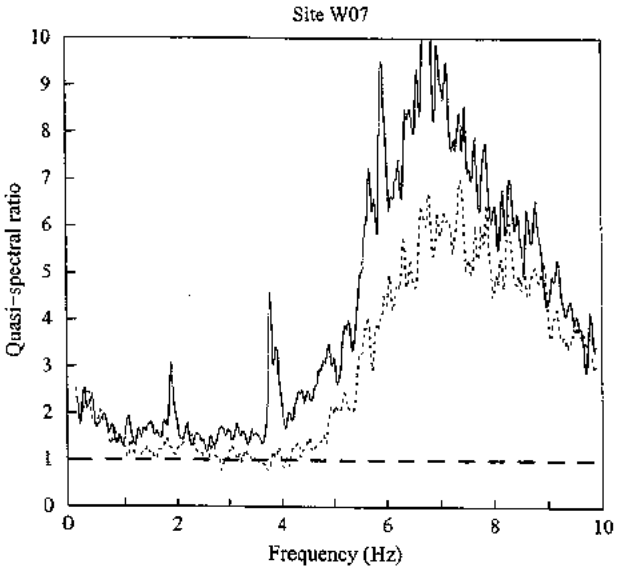

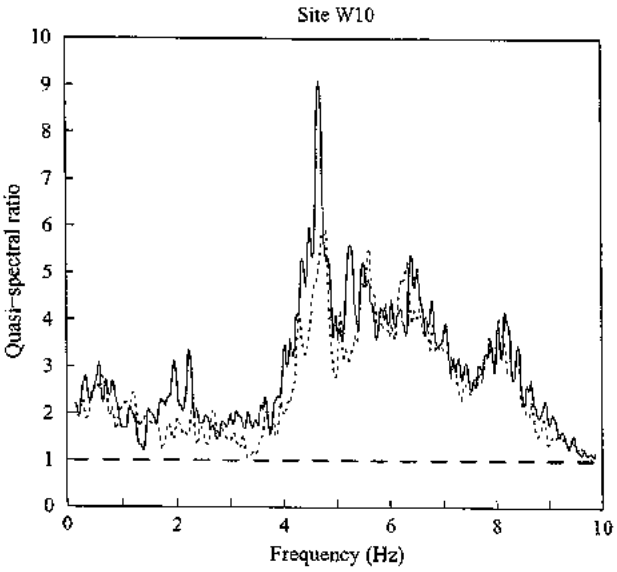

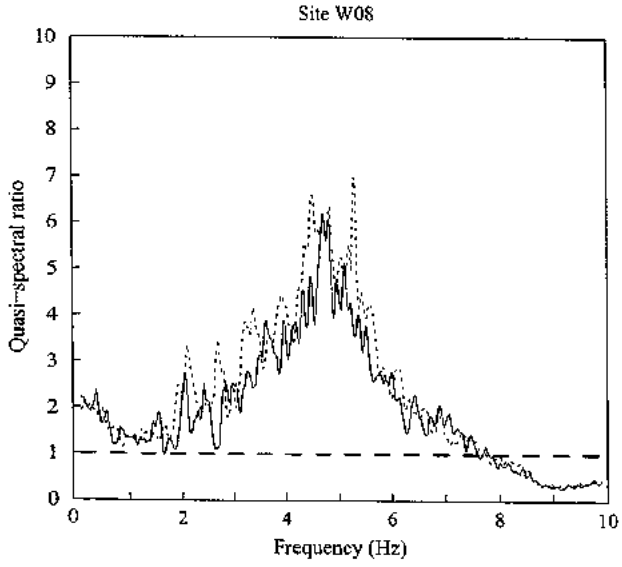

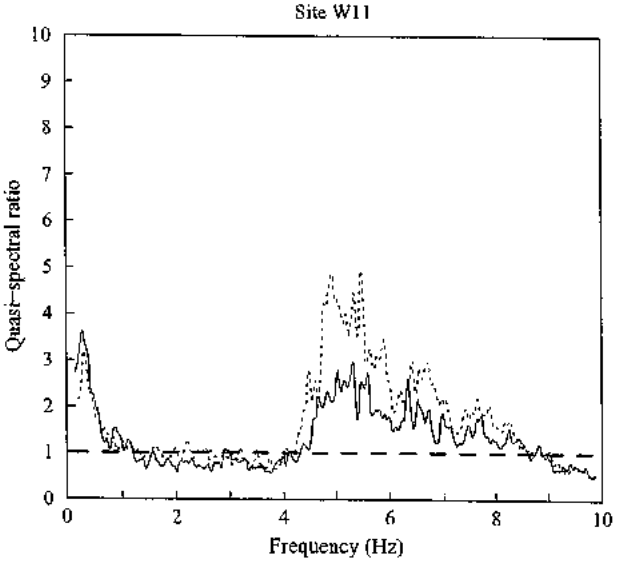

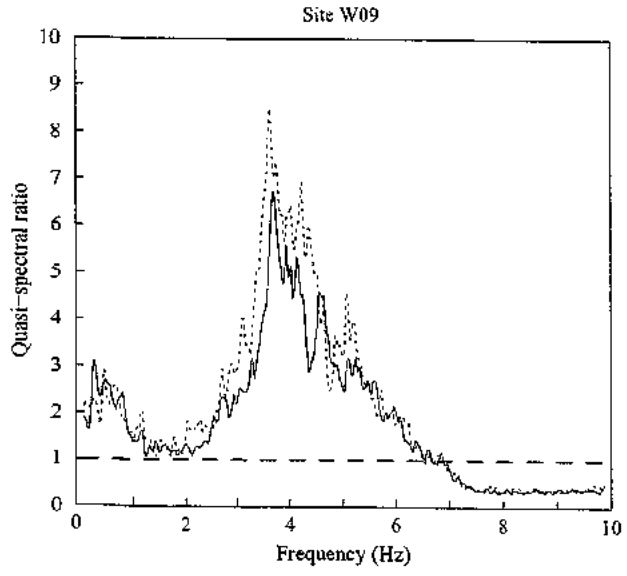

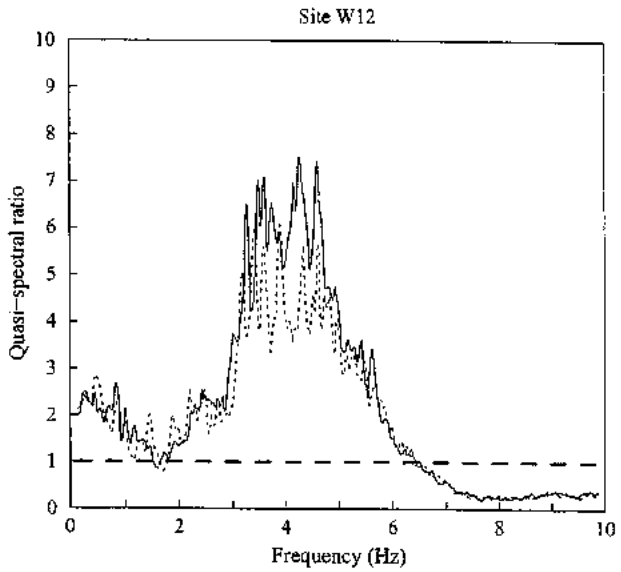

Whakatane Quasi–Spectral Ratios

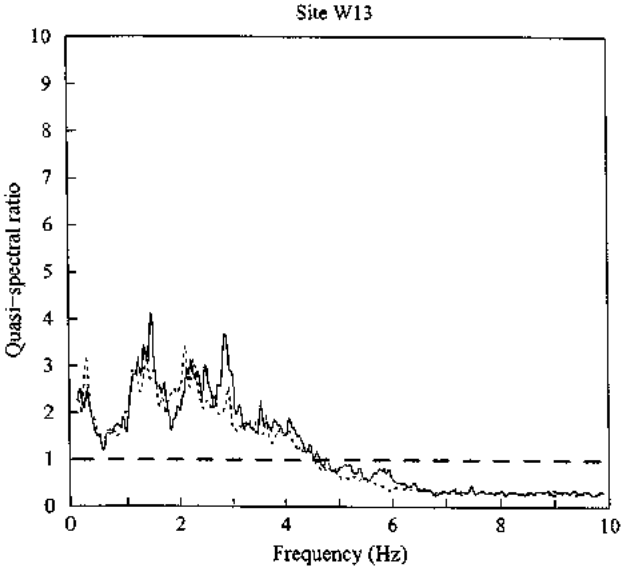

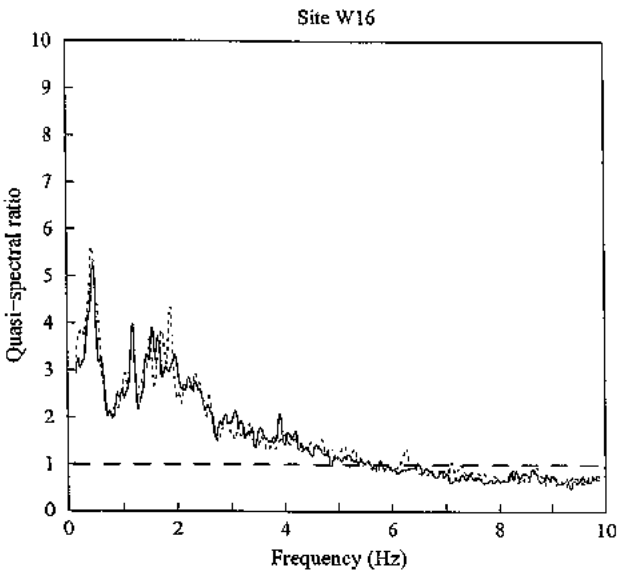

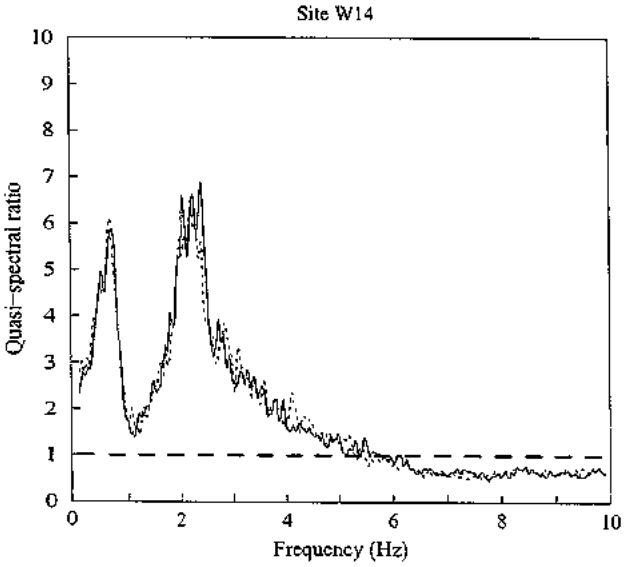

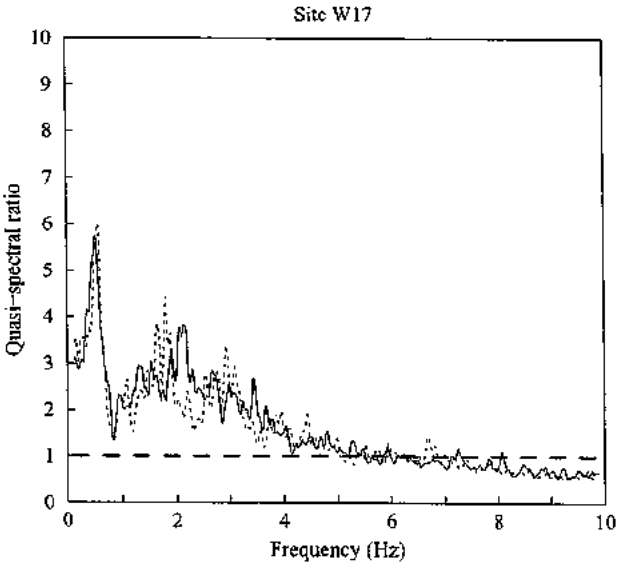

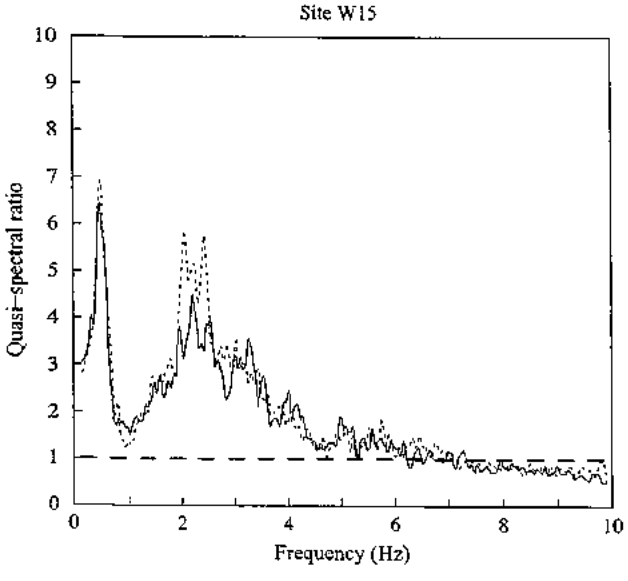

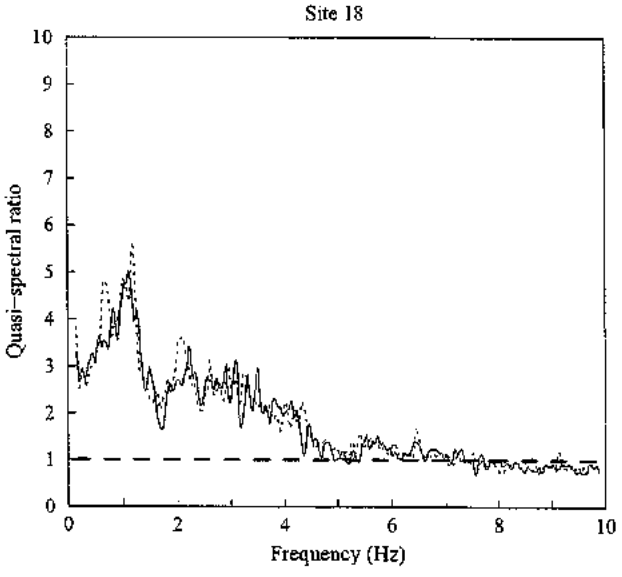

Whakatane Quasi–Spectral Ratios

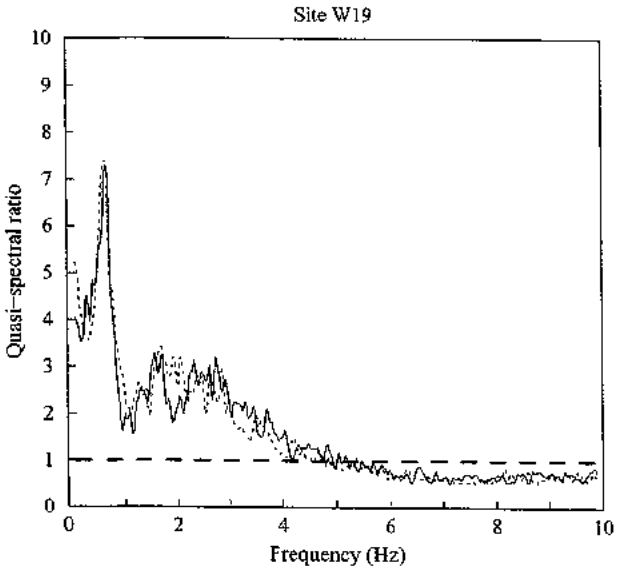

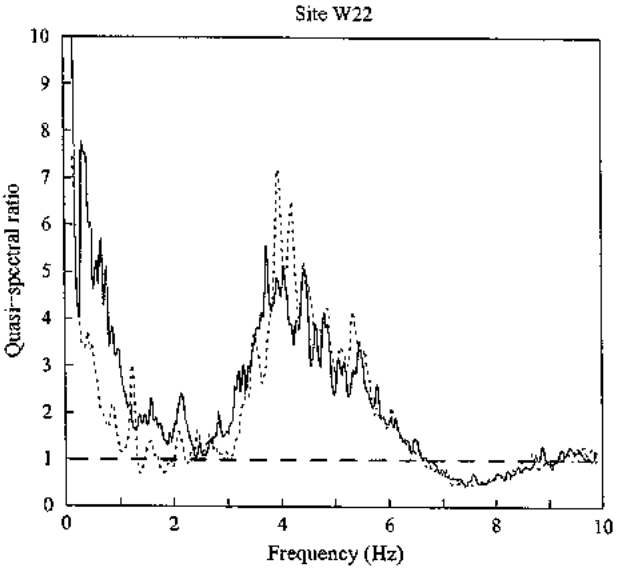

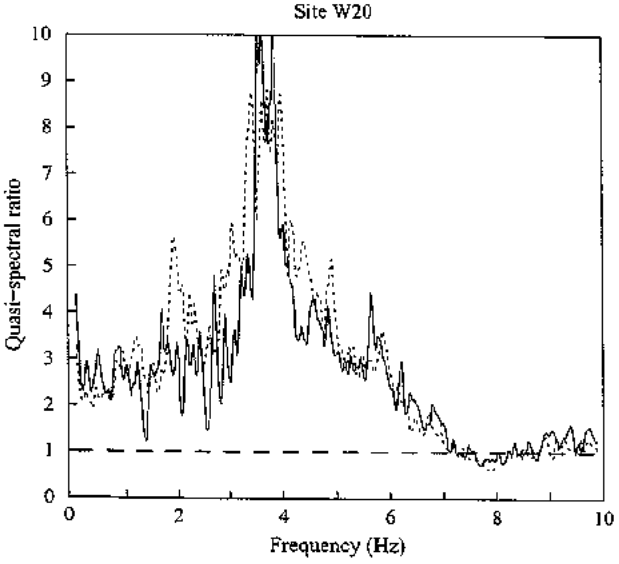

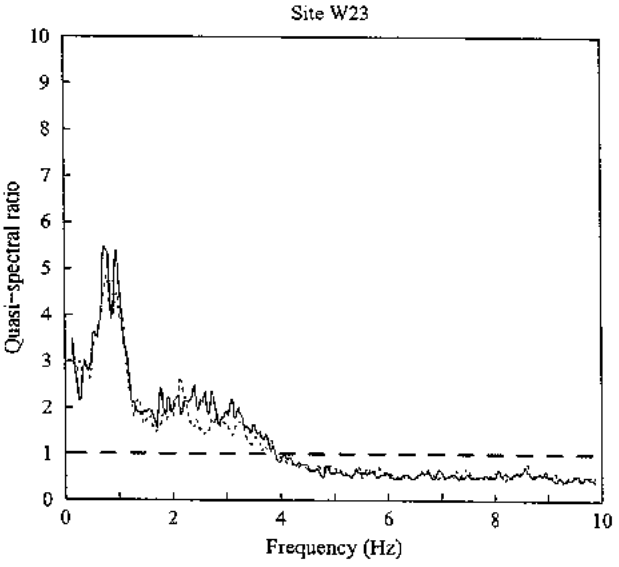

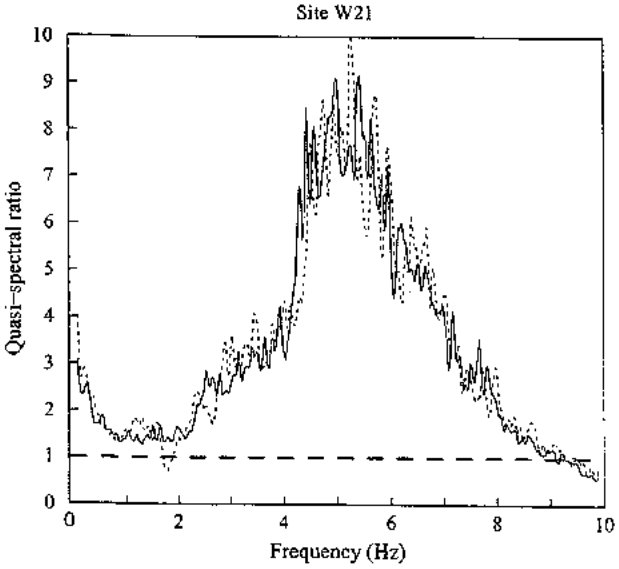

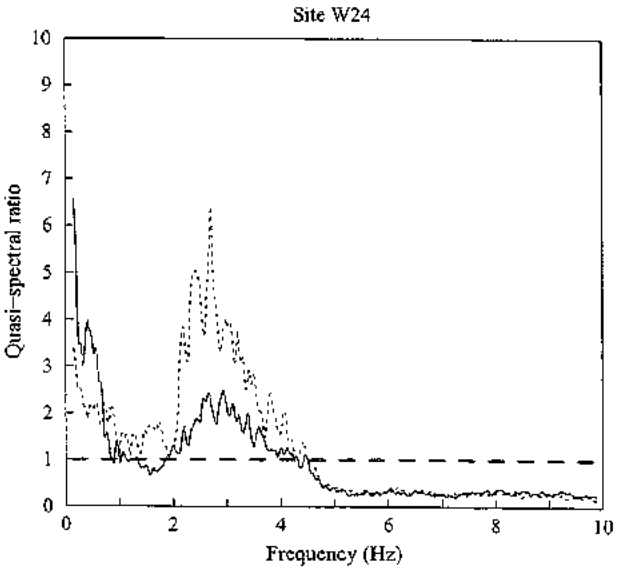

Whakatane Quasi–Spectral Ratios

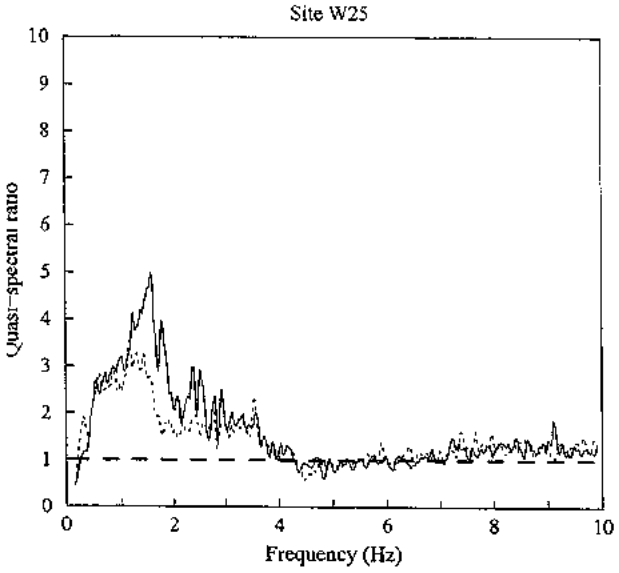

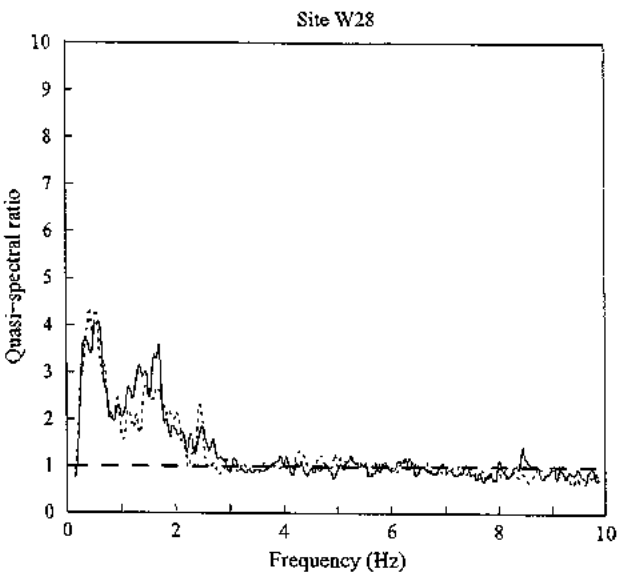

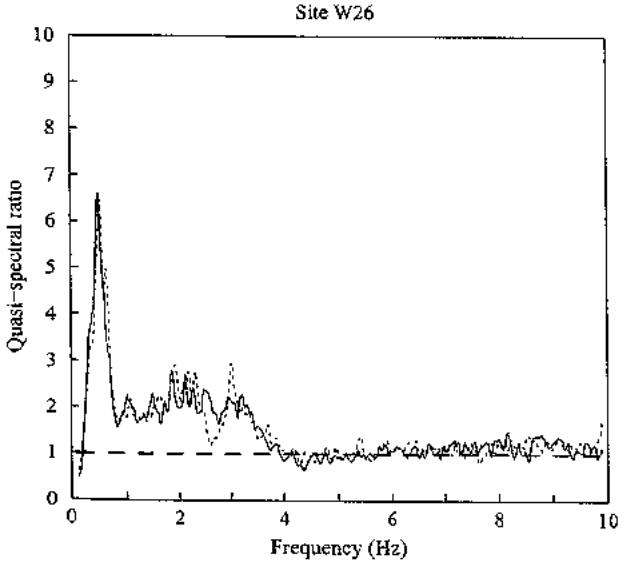

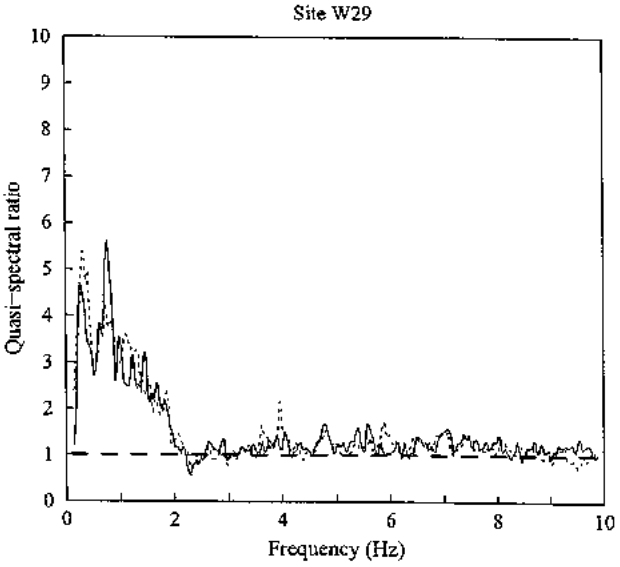

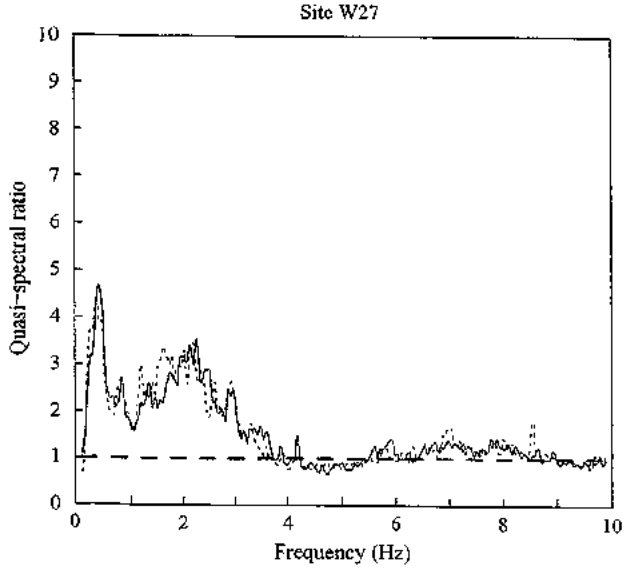

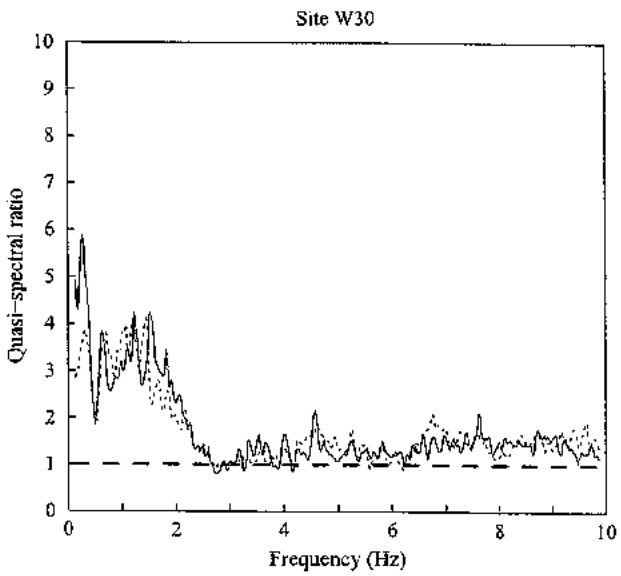

Whakatane Quasi–Spectral Ratios

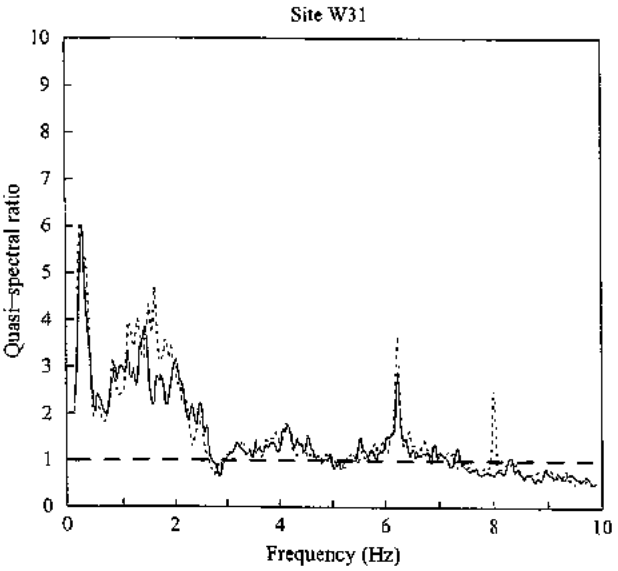

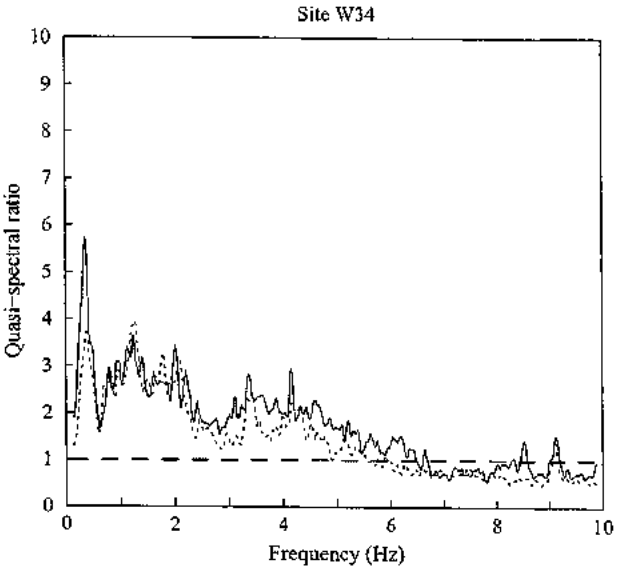

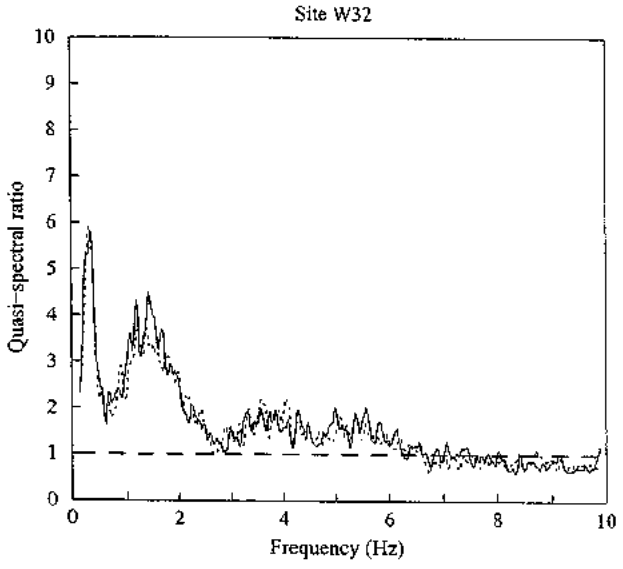

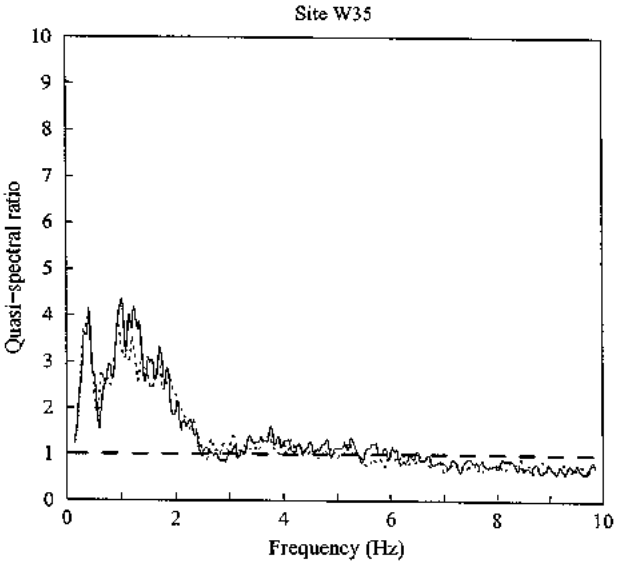

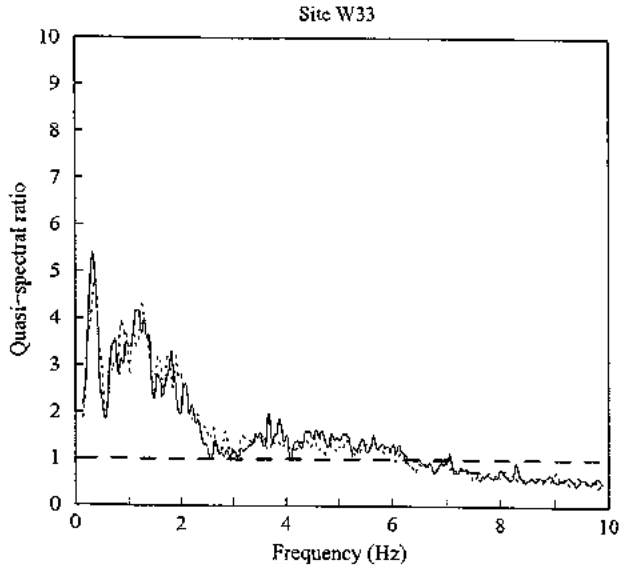

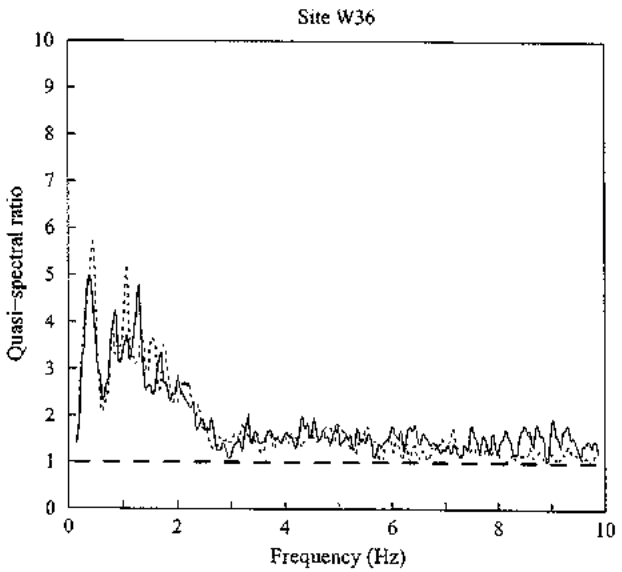

Whakatane Quasi–Spectral Ratios

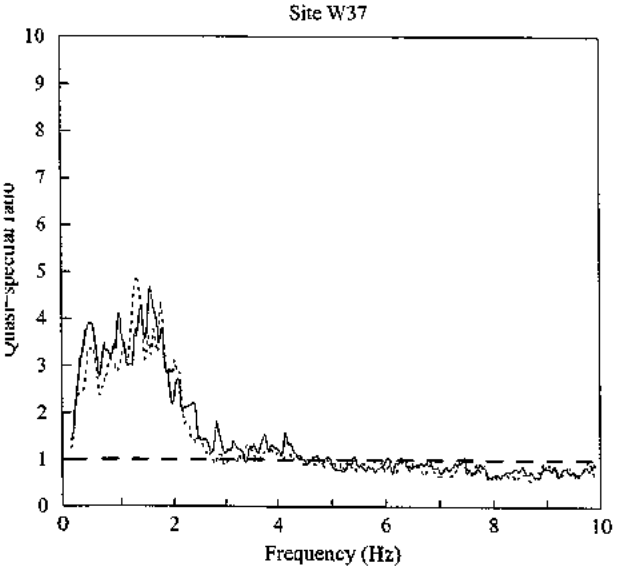

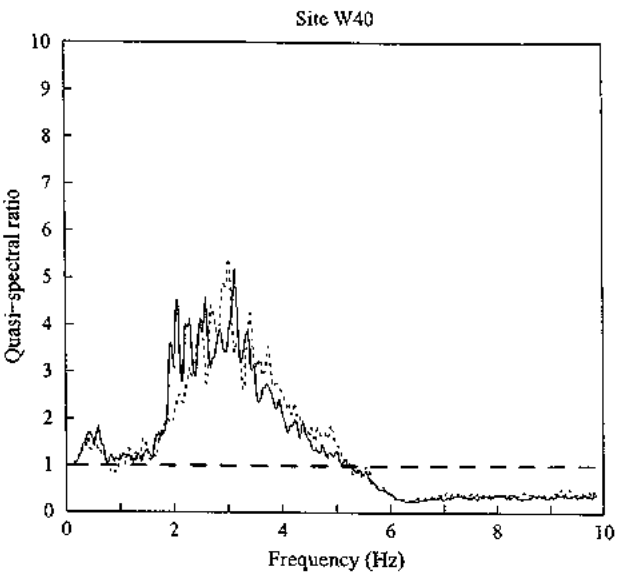

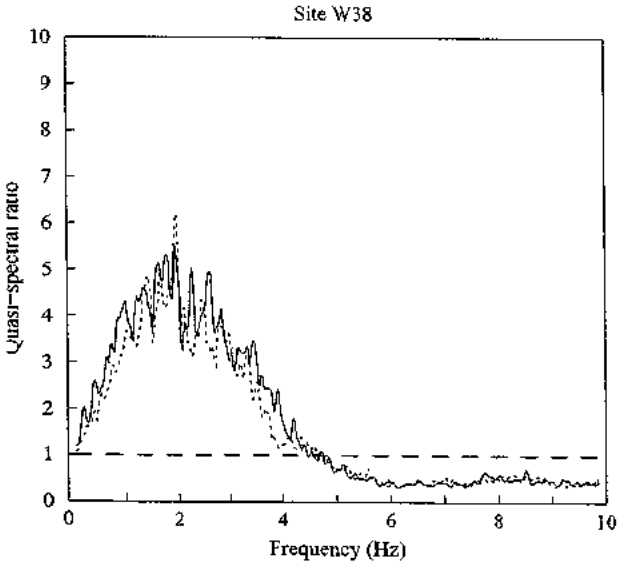

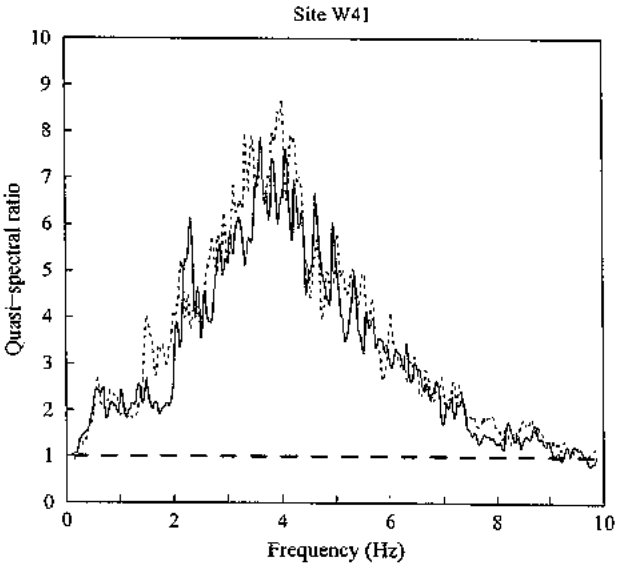

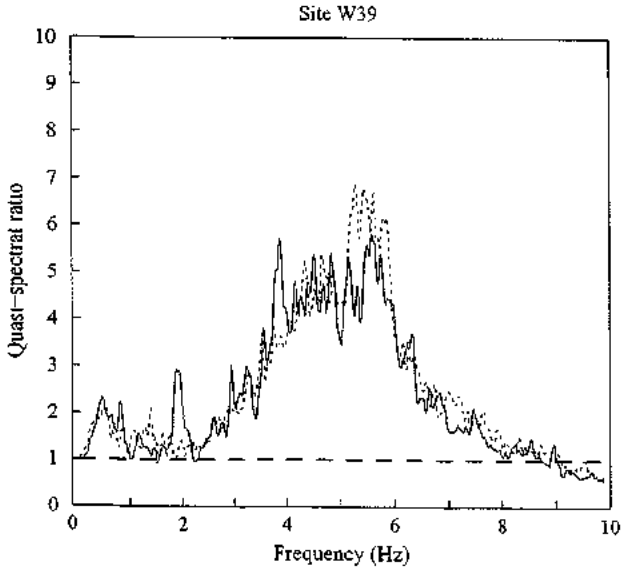

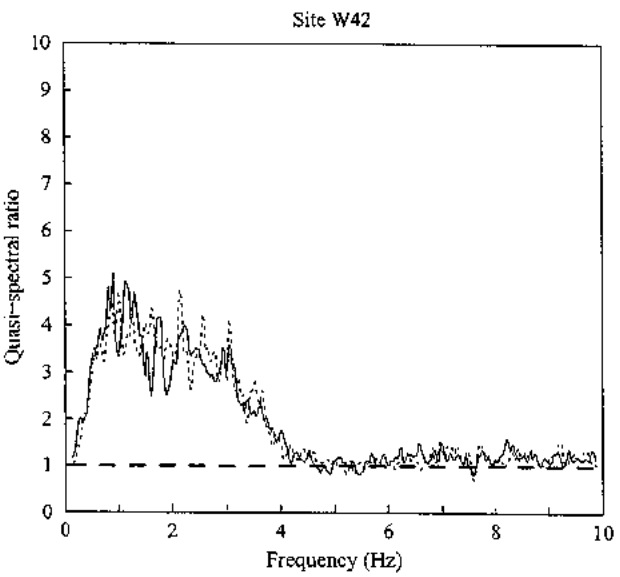

Whakatane Quasi-Spectral Ratios

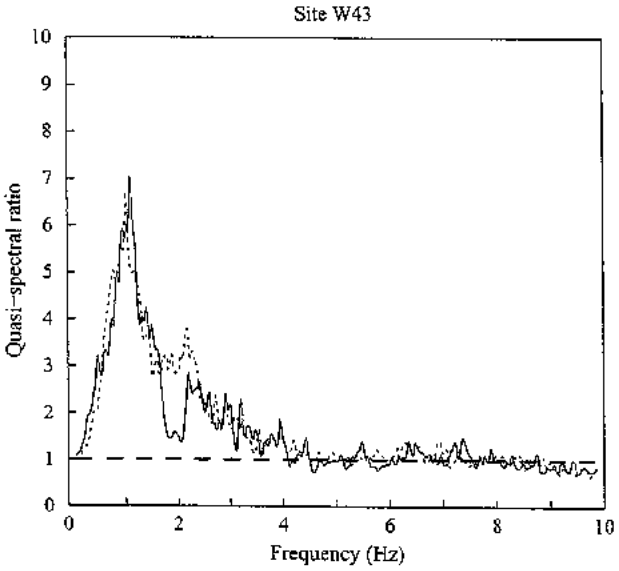

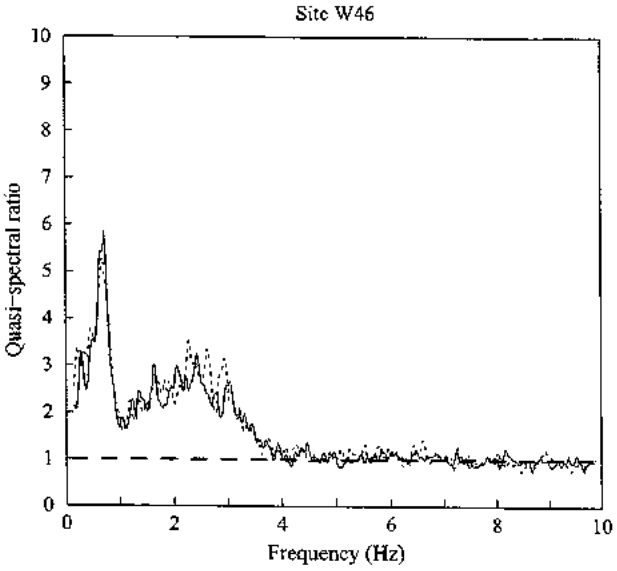

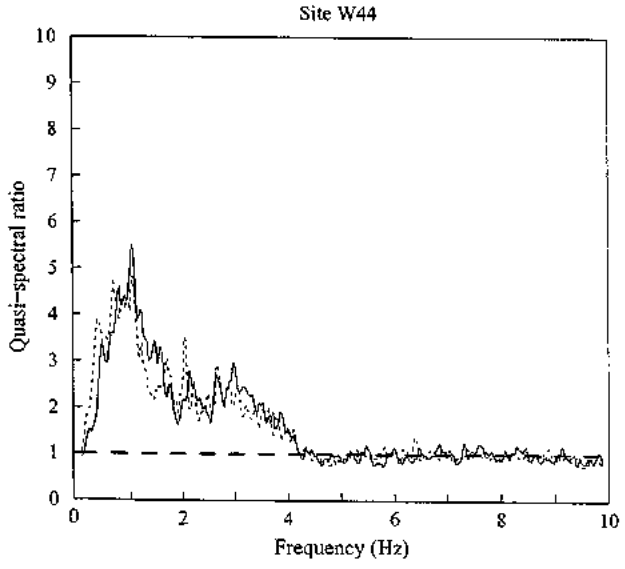

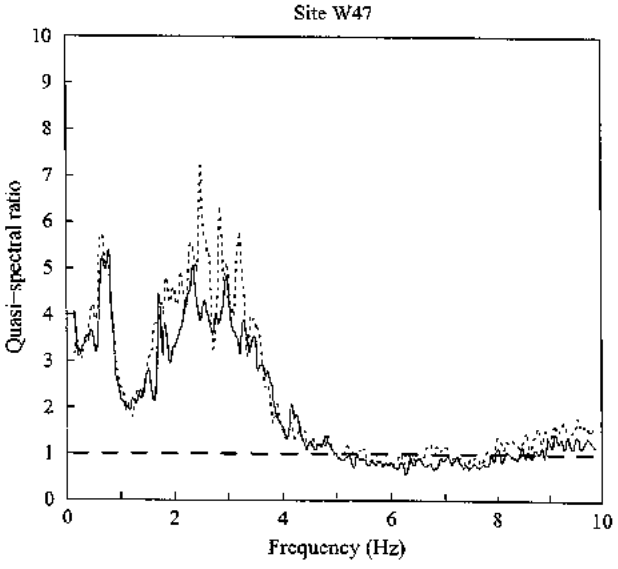

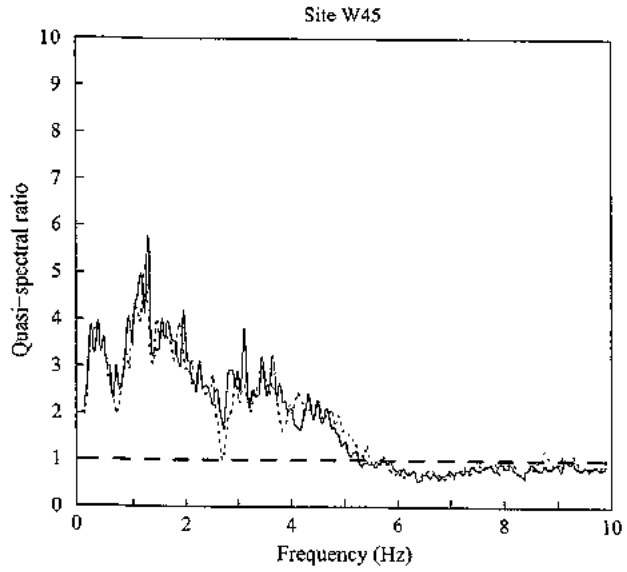

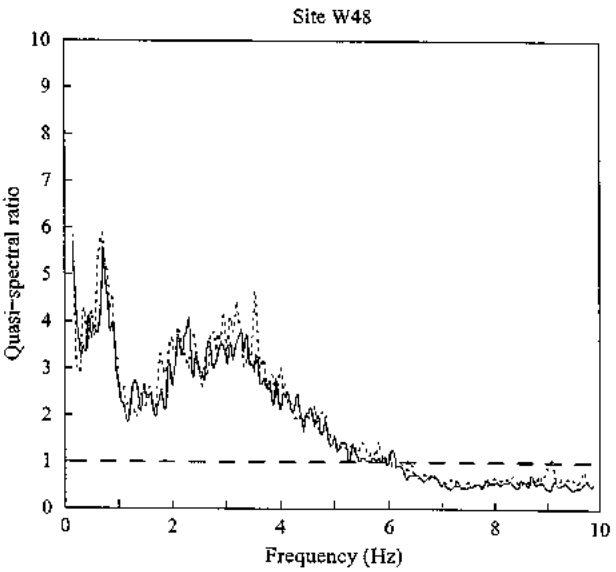

Whakatane Quasi–Spectral Ratios

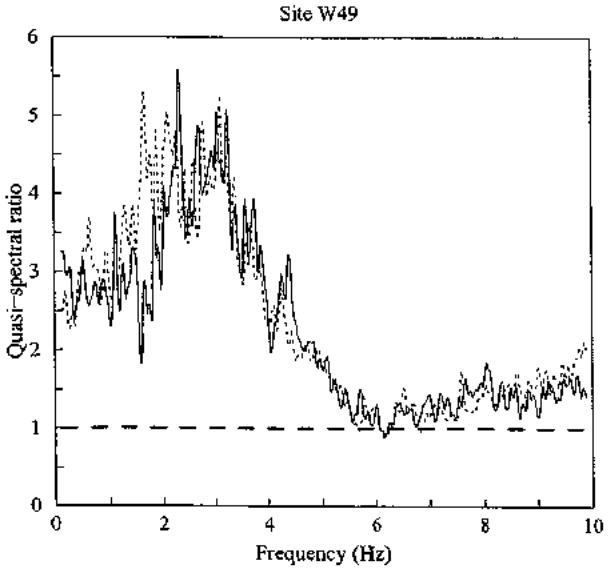

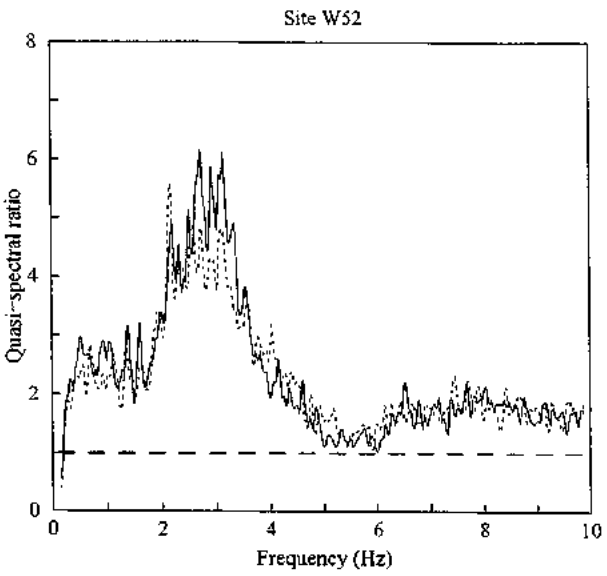

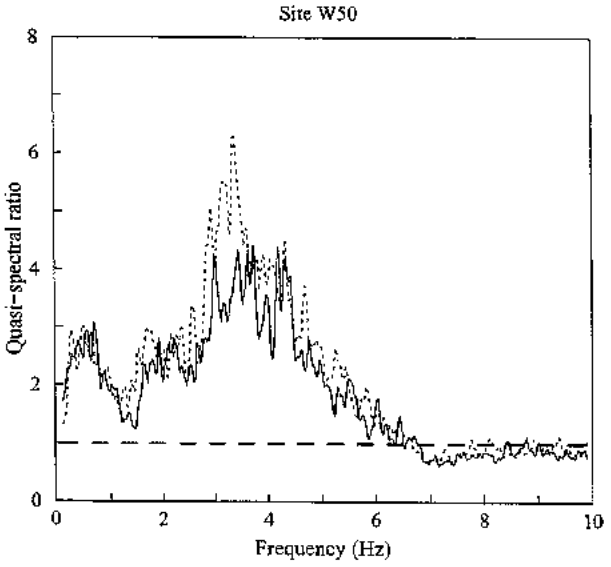

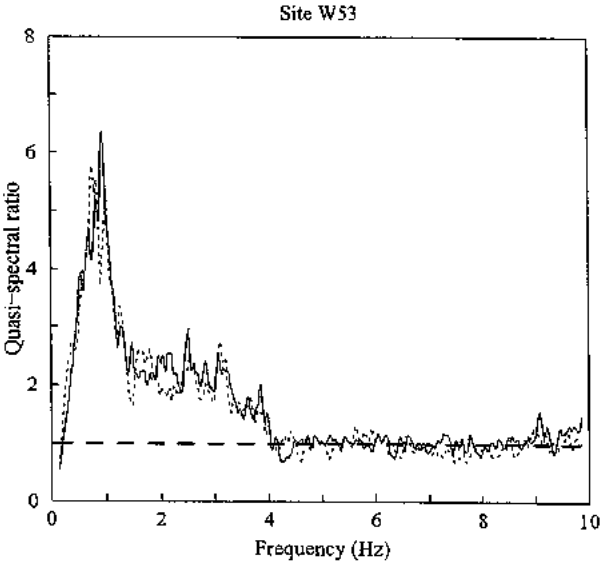

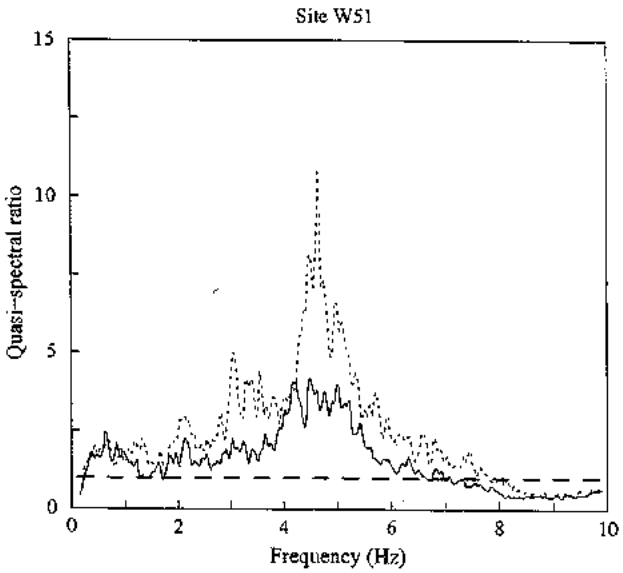

Whakatane Quasi–Spectral Ratios

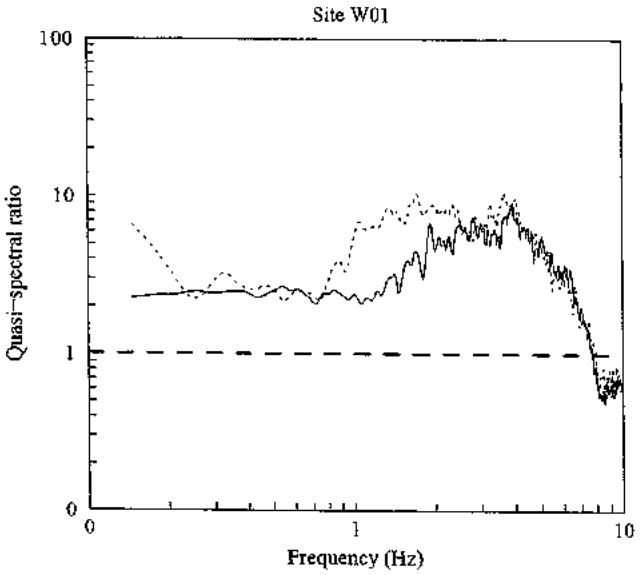

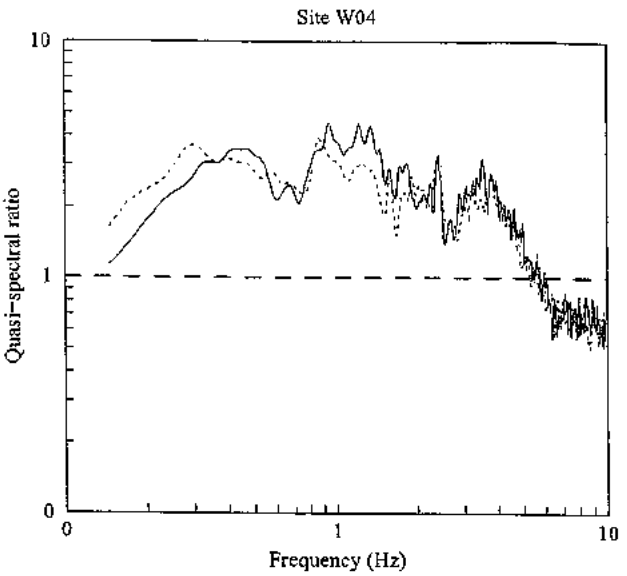

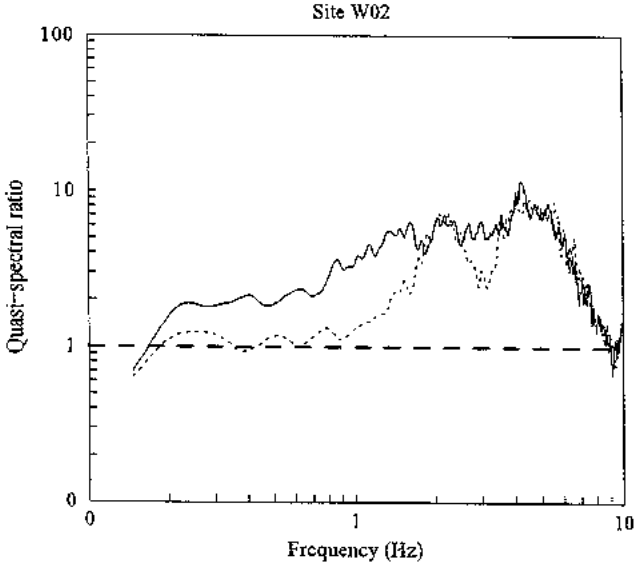

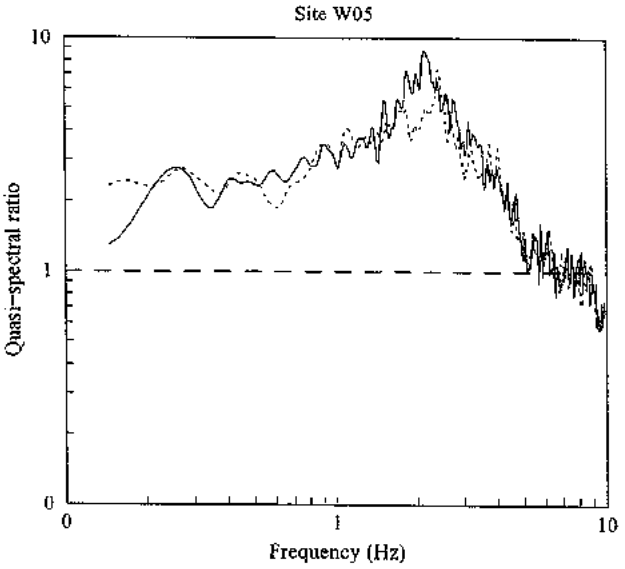

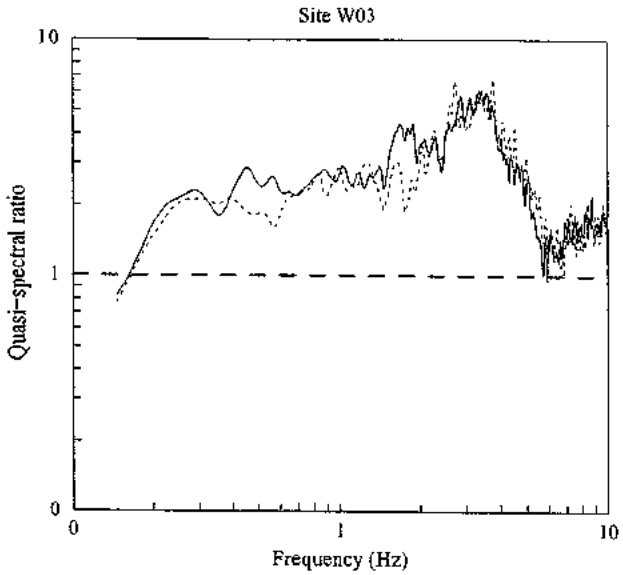

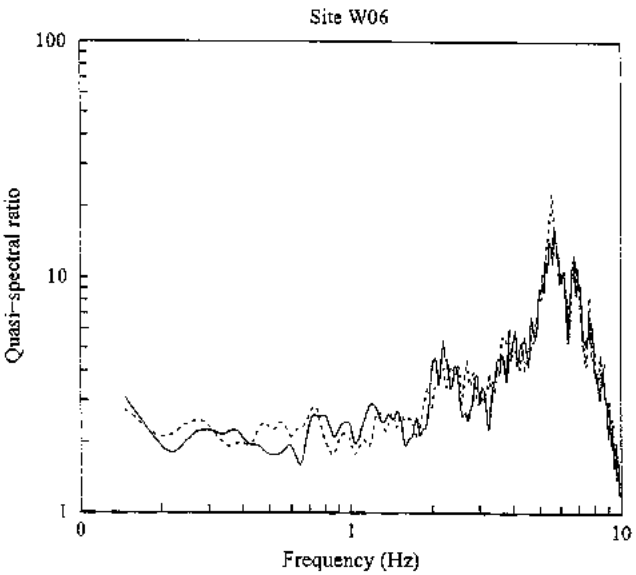

Whakatane Quasi–Spectral Ratios

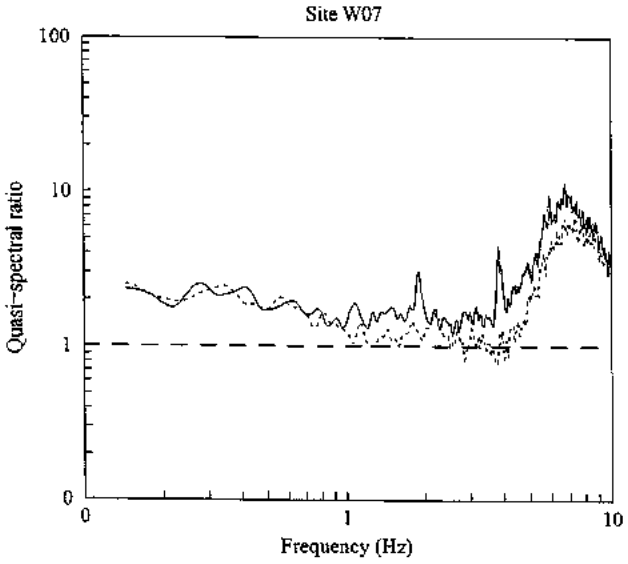

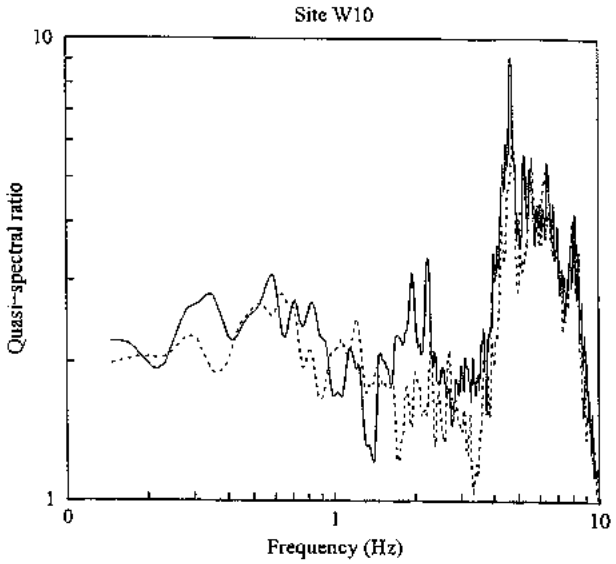

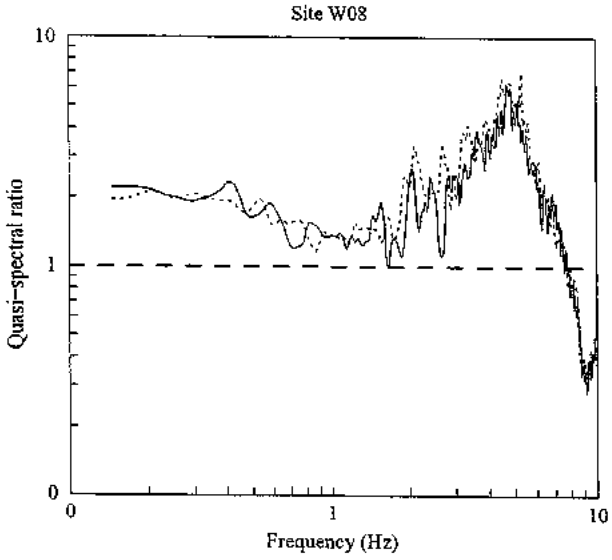

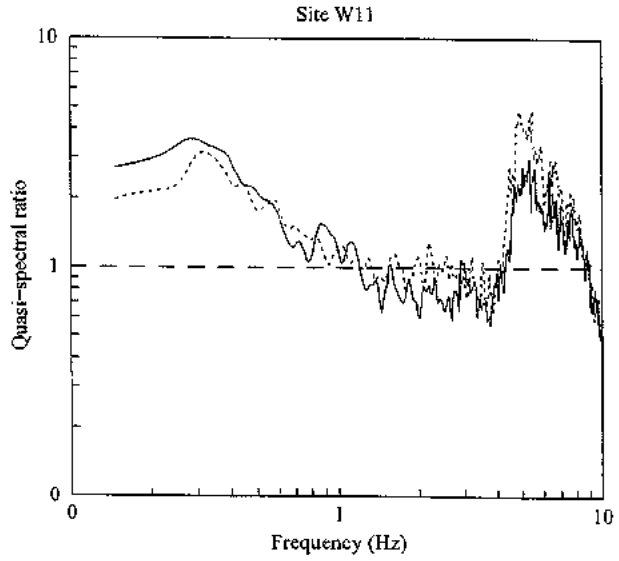

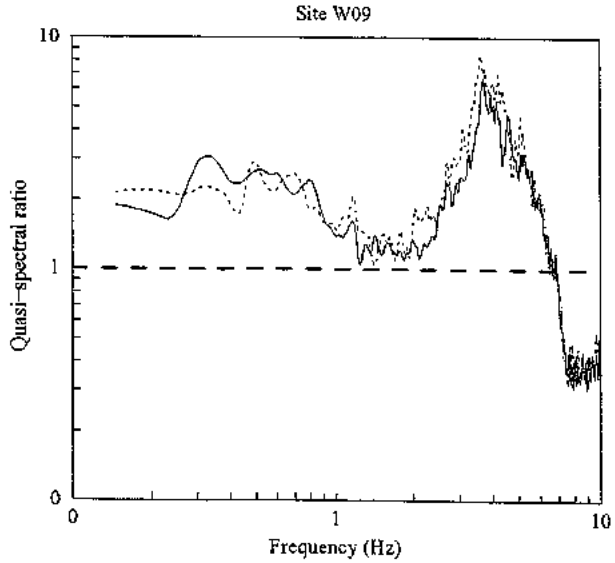

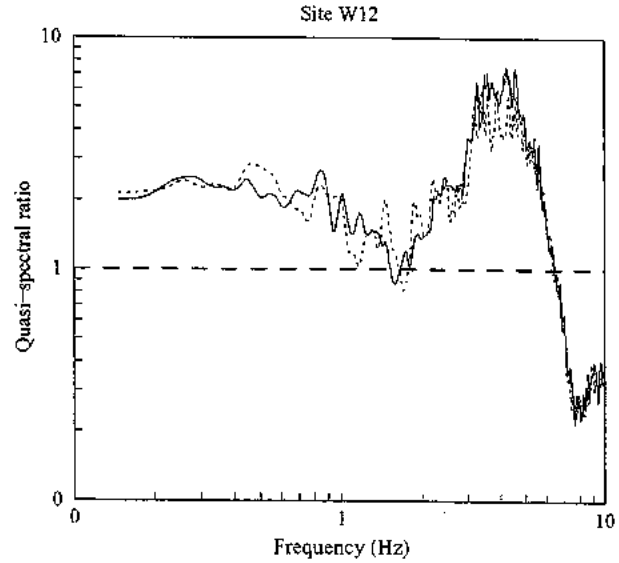

Whakatane Quasi-Spectral Ratios

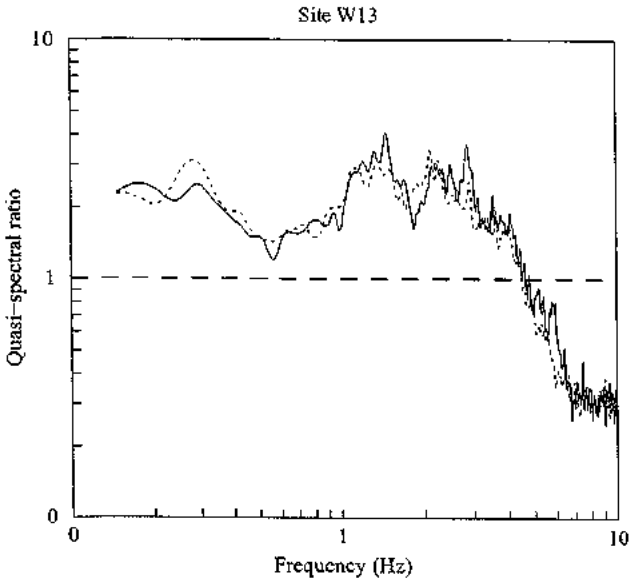

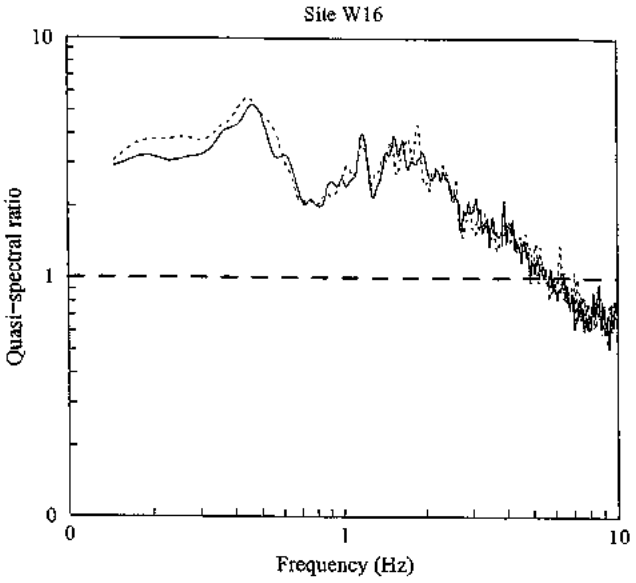

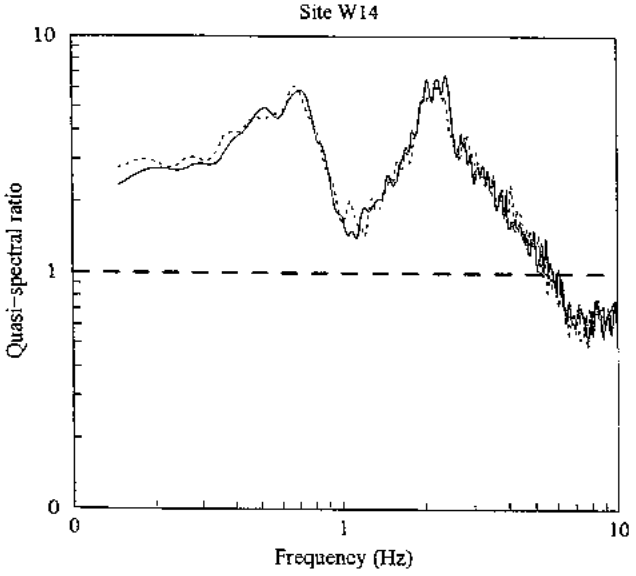

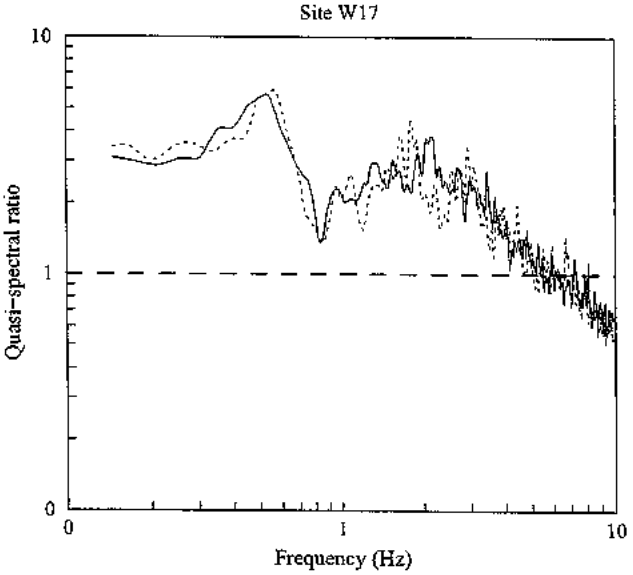

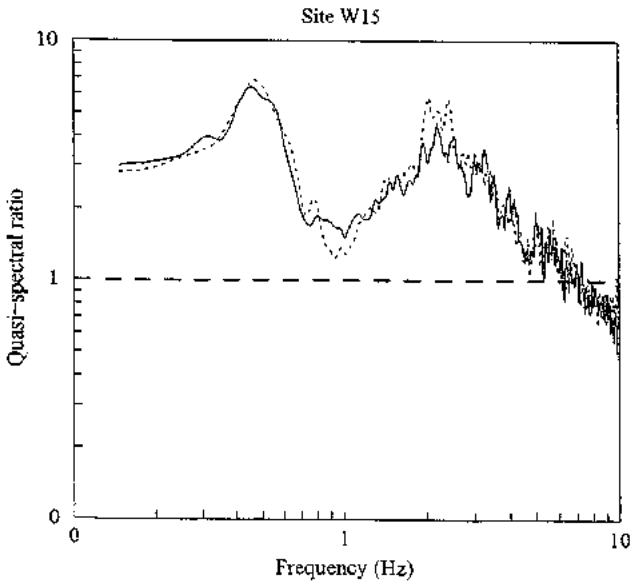

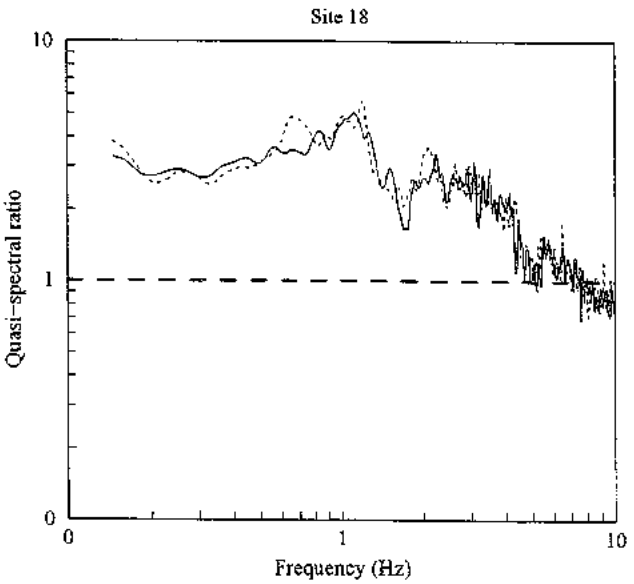

Whakatane Quasi–Spectral Ratios

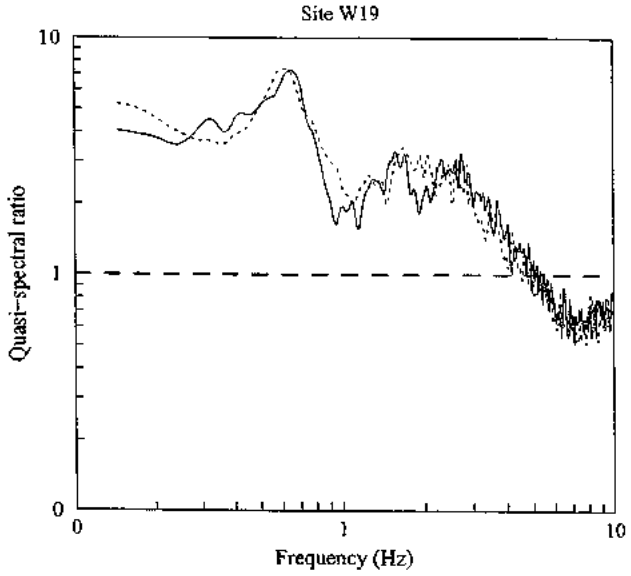

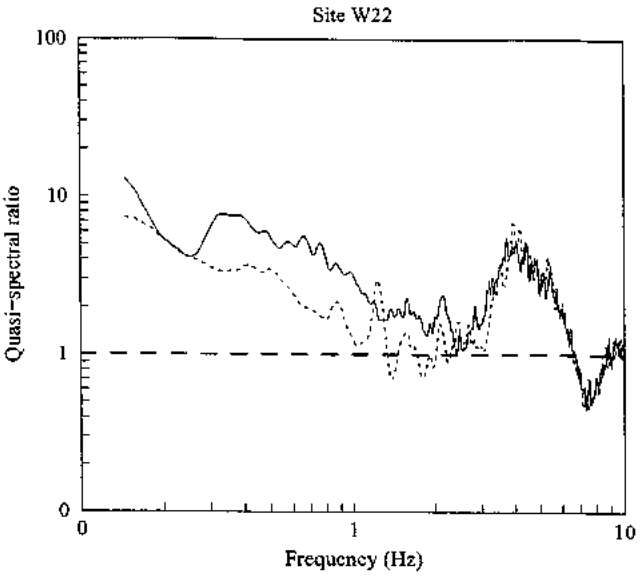

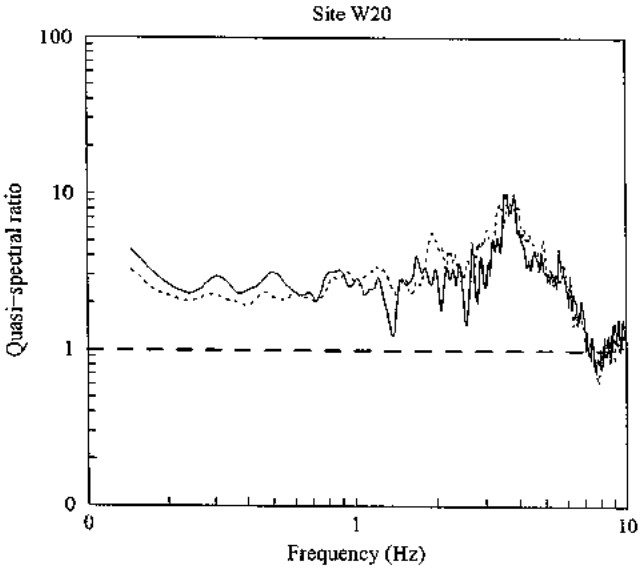

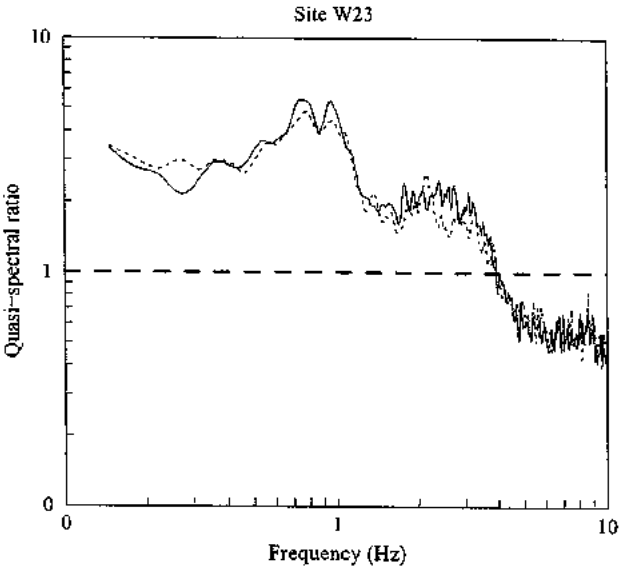

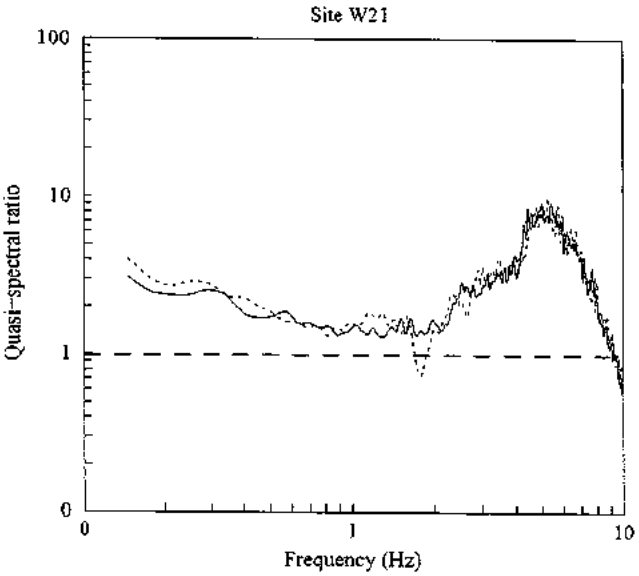

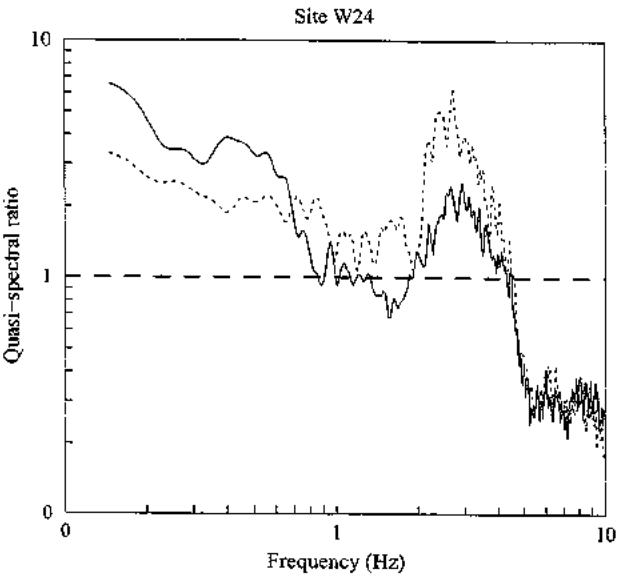

Whakatane Quasi–Spectral Ratios

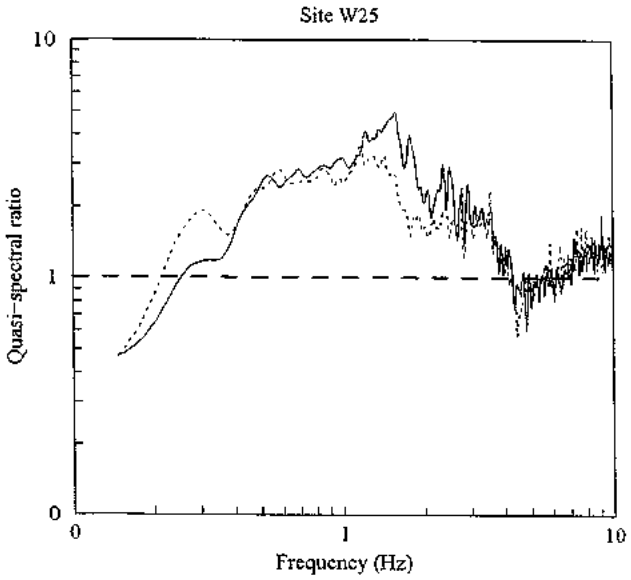

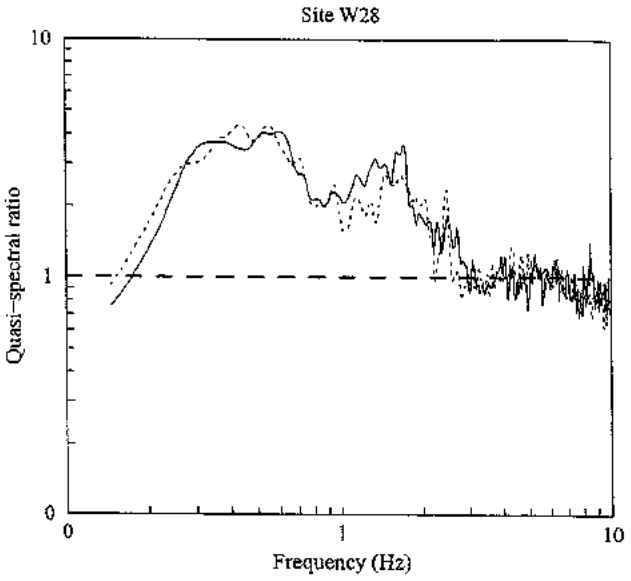

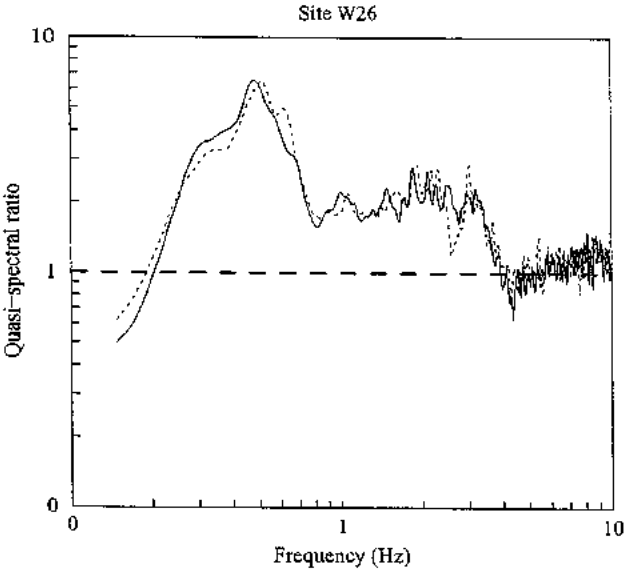

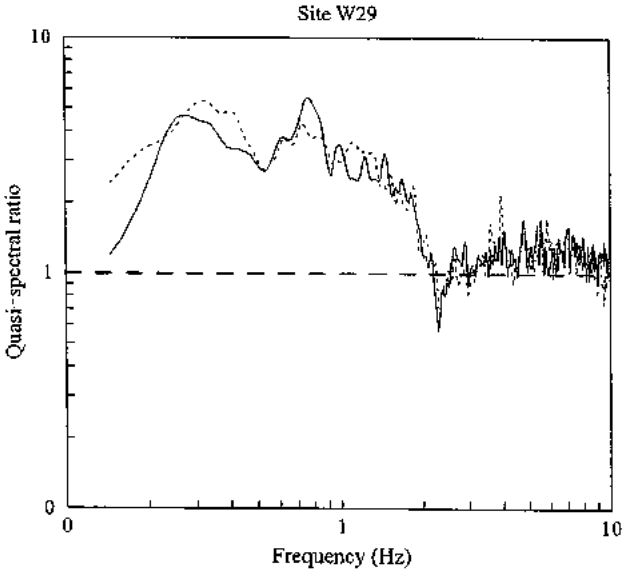

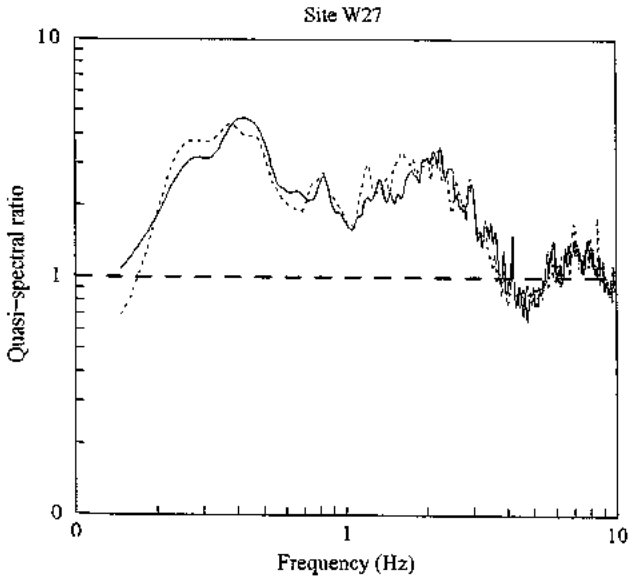

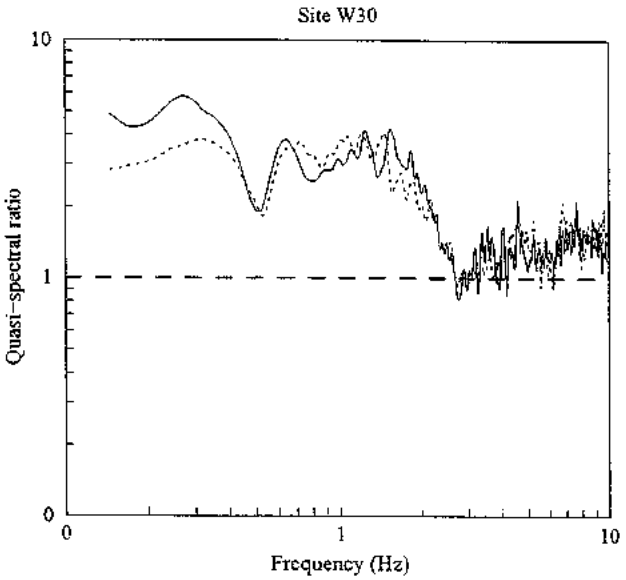

Whakatane Quasi-Spectral Ratios

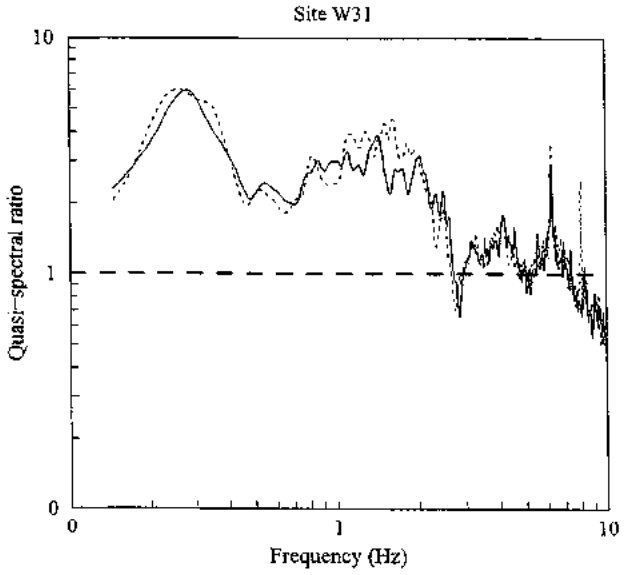

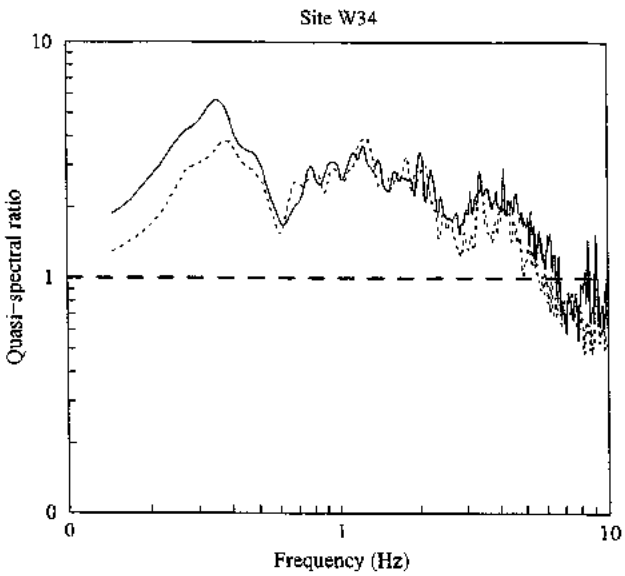

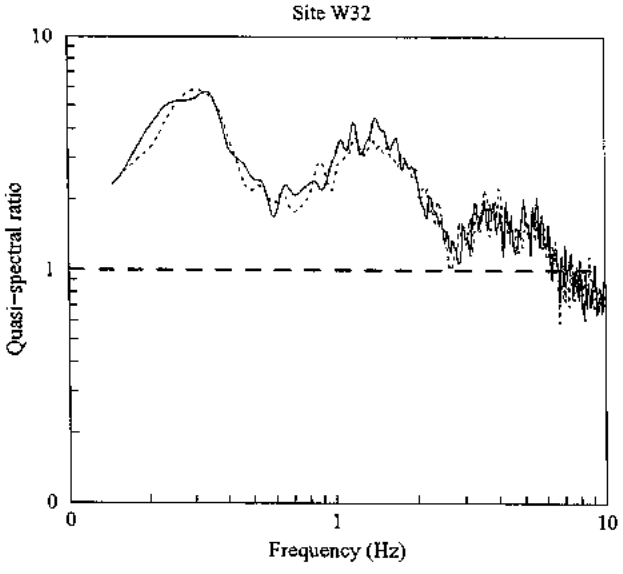

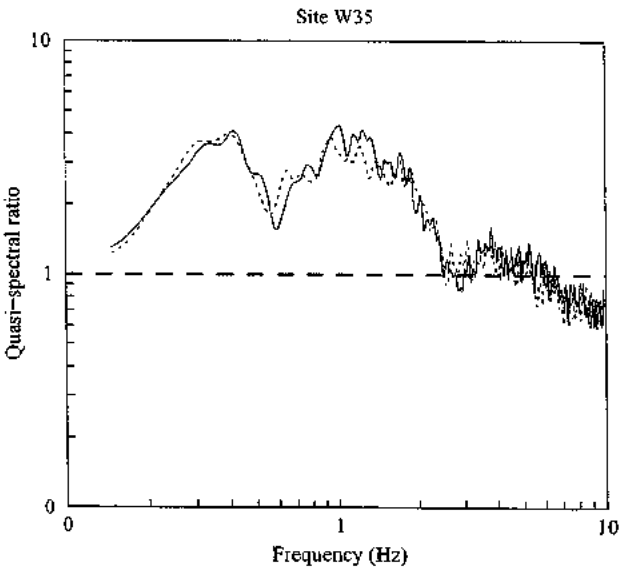

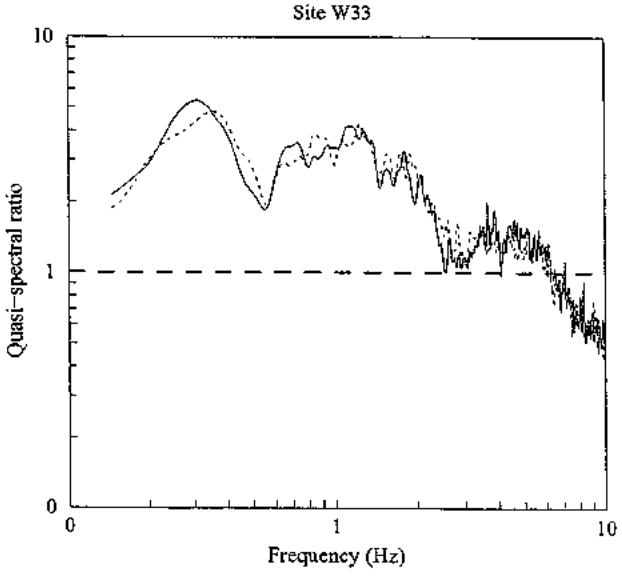

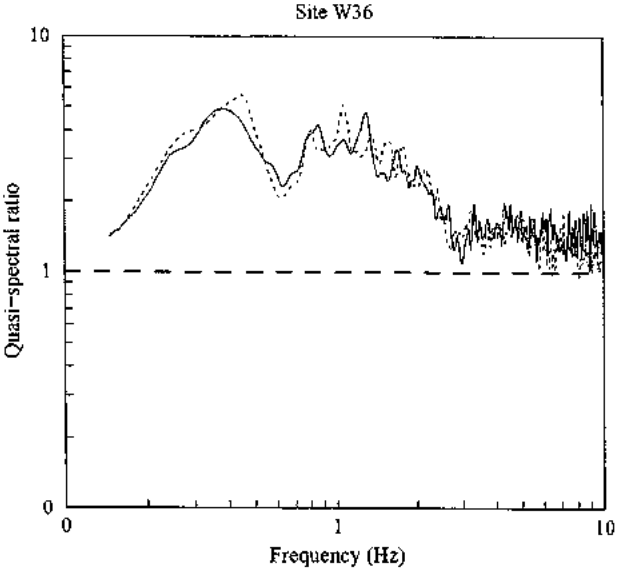

Whakatane Quasi-Spectral Ratios

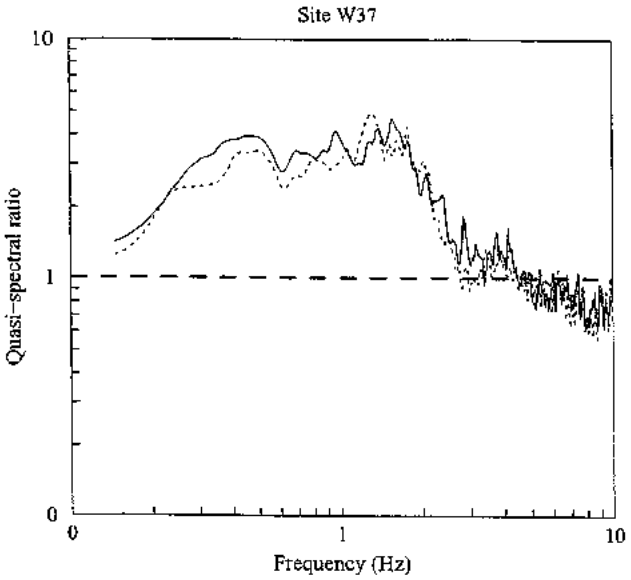

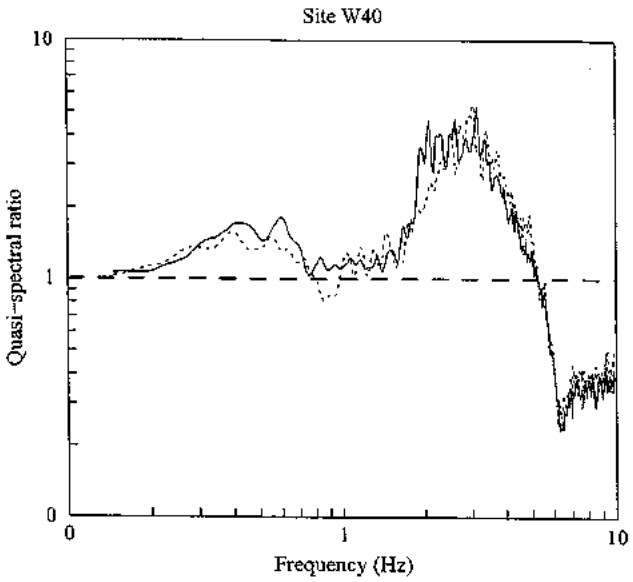

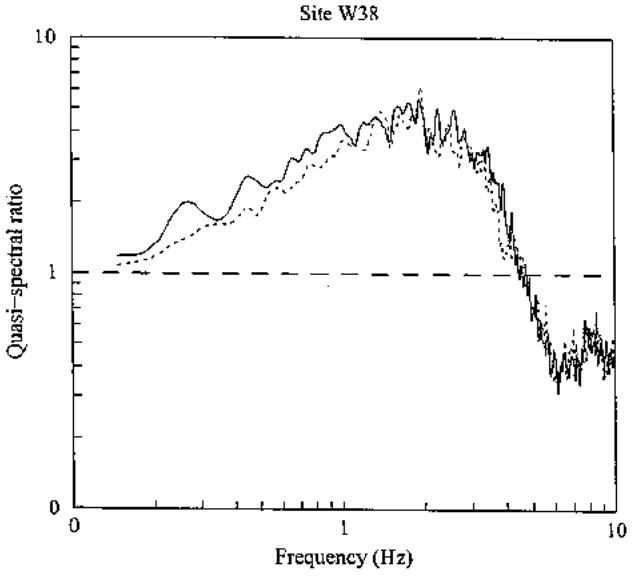

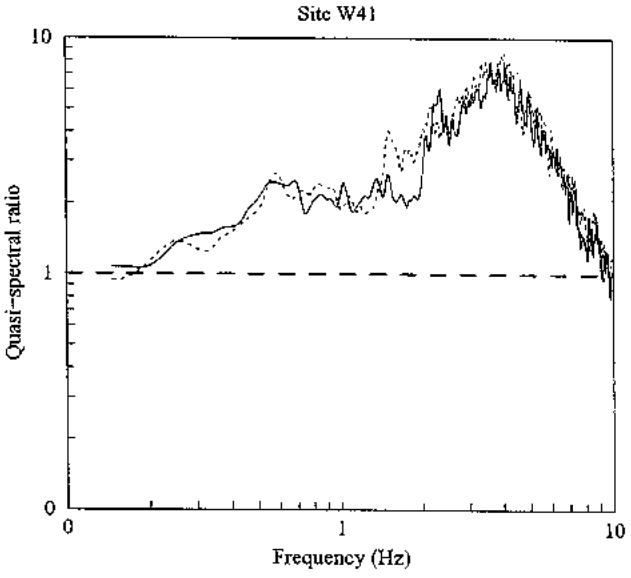

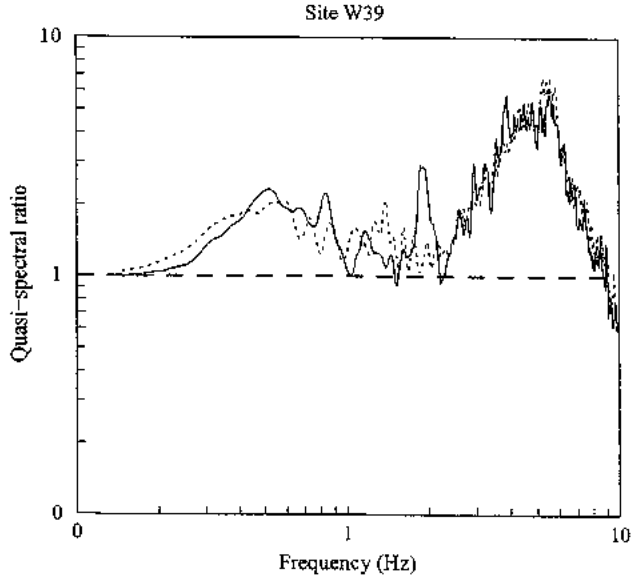

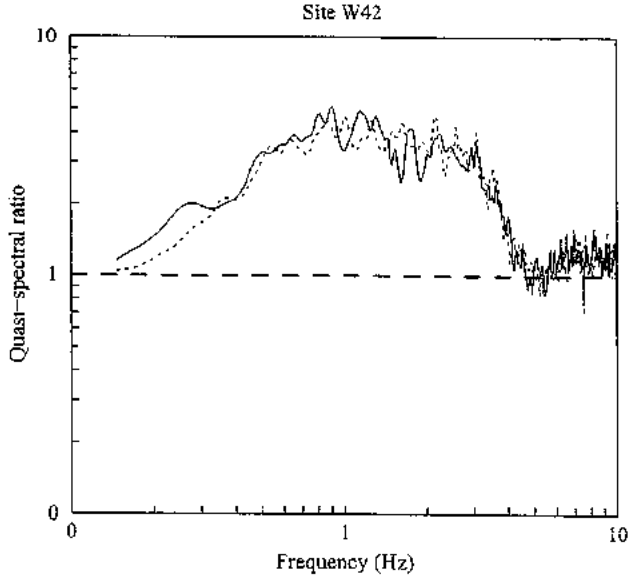

Whakatane Quasi–Spectral Ratios

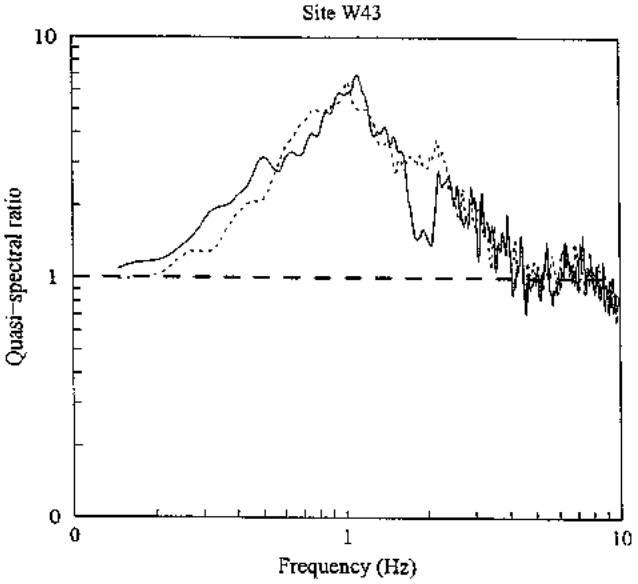

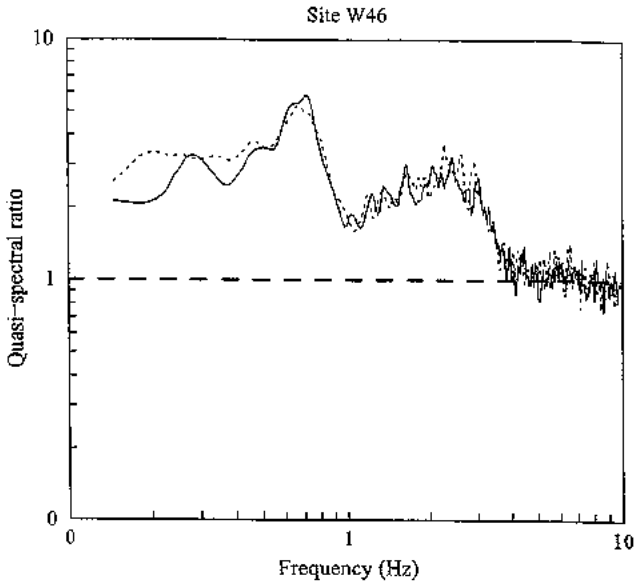

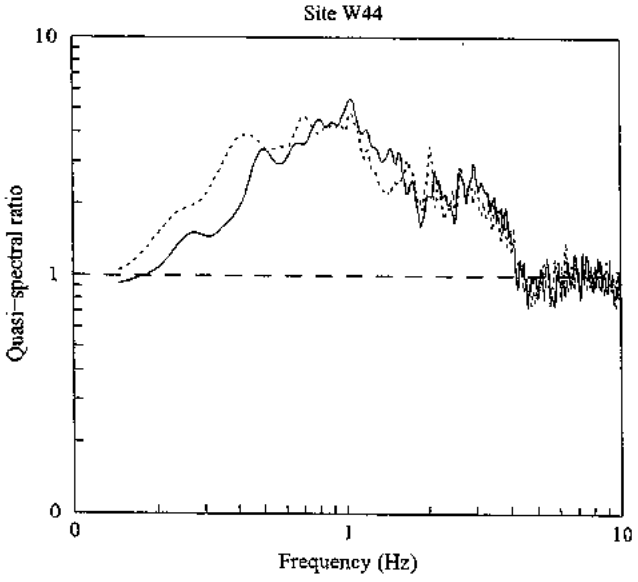

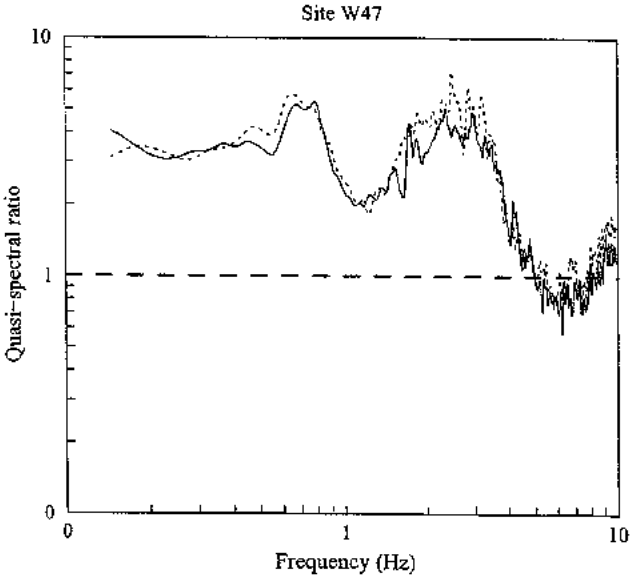

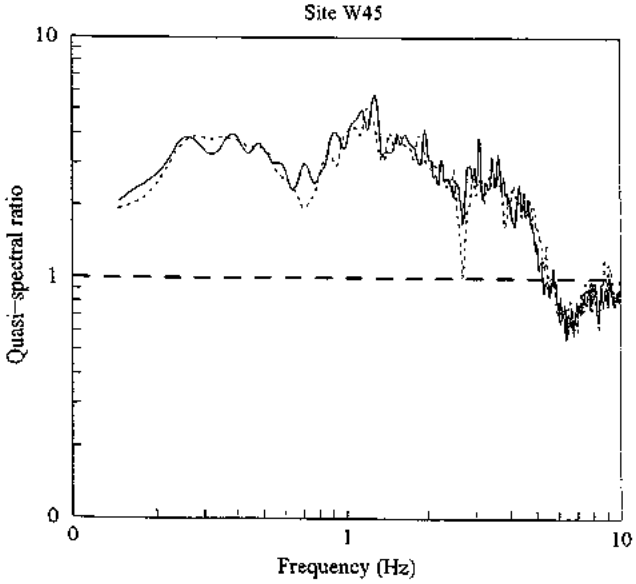

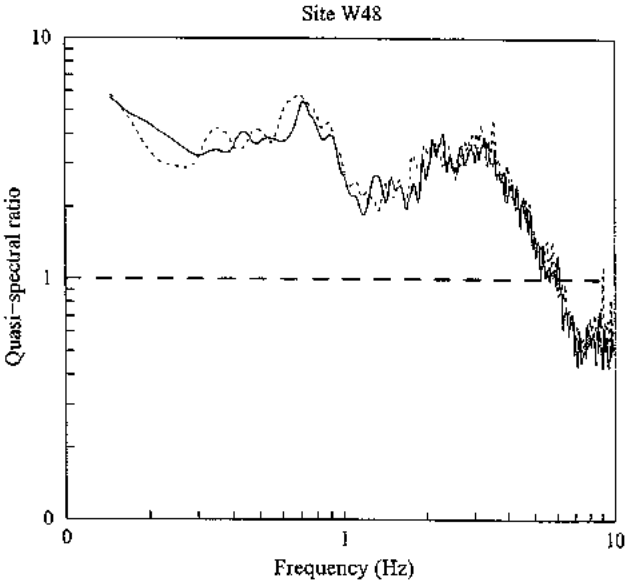

Whakatane Quasi-Spectral Ratios

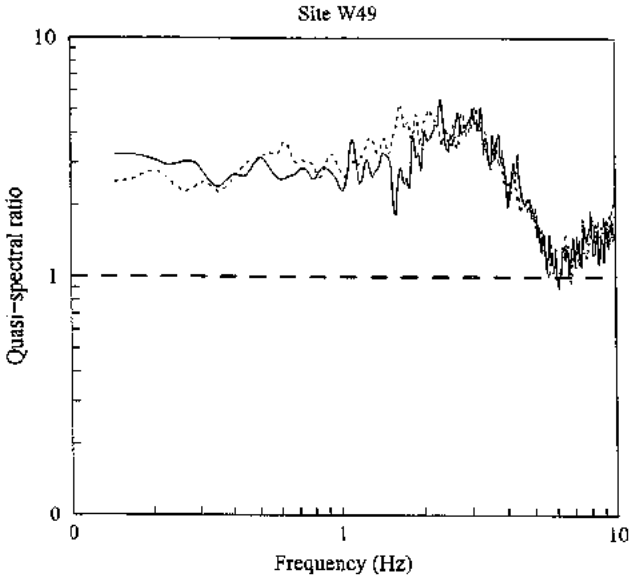

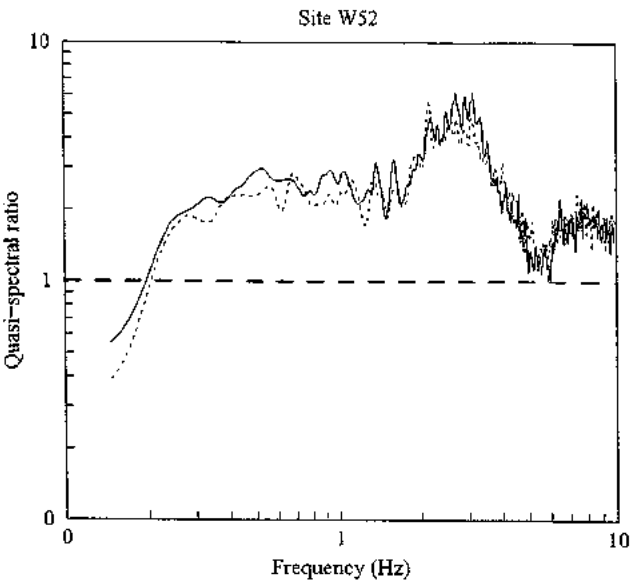

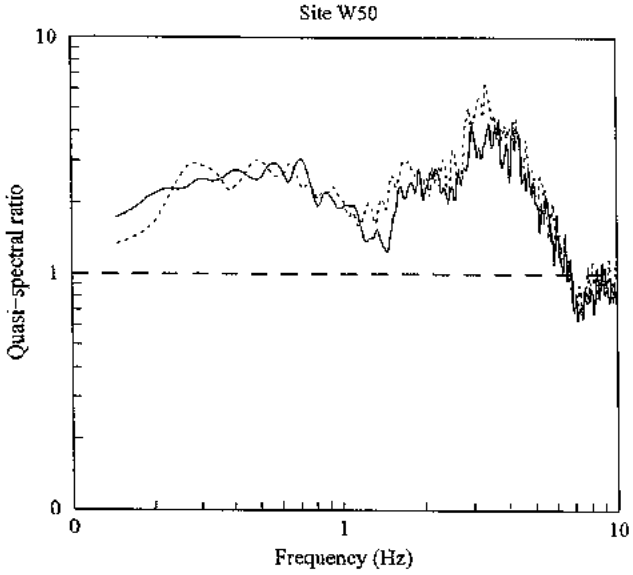

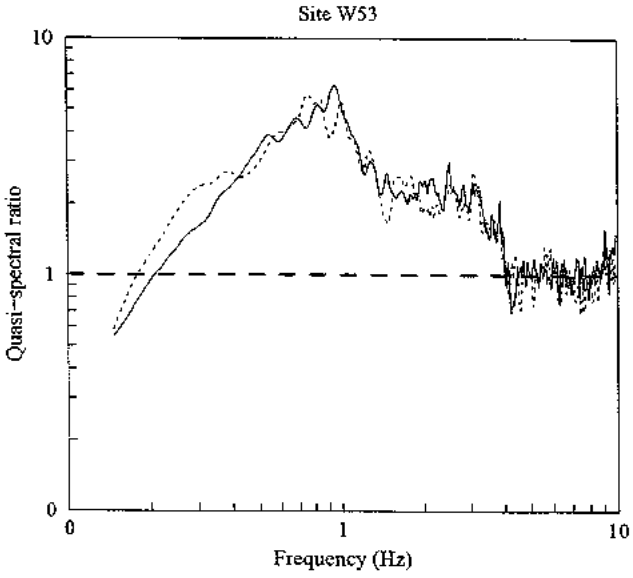

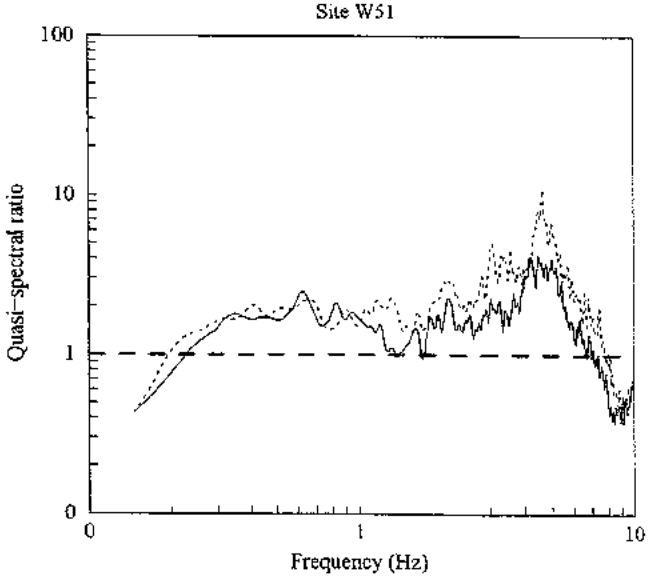

APPENDIX 3

SCPT Data

Seismic cone penetrometer and cone penetrometer results from the Whakatane urban area

CONTENTS

Data (for SCPT sites 1-8)
- Shear wave velocity profile
- Summary CPT data
  - Point Resistance
  - Friction Ratio
  - Pore Pressure
- Cone Resistance, friction ratio and sleeve friction
- Total vertical stress and effective vertical stress
- Cone resistance, dynamic pore pressure ratio and dynamic pore pressure
- Dynamic pore pressure, soil behaviour type and in-situ pore pressure
- Total cone resistance, total friction ratio, total sleeve friction and pore pressure ratio
- Normalised cone resistance, pore pressure ratio and normalised friction ratio
- Effective cone resistance
- Nett cone resistance, pore pressure ratio and excess pore pressure
- Relative density
- Internal friction angle and undrained shear strength
- Soil behaviour type index
- Equivalent SPT N60 value

For Rex Morpeth Park site (SCPT site 9)
- Shear wave velocity profile
- Summary CPT data
  - Point Resistance
  - Friction Ratio

1.0 SUMMARY

The Institute of Geological & Nuclear Sciences (GNS) has been commissioned by Environment Bay of Plenty to undertake a study of the earthquake shaking response and amplification potential of soils within the Whakatane urban area. As part of that study GNS commissioned a series of eight piezocone (CPTU) and seismic cone penetrometer (SCPT) probes that were done by Perry Drilling under the supervision of Barker Consulting. Previous CPT/SCPT probing work in the Whakatane area has been described by Barker (1995) and summary results of that work is also included here.

This appendix describes the methodology used in the acquisition of CPTU and SCPT data and the results of processing the data using standard procedures. SCPT probing enables the potential resonance at a site to be evaluated. The equipment and methods used for CPTU tests have been fully described in Stephenson and Barker (1989) and the equipment and methods used for SCPT tests have been fully described in Barker and Stephenson (1991), but a brief outline is given below.

The earthquake-amplifying behaviour of a soft site is primarily controlled by the shear wave velocity profile of the site. This primary control is modified by the lateral extent of the soft deposit, and by the soil type. A wide basin extent can lead to long duration shaking and a cohesionless soil can greatly reduce amplification.

2.0 EQUIPMENT AND METHODS

2.1 Cone Penetration Test (CPT/CPTU)

Cone penetrometry (CPT) is a well-established method of investigating soft or weak soil sites, and is described by Sanglerat (1972) and by Lunne et al (1997). A further refinement has been the addition of seismic sensing by Robertson et al (1986).

Cone penetrometry measurements can be expressed in terms of classification charts, which attempt to characterise the properties of soils on the basis of their tip resistance and side friction values. Although classification charts do not provide an accurate prediction of soil type based on grain size distribution they can provide a guide to soil behaviour type. CPT data do provide a repeatable index of the aggregate behaviour of the in situ soil in the immediate vicinity of the cone.

In general, dense fine granular sand and silt soils produce high cone resistance and low side friction while soft clay soils produce low cone resistance and high side friction. Organic soils tend to produce very low cone resistance and very high side friction and sensitive soils produce low cone resistance and low friction (Lunne et al, 1997).

Pore water pressure sensing adds useful information because the changes to porewater pressure induced as a cone moves through soils depend upon both the response of the soil fabric to shear stress and the hydraulic conductivity of the soil. It is accepted (Meigh, 1987) that the addition of a piezometer to a standard CPT cone allows better profiling of soils, but does not lead to any major improvement in identification of soils. Such a combined instrument is known as a piezocone, and tests using it are referred to as CPTU tests.

Piezocone penetrometry (Meigh, 1987) helps with the assessment of engineering parameters, particularly permeability and consolidation characteristics. One significant advantage of pore-water pressure measurements is that they offer better resolution of layers than do tip resistance or sleeve resistance measurements. This is because tip and sleeve measurements tend to integrate effects over a significant depth range whereas pore pressure measurements do not.

As a piezocone moves downwards, the measured pore-water pressure reflects the hydrostatic pressure that would be measured in the absence of any disturbance plus any pressure changes due to dilatancy effects. The pressure then tends to return to the undisturbed value as the pore fluid moves by diffusion. The resultant pressure versus depth characteristic is not easily interpreted, but general observations may be made.

Dou and Berrill (1993) state that "In layers of non-liquefiable cohesive soils, measurements of pore pressure u in the CPTU test show very high positive values, far greater than the static pore pressure u_s. In liquefiable soils, pore pressure u displays a strongly fluctuating character with a mean value that is negative or at least much lower than u_s. In non-liquefiable cohesionless soils, u is relatively stable and close to u_s." Based on this, and the fact that tip resistance and friction ratio are also related to liquefaction, piezocone measurements have been used as part of a pattern recognition system by Berrill *et al* (1995) and by Vreugdenhil (1995) to predict liquefaction potential.

The equipment and methods have been fully described in Stephenson and Barker (1989). The CPT probing at Whakatane was carried out in accordance with ASTM Standard D 5778-95.

2.2 Seismic Cone Penetration Test (SCPT)

The equipment and methods have been fully described in Barker and Stephenson (1991) and only a brief outline is given here. The seismic cone is attached to a standard CPT thrust rod and is pushed down close to the hole made by the CPT cone. A hammer blow at the surface generates a downward propagating horizontally polarised shear wave which is detected by a miniature geophone in the cone. The arrival is logged on a laptop personal computer for later processing. The process of generating and recording is repeated at 0.1m intervals.

3.0 DATA COLLECTION IN WHAKATANE

Cone penetrometry data was obtained from a number of sources. In particular cone penetrometry data was acquired from Christensen (1995) and file searching at the Whakatane District Council and Environment Bay of Plenty. This data is summarized in Table A3-1 along with data CPT investigations undertaken for this project.

Eight sites were selected for probing with a seismic cone penetrometer (SCPT) in addition to a previous site (Barker, 1995). In addition to obtaining the SCPT results normal cone penetrometer probing was also carried out at each of the 2003 sites and the results are presented here. At each site a CPTU (cone penetration test with pore water pressure measurements) was undertaken prior to the seismic test. This was undertaken by Perry Drilling Ltd using their 10 tonne Geomil equipment. The CPTU and SCPT tests were done about 0.5m apart.

4.0 RESULTS FOR WHAKATANE

4.1 CPT

The CPT data confirms the presence of a soft or weak layer in the urban area of Whakatane built on the flood plain of the Whakatane River. The data shows that this layer varies in thickness from 1 to 10 metres (usually 4-8 metres) and generally consists of fine-grained cohesionless materials (i.e. sand). By comparing the depth of the layer with the depth to the water table an assessment can be made of the likelihood of liquefaction to occurring (layers below this surface layer are generally sufficiently dense that they will not liquefy. The cone penetrometry sites are shown on Figure A3-1.

4.2 SCPT

There are three popular ways of condensing shear wave velocity profile information into a single parameter. These are to establish a site natural frequency, to establish the average shear wave velocity for the top 30m of the site (V_S30), and to establish a site NEHRP (US National Earthquake Hazard Reduction Program) category based on V_S30.The relationship between each of these, and the potential of the site to increase earthquake shaking damage, is imprecise, and it is possible to choose sites which appear identical according to these criteria, but which behave differently when shaken by earthquakes. On the one hand, a site whose velocity grades steadily downward will amplify less than a site which has a strong velocity discontinuity at depth. On the other hand, during strong shaking an non-cohesive site will amplify less than a cohesive site.

Of the nine sites (summarised in Table A3-2), three (Apanui School, Awatapu Park and Trident High School) show clear reflections from depth. A reflection implies a velocity

contrast and therefore a resonance, so natural frequencies of these sites may be assessed. It is tempting to do this by projecting the line of downward-going arrivals and the line of upward-going arrivals to their point of intersection, and taking the time of this intersection to be a quarter of the site natural period. However the waves involved may be dispersive, so that arrival times are overestimated, and natural periods erroneously increased. The approach adopted here is to construct a velocity profile using well-defined, non-dispersed arrivals in conjunction with a layer thickness derived from CPT data. Both the best-guess estimate, and the minimum value, of the site frequency are given here.

Table A3-1: Summary of cone penetrometry data from literature, files and work undertaken for this project. Site locations are shown on Figure A3-1.

Location	Figure A3-1 code	Data Source	Hole no	Water level	Soft layer	Liquefiable
Awatapu Drive	3	Beetham et al 2003	SCPT1	3	7.2	yes
James Street Loop	JSL	Christensen 1995	JSL001	1	6.2	yes
James Street Loop	JSL	Christensen 1995	JSL002	0.8	6.4	yes
James Street Loop	JSL	Christensen 1995	JSL003	1.8	8.2	yes
James Street Loop	JSL	Christensen 1995	JSL004		7.8	yes
James Street Loop	JSL	Christensen 1995	JSL005	1.9	10.3	yes
James Street Loop	JSL	Christensen 1995	JSL006		10	yes
James Street Loop	JSL	Christensen 1995	JSL007	1.2	7	yes
James Street Loop	JSL	Christensen 1995	JSL008	1.2	6.7	yes
Awatapu Park	2	Beetham et al 2003	SCPT3	3	5	yes
Hospital	4	Beetham et al 2003	SCPT4	3	6	no
Hospital	HSP	Christensen 1995	HSP001	>4.0	3.5	no
Hospital	HSP	Christensen 1995	HSP002	>4.0	2.8	no
Hospital	HSP	Tonkin & Taylor, 1988	CP1	4.4	3	no
Hospital	HSP	Tonkin & Taylor, 1988	CP2	4.4	2.6	no
Hospital	HSP	Tonkin & Taylor, 1988	CP3	4.4	3.2	no
Hospital	HSP	Tonkin & Taylor, 1988	CP4	4.4	3.5	no
Hospital	HSP	Tonkin & Taylor, 1988	CP5	4.4	2.6	no
Hospital	HSP	Tonkin & Taylor, 1988	BH1	4.4		no
St Joseph School	5	Beetham et al 2003	SCPT5	3	2.4	no
Warren Park	8	Beetham et al 2003	SCPT6	3	3.8	no
Apanui School	7	Beetham et al 2003	SCPT7	3	3.4	no
Peace Park	9	Beetham et al 2003	SCPT8	3	7.8	yes
Pumping Station	SPS	Christensen 1995	SPS001	1.4	8.3	yes
Trident High School	1	Beetham et al 2003	SCPT9	3	10.5	yes
Whakatane Pony Club	WPC	Christensen 1995	WPC001	2.4	8.6	yes
Whakatane Pony Club	WPC	Christensen 1995	WPC002	2.2	8.3	yes
Whakatane Pony Club	WPC	Christensen 1995	WPC003	1.9	6.8	yes
Whakatane Pony Club	WPC	Christensen 1995	WPC004	4	7.6	yes
Rex Morpeth Park	6	Barker 1995	SCPT11	?	4	no
Landing Road Bridge	LRB	Christensen 1995	LRB001		5.4	yes
Landing Road Bridge	LRB	Christensen 1995	LRB002		4.8	yes
Landing Road Bridge	LRB	Christensen 1995	LRB003		6.1	yes
Landing Road Bridge	LRB	Christensen 1995	LRB004		6.5	yes
Landing Road Bridge	LRB	Christensen 1995	LRB005		7.3	yes
Landing Road Bridge	LRB	Christensen 1995	LRB006		6.5	yes
Landing Road Bridge	LRB	Christensen 1995	LRB007	1	6.3	yes
Landing Road Bridge	LRB	Christensen 1995	LRB008/9		6.5	yes
Landing Road Bridge	LRB	Christensen 1995	LRB010		6.1	yes
Landing Road Bridge	LRB	Christensen 1995	LRB011		5.3	yes
Landing Road Bridge	LRB	Christensen 1995	LRB012		8.1	yes
Landing Road Bridge	LRB	Christensen 1995	LRB013		7.5	yes
New World	NW	Tonkin & Taylor, 2002				yes
Strand Development	SD	Tonkin & Taylor, 2002	1	2.5		yes
Strand Development	SD	Tonkin & Taylor	2	2.1		yes
Strand Development	SD	Tonkin & Taylor	3	2.1		yes
Strand Development	SD	Tonkin & Taylor	4	2.1		yes
Strand Development	SD	Tonkin & Taylor	5	dry		no
Strand Development	SD	Tonkin & Taylor	6	1.8		yes
Strand Development	SD	Tonkin & Taylor	CP4	2	6.5	yes
Strand Development	SD	Tonkin & Taylor	CP5	2	5.5	yes
Strand Development	SD	Tonkin & Taylor	CP6	2	6	yes
Strand Development	SD	Tonkin & Taylor	CP11	2	6	yes
Whakatane DC	WDC	Murray-North			6	yes
EBOP	EBOP	BH Consultants	CPT1		5	yes
EBOP	EBOP	BH Consultants	CPT2		4	yes
EBOP	EBOP	BH Consultants	CPT3		5	yes
EBOP	EBOP	BH Consultants	CPT4		1	no
EBOP	EBOP	BH Consultants	CPT5		5	yes
EBOP	EBOP	BH Consultants	CPT6		4	yes

Table A3-2: Derived ground class for the SCPT sites using NHERP, NZ code (site period (SP) or geological model (GM)) and Nakamura results (from this study).

Site No.	Site natural frequency (Hz) (Reciprocal ground period (seconds))			Shear wave velocity (m/s) for V_s30			Ground Class Code from various sources				
	Min	Pre-dicted	Max	Min.	Av.	Max.	NHERP	NZ code		Naka-mura	Selected
								GM	SP		
1	1.45 (0.69)	1.66 (0.60)		168	176	185	E	D	C/D	C/D	**D**
2	1.44 (0.70)	1.94 (0.52)		156	197	232	D	D	C	D	**D**
3			2.90 (0.34)				D	D		D	**D**
4			3.70 (0.27)				D	D		D	**D**
5			6.60 (0.15)				D	C		D	**D**
6							C	C		C	**C**
7	1.84 (0.54)	2.58 (0.38)		151	217	283	D	C	C	C	**C**
8		2.00 (0.50)		152	199	238	D	C	C	D	**D**
9		3.20 (0.31)		120	240	370	C	C	C	C	**C**

The minimum value is based upon the possibility that a strong line of reflections may define a boundary below the CPT-indicated boundary. It is obtained by assuming that the layer-propagation time is where the downward-going and upward-going arrival lines intersect. The maximum value for V_S30 is assessed by assuming infinite velocity below the measured value, and the minimum value for V_S30 by assuming the velocity in the deepest layer is continued to 30 metres. However, the best guess is given by assuming a velocity of 500m/s below either the "basement" or the greatest SCPT depth if no "basement" is defined.

Site1: Trident High School - this site is dominated by a layer of thickness 26.5m which is predicted to have a natural frequency of 1.66Hz. The minimum possible natural frequency is 1.45 Hz. 168m/s < V_S30< 185m/s (176m/s when 500m/s is assumed in the "basement"). NEHRP category E on the basis that the velocity in the top layer is close to the bounding value of 180m/s, and unlikely to be sufficiently stiff for the remaining 12m to push it to D.

Site 2: Awatapu Park - this site is dominated by a layer of thickness 18m which is predicted to have a natural frequency of 1.94Hz.The minimum possible natural frequency is 1.44Hz. 156m/s < V_S30< 232m/s (197m/s when 500m/s is assumed in the "basement").NEHRP category D on the basis that the velocity in the top layer is close to the bounding value of 180m/s, and unlikely to be sufficiently stiff for the remaining 12m to push it to C.

Site 7: Apanui School – this site is dominated by a layer of thickness 14m which is predicted to have a natural frequency of 2.58Hz.The minimum possible natural frequency is 1.84Hz. 151m/s < V_S30< 283m/s (217m/s when 500m/s is assumed in the "basement"). NEHRP

category is D on the basis that the velocity in the top layer is close to the bounding value of 180m/s, and likely to be sufficiently stiff for the remaining 16m to push it from E to D.

Two other sites (Warren Park and Peace Park) each have a surface layer which is well constrained by CPT data, and for which the likely resonant frequency and NEHRP category may be calculated.

Site 8: Warren Park – this site is dominated by a layer of thickness 16.5m which is predicted to have a natural frequency of 2.0Hz152m/s < V_S30< 238m/s (199m/s when 500m/s is assumed in the "basement").NEHRP category D on the basis that the velocity in the top layer is close to the bounding value of 180m/s, and unlikely to be sufficiently stiff for the remaining 13.5m to push it to C.

Site 9: Peace Park – this site is dominated by a layer of thickness 8.1m which is predicted to have a natural frequency of 3.2Hz120m/s < V_S30 < 370m/s (240m/s when 500m/s is assumed in the "basement").NEHRP category D or possibly C on the basis that the velocity in the top layer is close to the bounding value of 180m/s. However it could be sufficiently stiff for the remaining 22m to push it to C.

The remaining three sites (St Joseph's School, Whakatane Hospital and Awatapu Drive) do not have an SCPT reflection, nor is it clear that a clear CPT-bounded layer exists. In these circumstances it is only possible to calculate bounding values for resonant frequency and NEHRP category.

Site 3: Awatapu Drive – Between 4m and 12.5m the relatively high velocity of 204m/s, assuming it continues or increases with depth, implies a NEHRP category of D, although a substantial velocity increase below 12.5m could push the site to C.Maximum site natural frequency is 2.9Hz.

Site 4: Whakatane Hospital – Between 5m and 10.5m the velocity of 162m/s is close to the bounding value of 180m/s, implying a likely NEHRP category of D, although a substantial velocity increase below 10.5m could push the site to C. Maximum site natural frequency is 3.7Hz.

Site 5: St Joseph's School –Between 2m and 6.5m the velocity of 175m/s is close to the bounding value of 180m/s, implying a likely NEHRP category of D, although a substantial velocity increase below 6.5m could push the site to C. Maximum site natural frequency is 6.6Hz.

At Rex Morpeth Park (probed in 1995) tip resistance increased steadily with depth, and together with the accumulated side friction, prevented penetration below 7.4m. No estimate of layer thickness may be made, and there were no reflections in the SCPT trace.

Site 6: Rex Morpeth Park – the shear wave velocity of 205m/s between 5.5m and 7.4m, and the near surface shear wave velocity of 144m/s suggest that the NEHRP category is most likely C, but that D cannot be ruled out

In general the Whakatane SCPT profiles indicate that amplification of earthquake shaking should be taken seriously, with many of the sites being comparable with the lower Hutt Valley. However none of the sites approaches the extreme nature of Wainuiomata or the Valley of Mexico.

5.0 REFERENCES

Barker, P.R., 1995:

Barker, P.R., and Stephenson, W.R., 1991: The seismic CPT probe as a tool for predicting seismic response of flexible sediments. *Proceedings of Pacific Conference on Earthquake Engineering, Vol 3:181-190, Auckland, New Zealand.*

Berrill, J.B., Christensen, S.A., Davis R.O., Dou Yiqiang, and Vreugdenhil, R.A. (1995): The CPTU test and liquefaction: some New Zealand Results, *Proc. IS TOKYO '95, Tokyo, pp, 917-922.*

Bruce Henderson Consultants, 1993: Environment Bay of Plenty Building geotechnical investigations; Unpublished report held on Whakatane District Council Files.

Christensen, S.A., 1995: Liquefaction of cohesionless soils in the March 2, 1987 Edgecumbe earthquake, Bay of Plenty, New Zealand, and other earthquakes. Research Report 95-1, Department of Civil Engineering, University of Canterbury, Christchurch, New Zealand.

Dou., Yiqiang and Berrill, J.B. (1993): A pattern recognition approach to evaluation of soil liquefaction potential using piezocone data. *Soil dynamics and earthquake engineering, 12(2) 91-102.*

Lunne,T., Robertson. P.K. and Powell, J.J.M. (1997): Cone testing in geotechnical practice. *London, Blackie Academic & Professional.*

Meigh, A. C. (1987): Cone penetration testing methods and interpretation. *Butterworths, London, 1987.*

Murray-North, 19??: Whakatane District Council Building geotechnical investigations; Unpublished report on Whakatane District Council Files.

Robertson, P. K., Campanella, R. G., Gillespie, D., Rice, A., (1986): Seismic CPT to measure in situ shear wave velocity, *Journal of Geotechnical Engineering,* 112 (8), p. 791-803.

Sanglerat, G. The penetrometer and soil exploration. (1972): *Amsterdam: Elsevier, 1972. 464p.*

Stephenson, W.R., and Barker, P.R., 1989: Seismic response of soil materials around Edgecumbe, Bay of Plenty, New Zealand. *New Zealand Journal of Geology and Geophysics 32:175-180.*

Tonkin and Taylor Ltd, 2002: Whakatane New World Supermarket Geotechnical Investigation; Unpublished report May 2002 (Ref: 19838.001) held on Whakatane District Council Files.

Vreugdenhil, R.A. (1995): Interpretation of piezocone data and its use in estimating seismic liquefaction potential. *PhD Thesis, University of Canterbury, Christchurch, New Zealand, 183p.*

Awatapu Drive

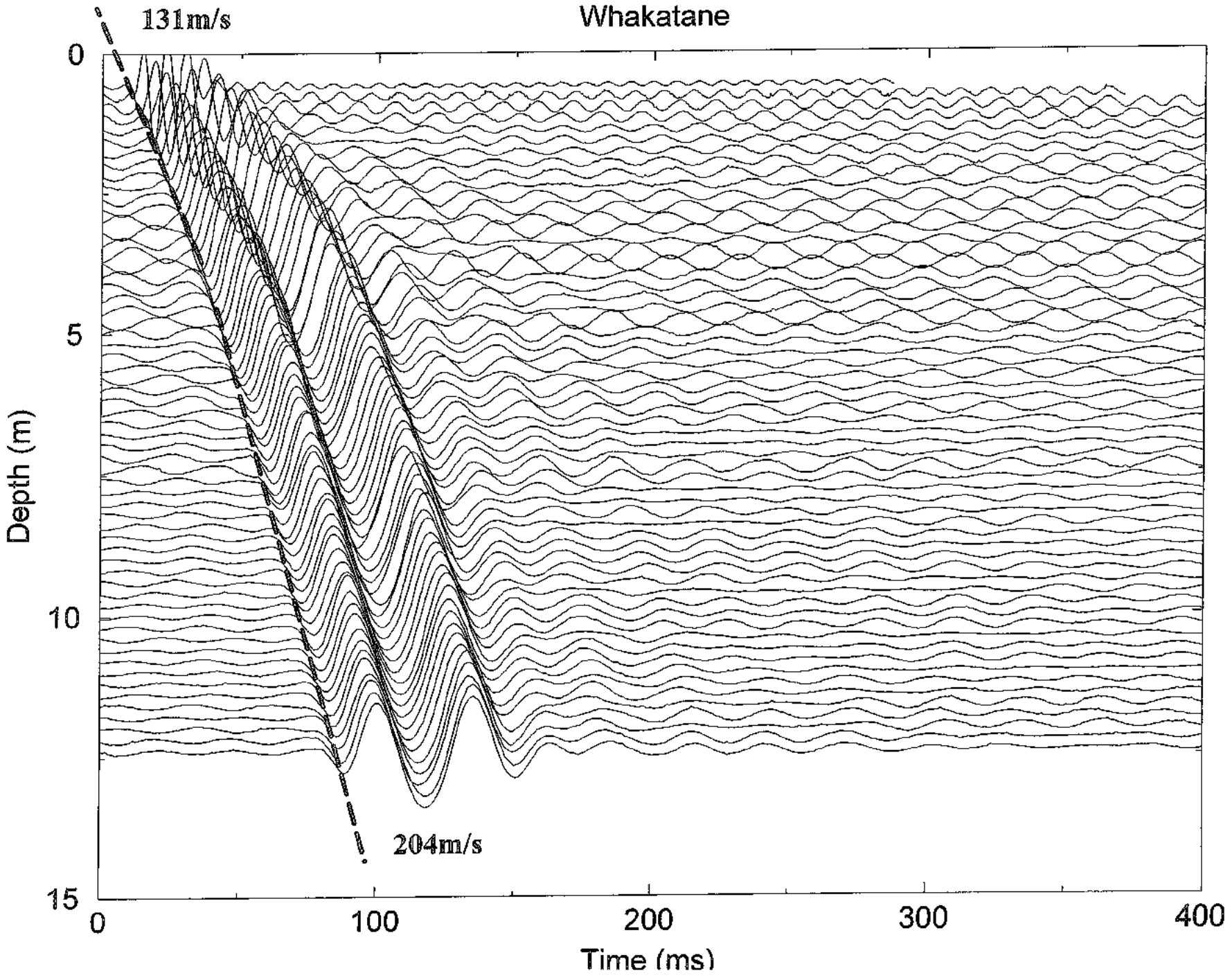

Awatapu Drive
Whakatane

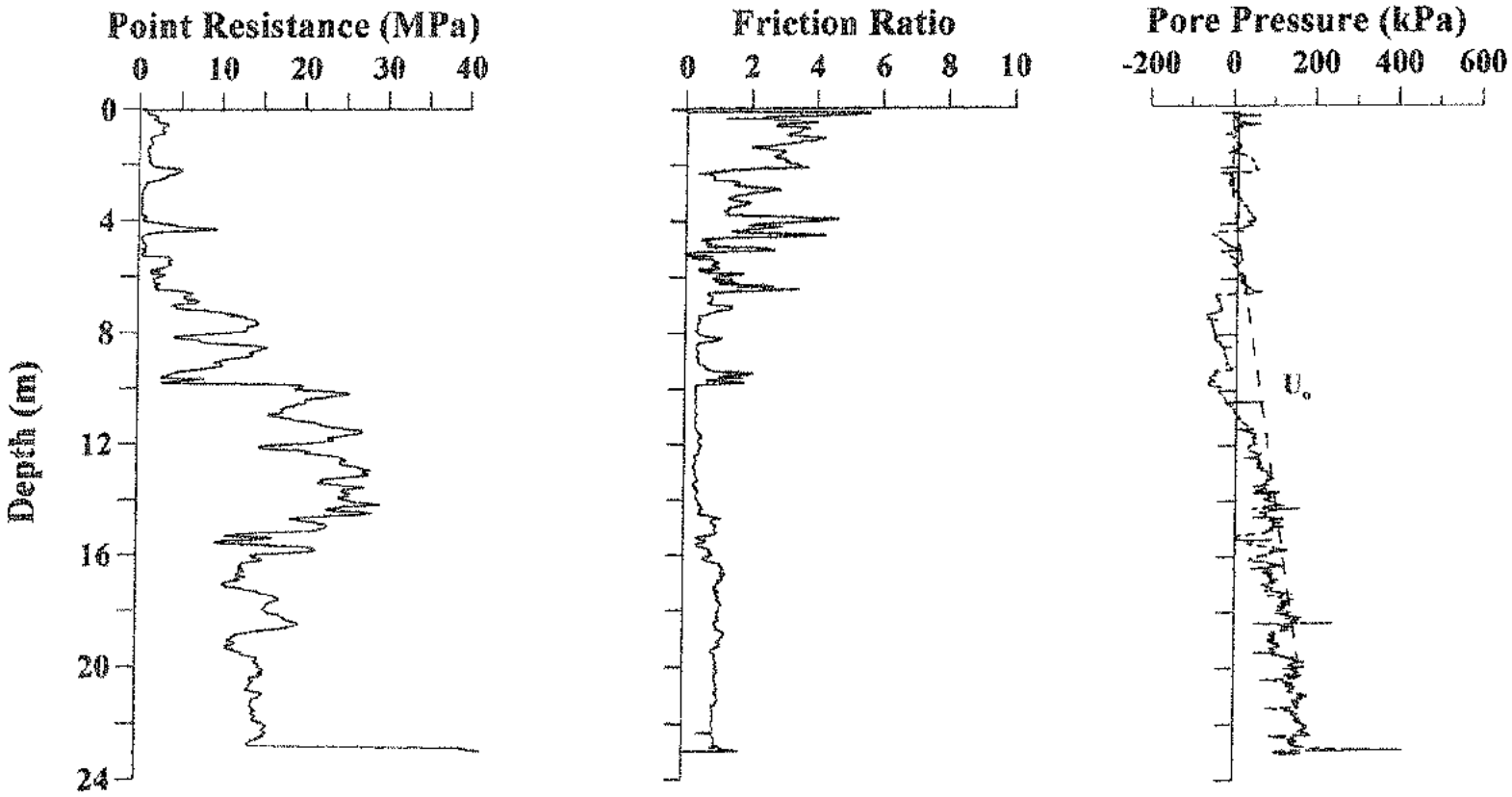

Awatapu Park

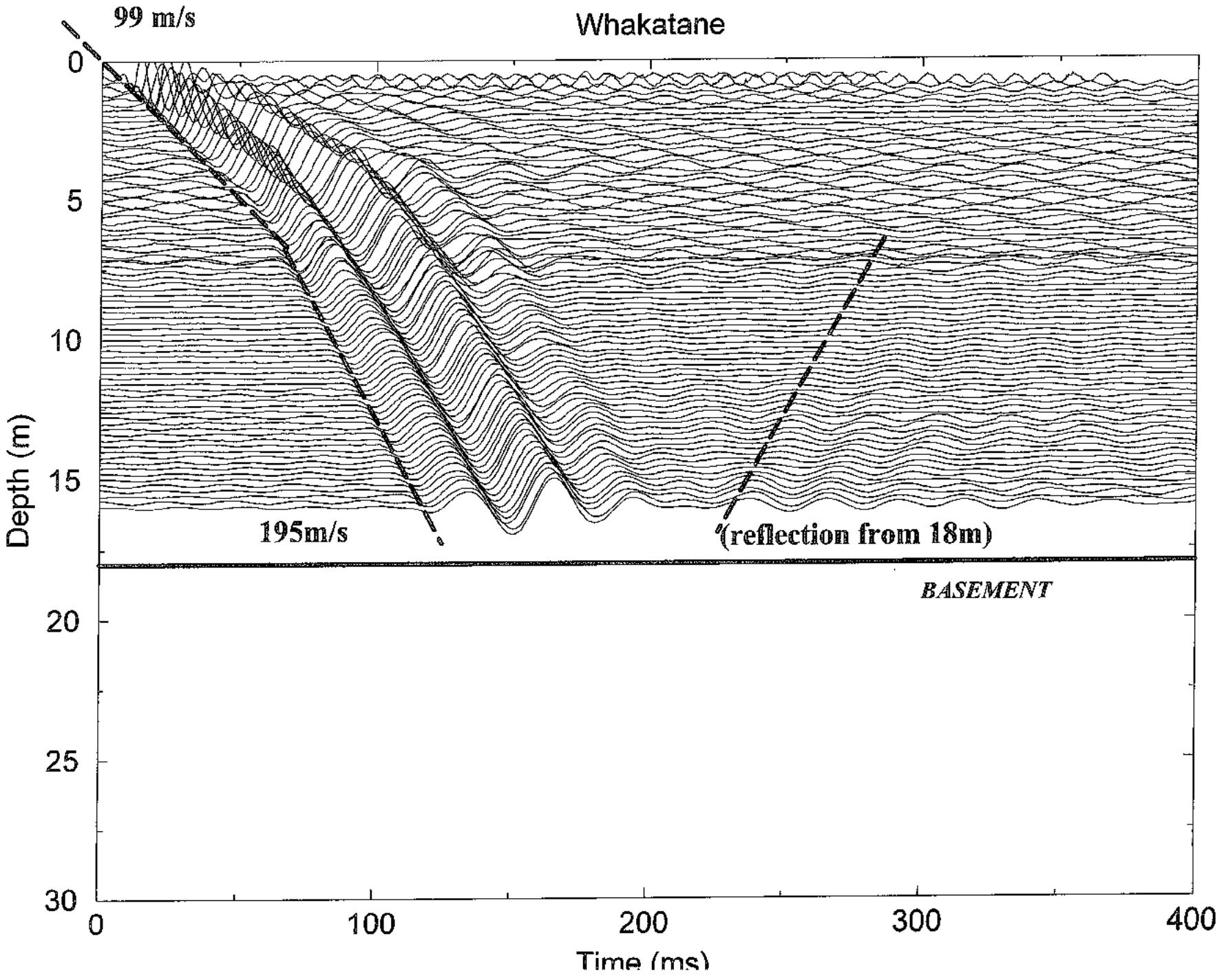

Awatapu Park
Whakatane

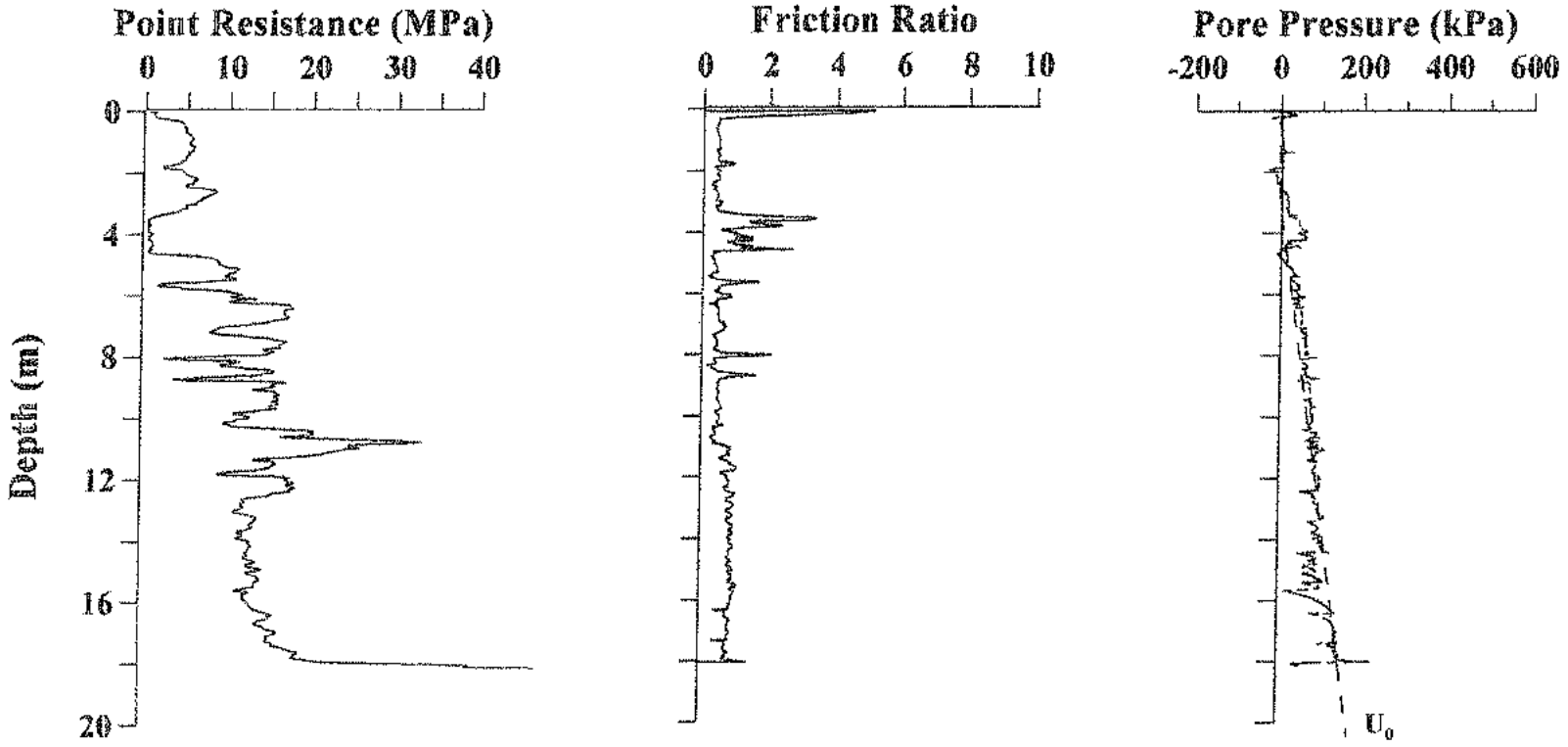

Whakatane Hospital

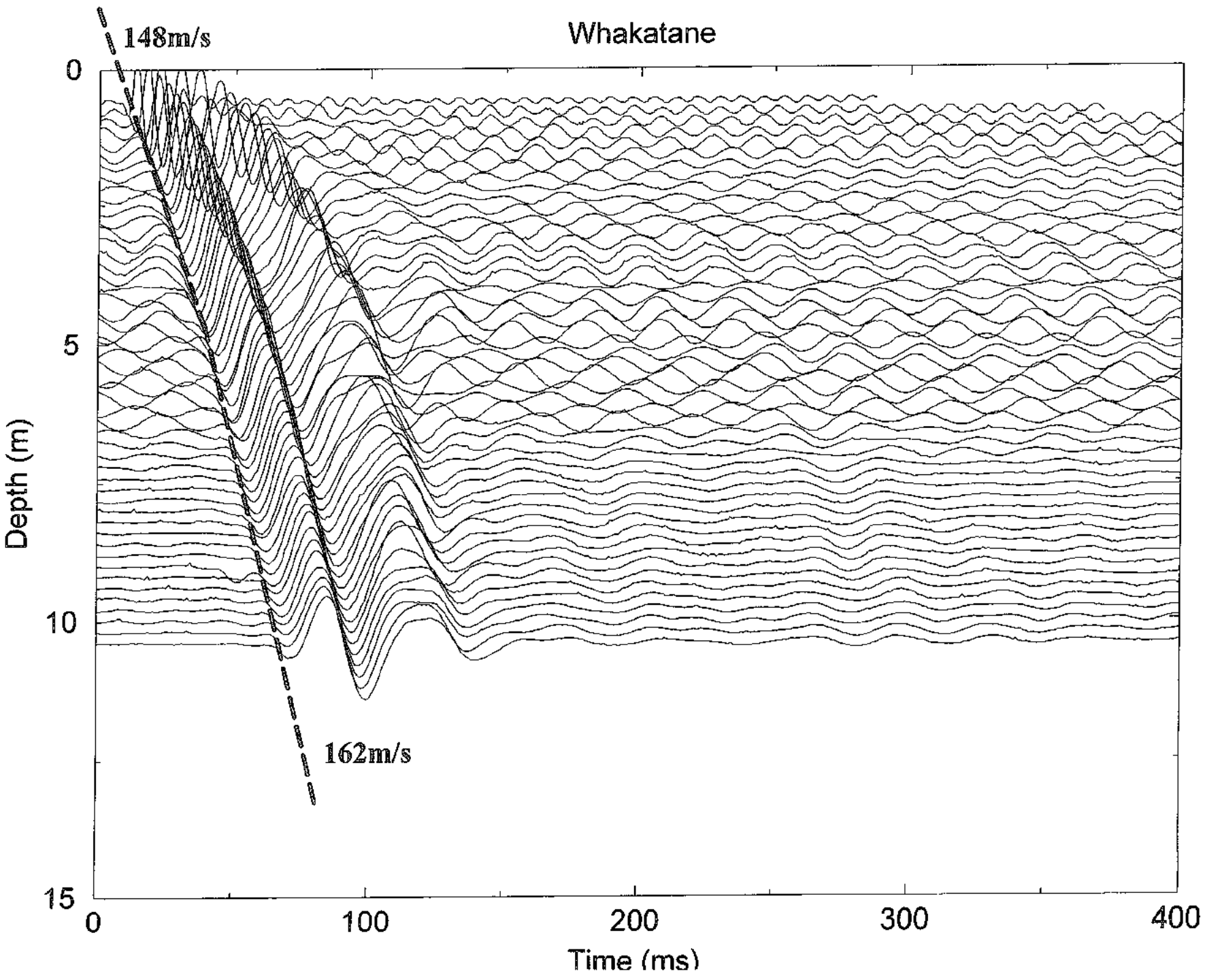

Hospital
Whakatane

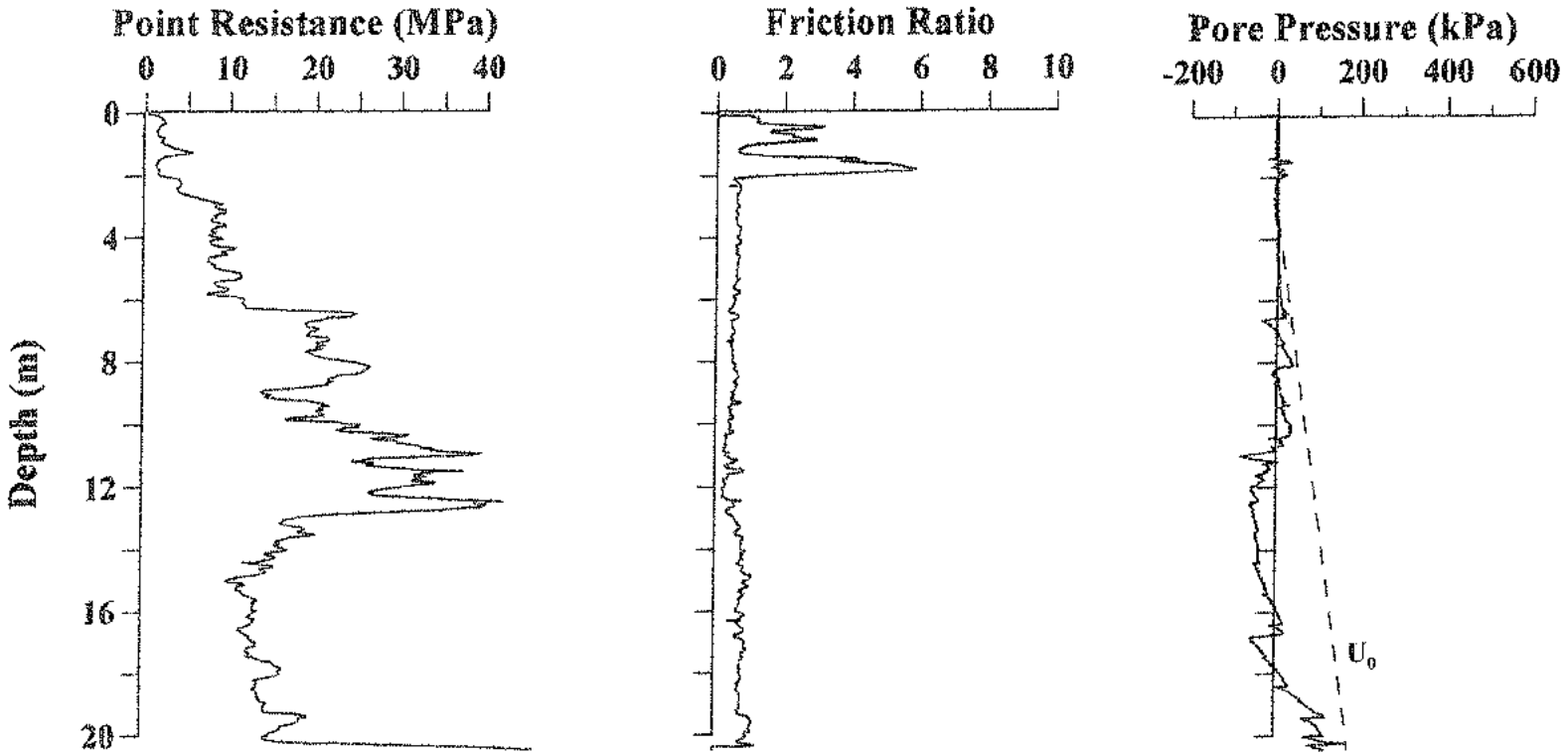

St Joseph School

Whakatane

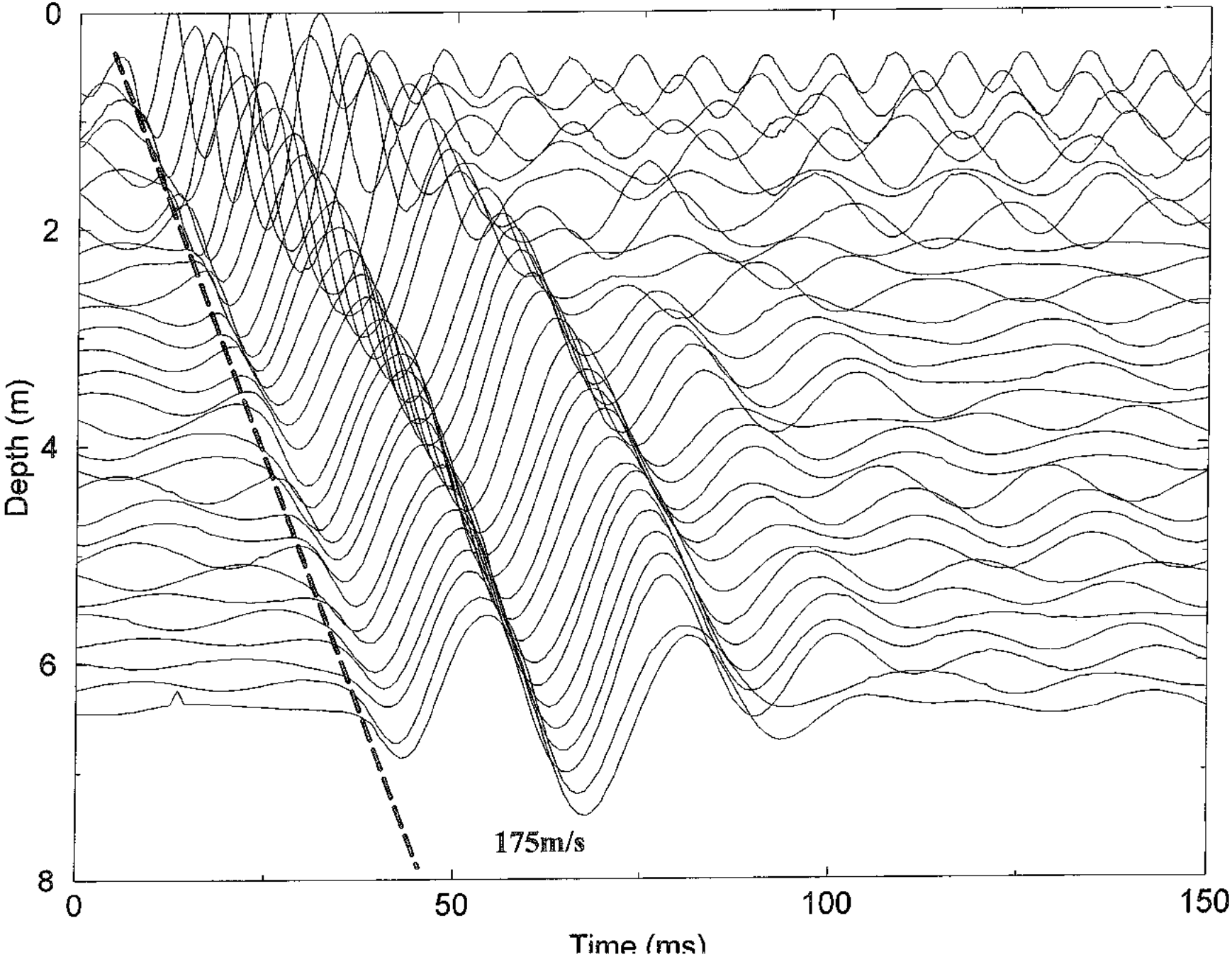

St Joseph School
Whakatane

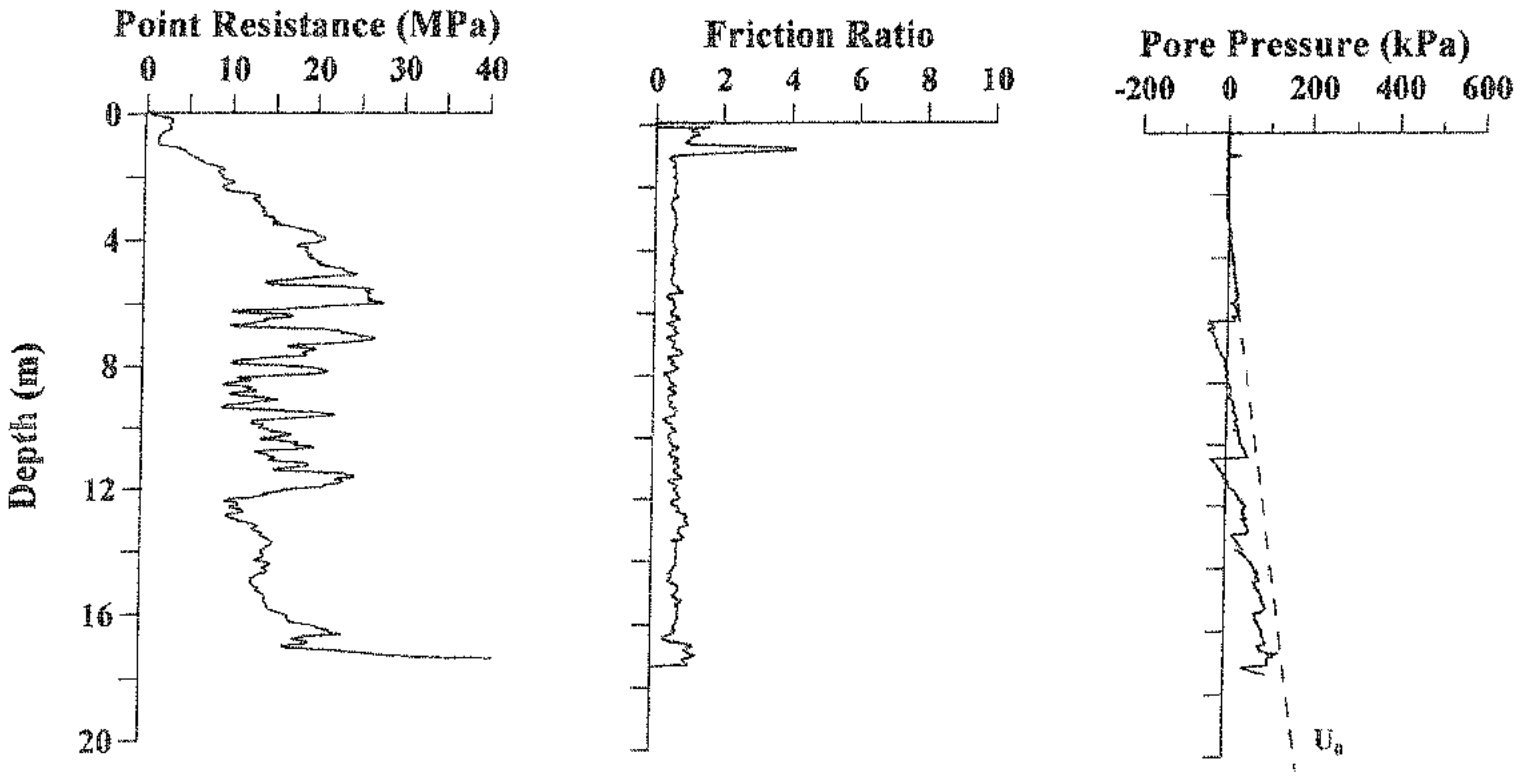

Warren Park

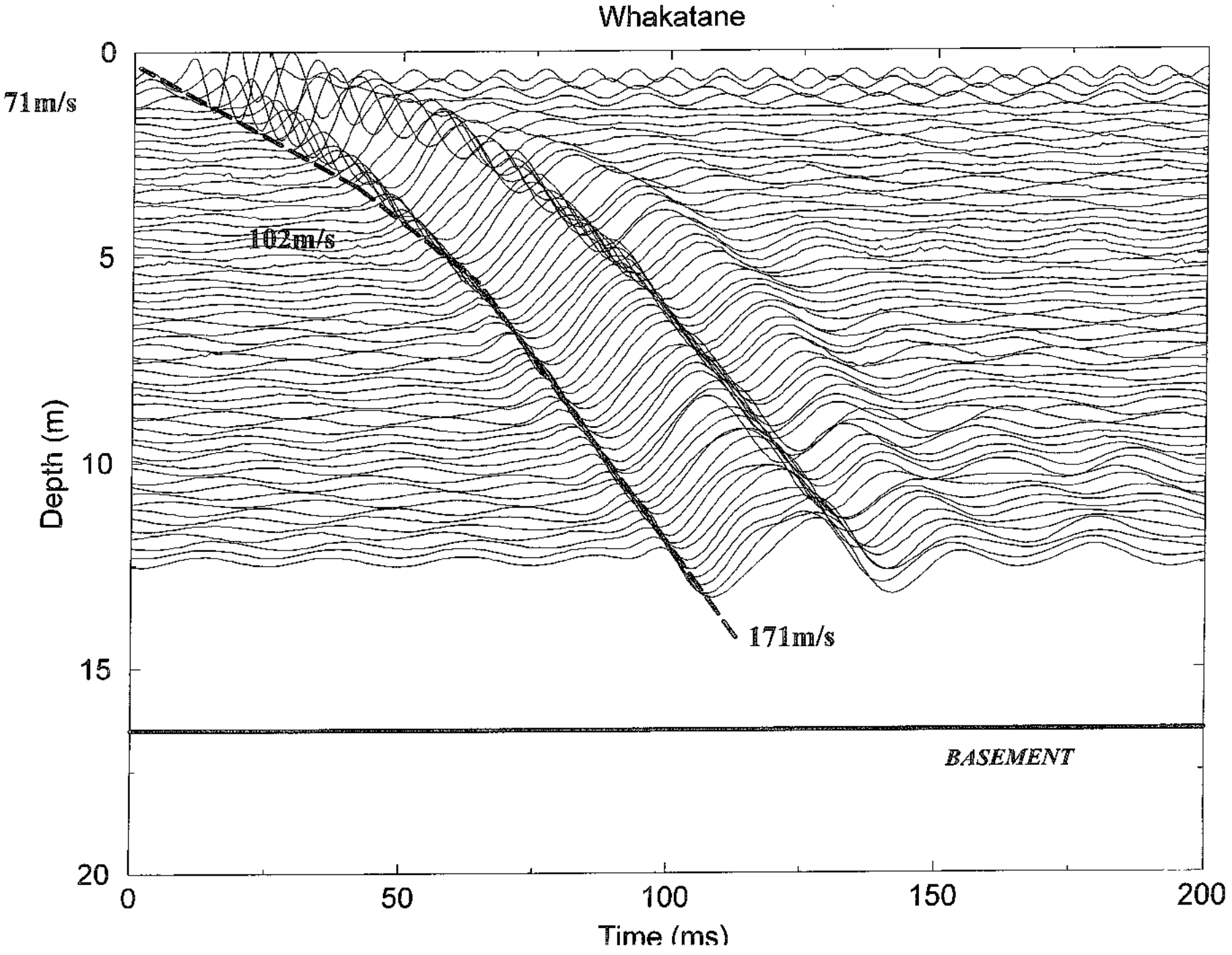
Whakatane
71m/s
102m/s
171m/s
BASEMENT
Depth (m)
0
5
10
15
20
0
50
100
150
200
Time (ms)

Warren Park
Whakatane

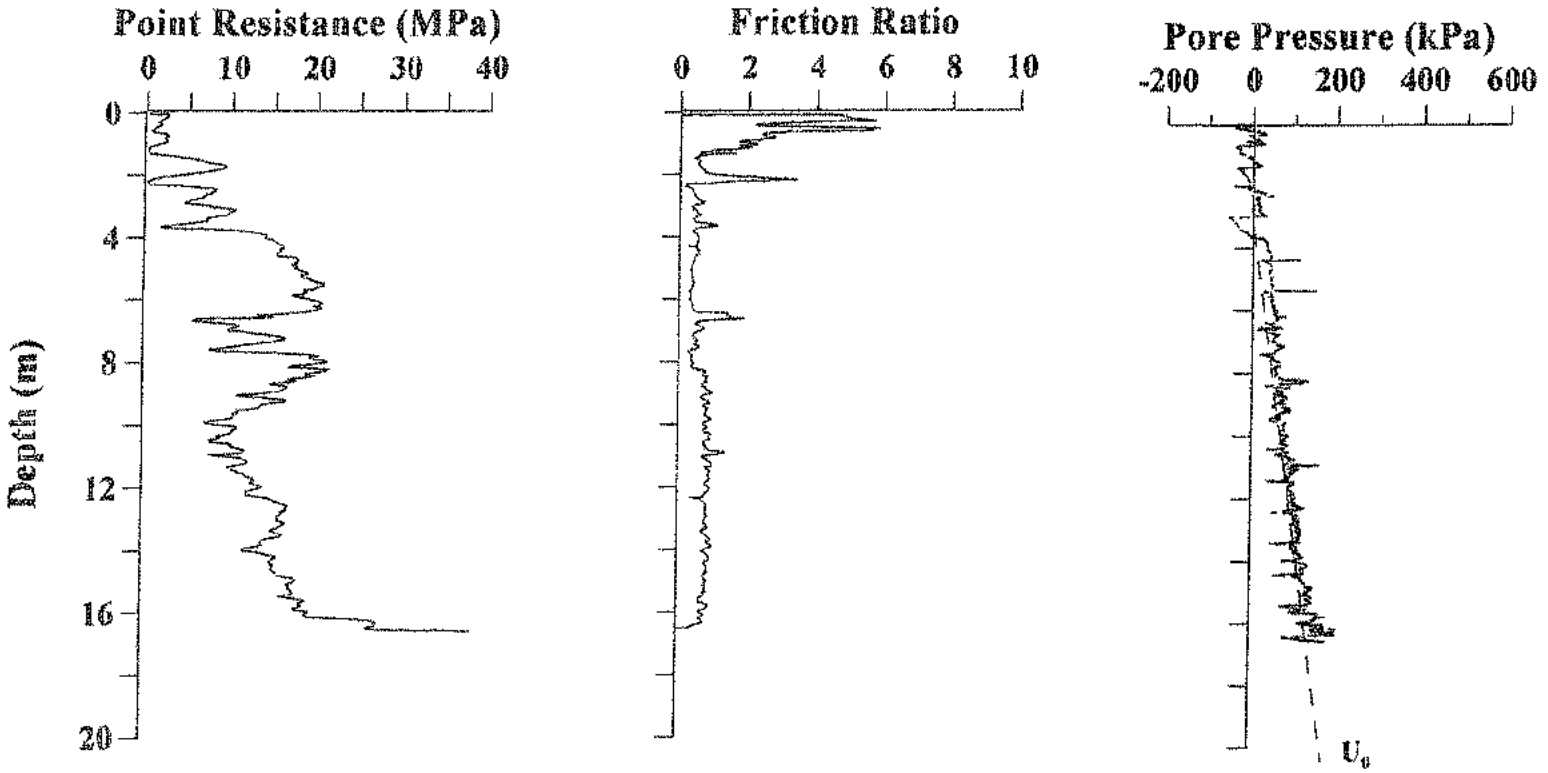

Apanui School

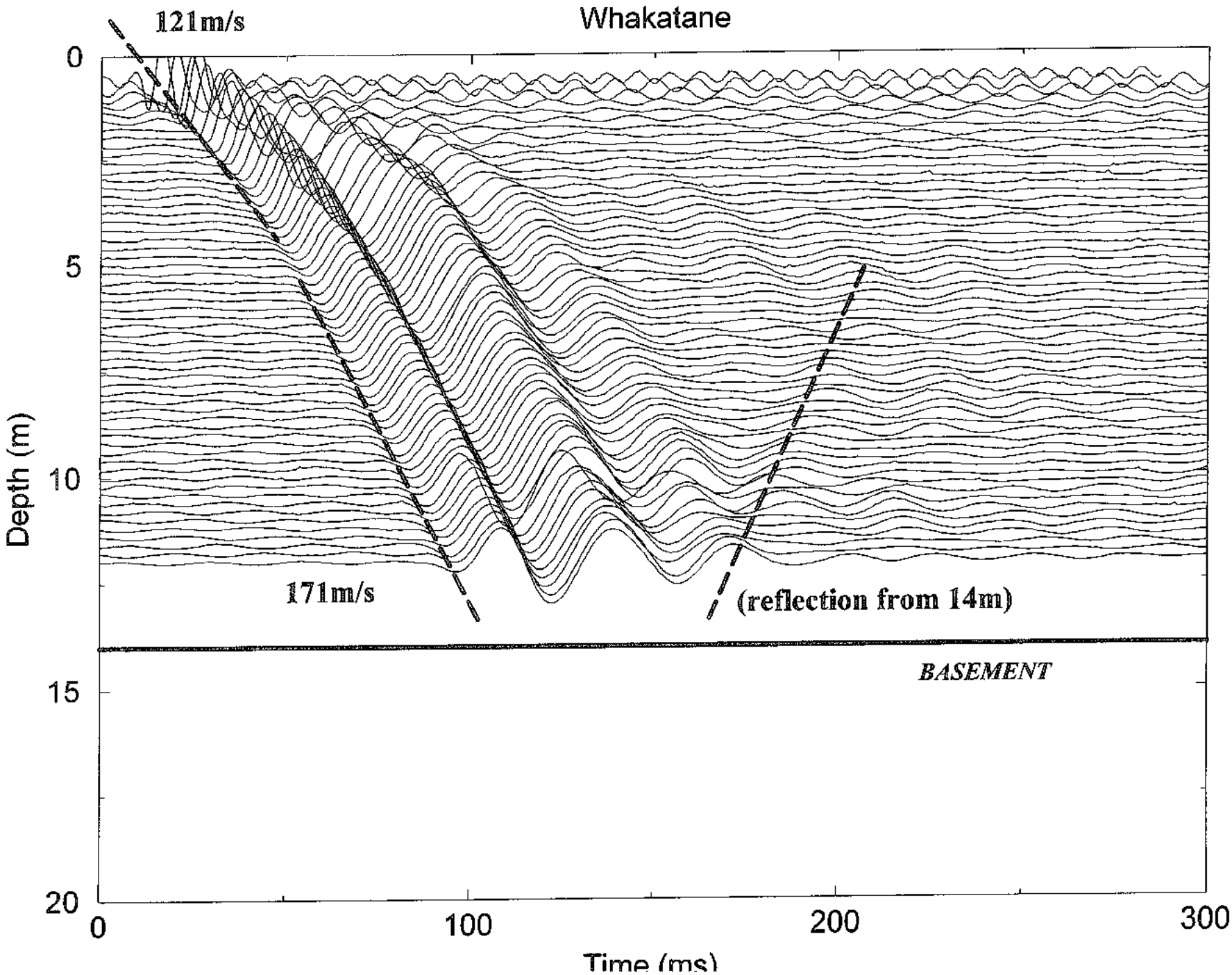

Apanui School
Whakatane

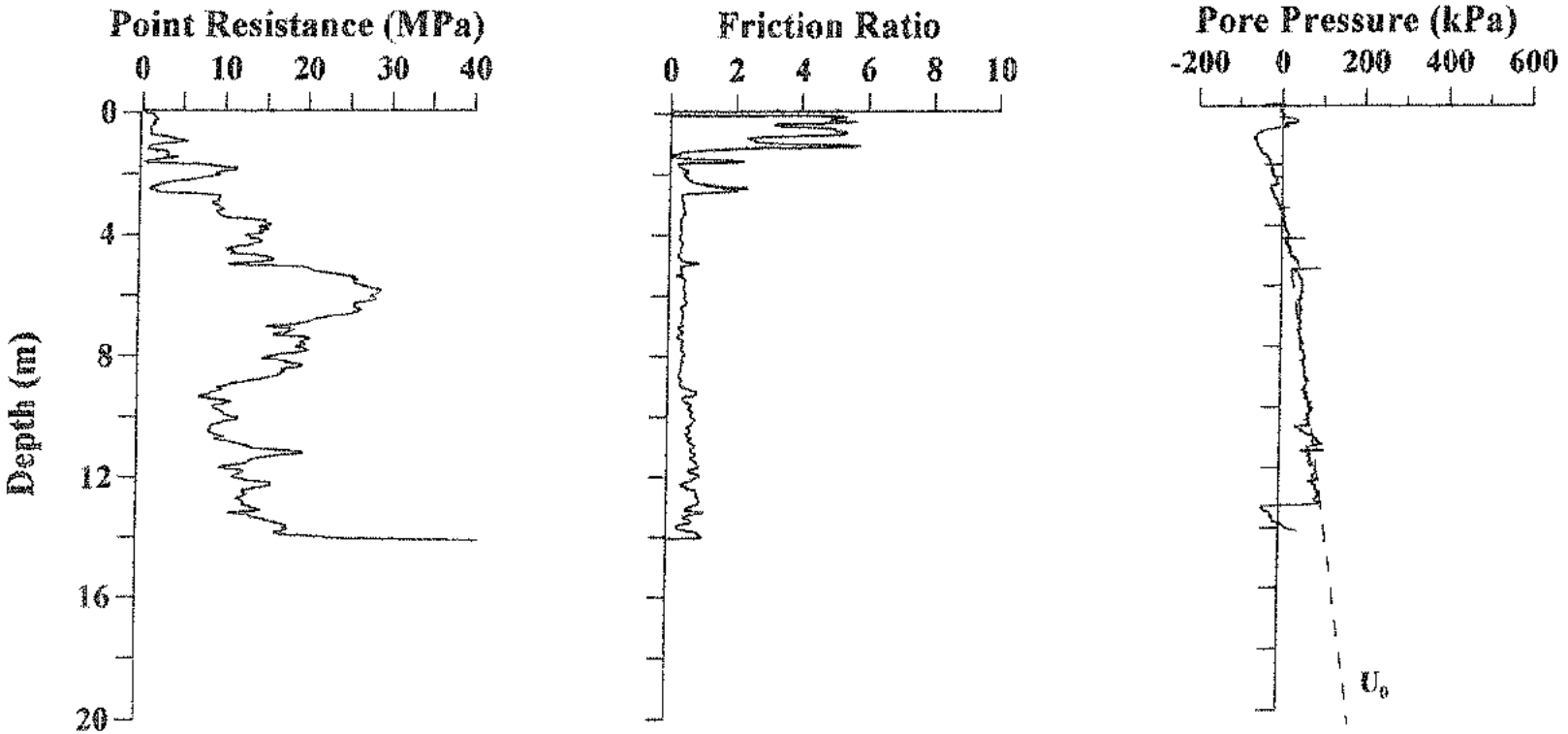

Peace Park

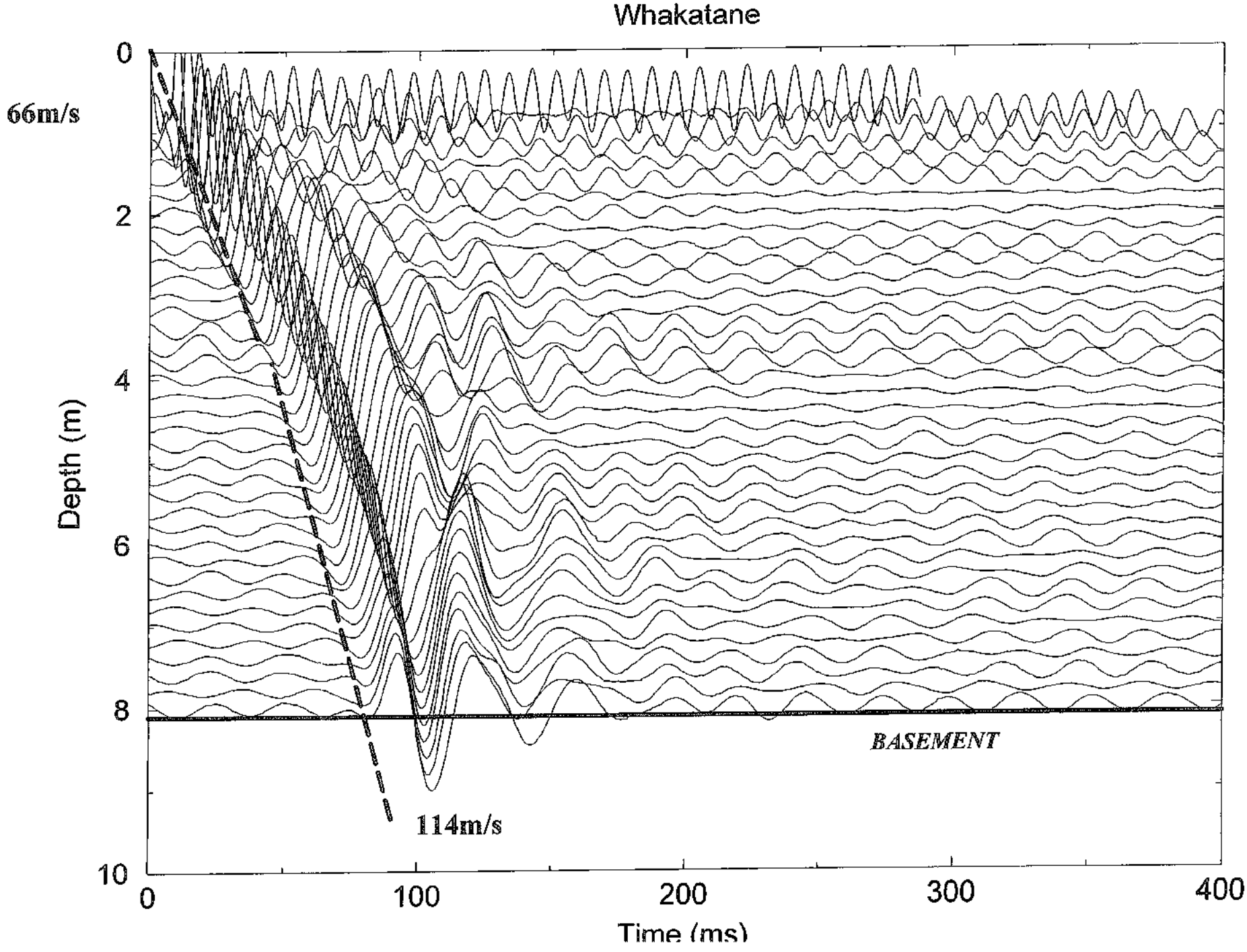
Whakatane
66m/s
114m/s
BASEMENT
Depth (m)
0
2
4
6
8
10
0
100
200
300
400
Time (ms)

Peace Park
Whakatane

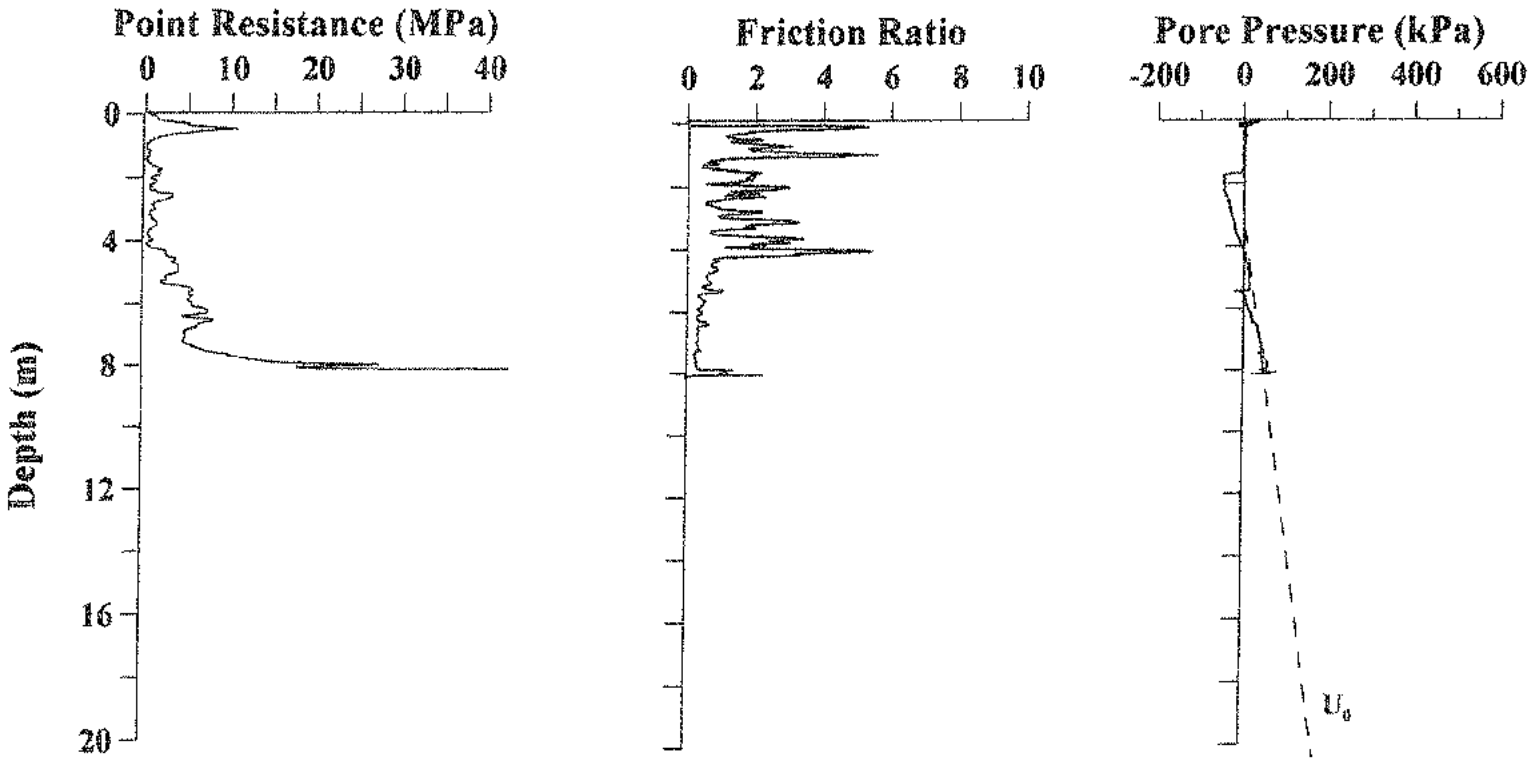

Trident High School

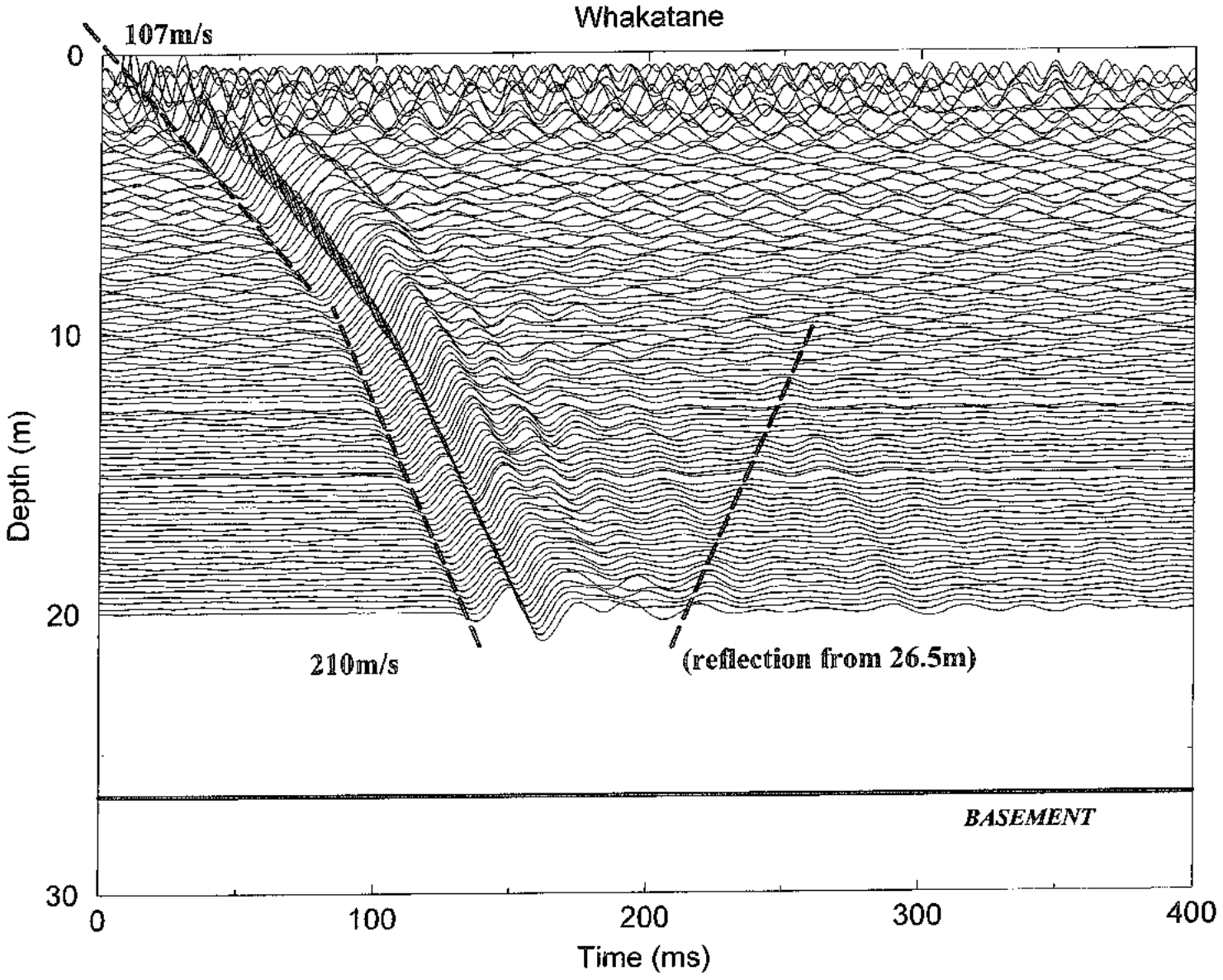

Trident High School
Whakatane

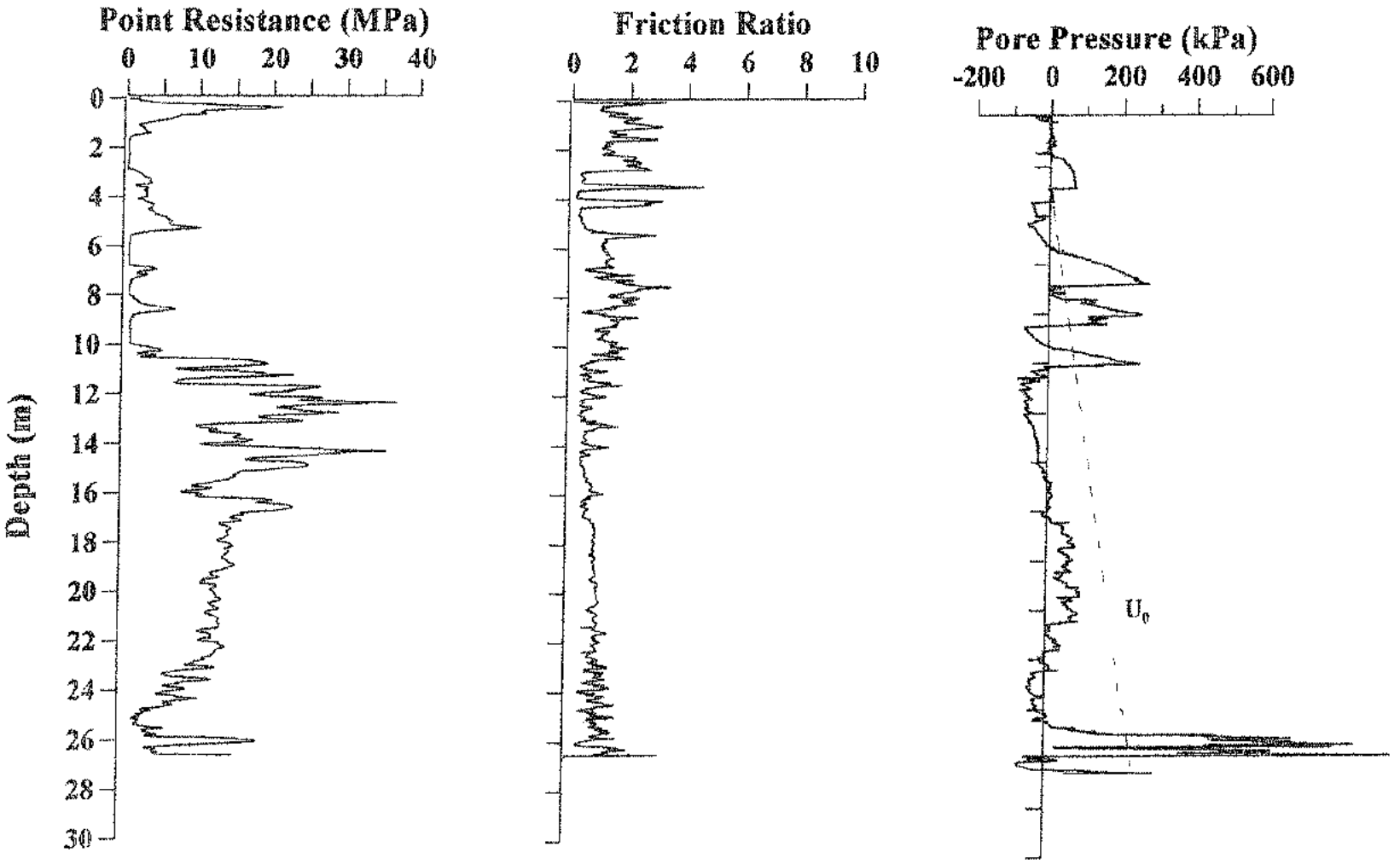

Rex Morpeth Park

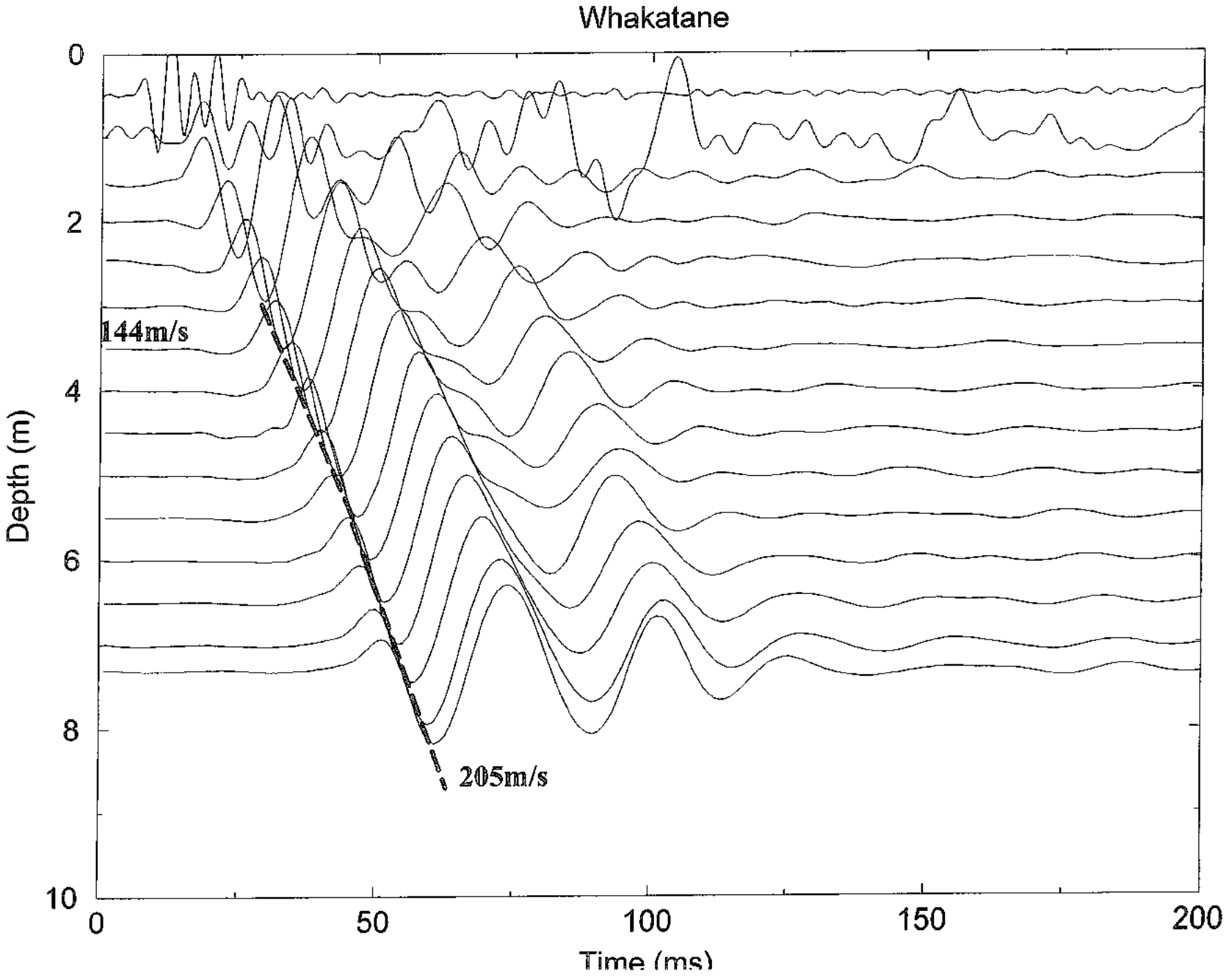

Rex Morpeth Park
Whakatane

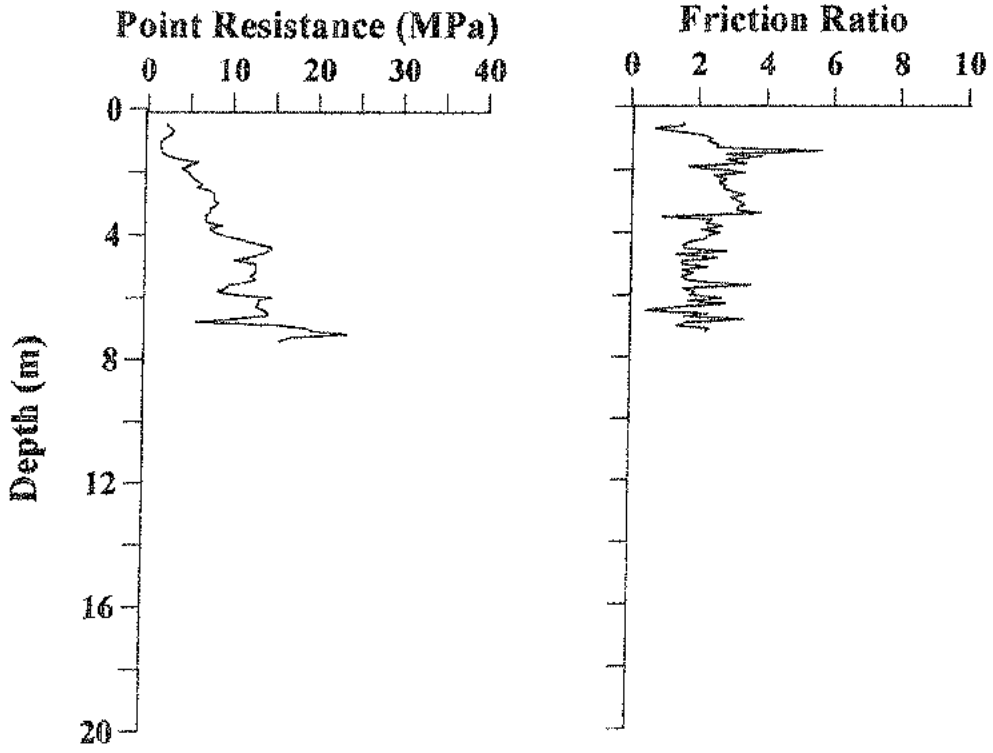

APPENDIX 4

MM Intensity descriptions

CONTENTS

1.0 Table 8 — Proposed environmental criteria for the N Z Modified Mercalli Intensity Scale

MODIFIED MERCALLI INTENSITY SCALE - N Z 1996 *(Dowrick, 1996)* *1996 Environmental Criteria*	REVISED MODIFIED MERCALLI INTENSITY SCALE – N Z 1997 *(Hancox et al., 1997)* *Proposed Environmental Criteria* [2]
MM6 Trees and bushes shake, or are heard to rustle. Loose material may be dislodged from sloping ground, e. g. existing slides, talus slopes, shingle slides.	**MM6** Trees and bushes shake, or are heard to rustle. Loose material dislodged on some slopes, e.g. existing slides, talus and scree slope. A few very small ($\leq 10^3$ m^3) soil and regolith slides and rock falls from steep banks and cuts. A few minor cases of liquefaction (sand boil) in highly susceptible alluvial and estuarine deposits.
MM7 Water made turbid by stirred up mud. Small slides such as falls of sand and gravel banks, and small rock falls from steep slopes and cuttings. Instances of settlement of unconsolidated or wet or weak soils. Some[1] fine cracks appear in sloping ground. A few[1] cases of liquefaction (e.g. small water & sand ejections).	**MM7** Water made turbid by stirred up mud. Very small ($\leq 10^3$ m^3) disrupted soil slides and falls of sand and gravel banks, and small rock falls from steep slopes and cuttings are common. Fine cracking on some slopes and ridge crests. A few small to moderate landslides (10^3 –10^5 m^3), mainly rock falls on steeper slopes (>30°) such as gorges, coastal cliffs, road cuts and excavations. Small discontinuous areas of minor shallow sliding and mobilisation of scree slopes in places. Minor to widespread small failures in road cuts in more susceptible materials. A few instances of non-damaging liquefaction (small water and sand ejections) in alluvium.
MM8 Cracks appear on steep slopes and in wet ground. Small to moderate slides in roadside cuttings and unsupported excavations. Small water and sand ejections, and localised lateral spreading adjacent to streams, canals, and lakes etc.	**MM8** Cracks appear on steep slopes and in wet ground. Significant landsliding likely in susceptible areas. Small to moderate (10^3-10^5 m^3) slides widespread; many rock and disrupted soil falls on steeper slopes (steep banks, terrace edges, gorges, cliffs, cuts etc). Significant areas of shallow regolith landsliding, and some reactivation of scree slopes. A few large (10^5-10^6 m^3) landslides from coastal cliffs, and possibly large to very large ($\geq 10^6$ m^3) rock slides and avalanches from steep mountain slopes. Larger landslides in narrow valleys may form small temporary landslide-dammed lakes. Roads damaged and blocked by small to moderate failures of cuts and slumping of road-edge fills. Evidence of soil liquefaction common, with small sand boils and water ejections in alluvium, and localised lateral spreading (fissuring, sand and water ejections) and settlements along banks of rivers, lakes, and canals etc.

NOTES:

(1) "Some or "a few" indicates that threshold for a particular effect or response has just been reached at that intensity.

(2) Intensity is principally a measure of damage. Environmental damage (response criteria) occurs mainly on susceptible slopes, and in certain materials, hence the effects described above may not occur in all places, but can be used to reflect the average or predominant level of damage (or MM intensity) in a given area.

[Page 1 of 2]

MODIFIED MERCALLI INTENSITY SCALE - N Z 1996 *(Dowrick, 1996)* *1996 Environmental Criteria*	REVISED MODIFIED MERCALLI INTENSITY SCALE - N Z 1997 *(Hancox et al., 1997)* *Proposed Environmental Criteria* [2]
MM9 Cracking on ground conspicuous. Landsliding general on steep slopes. Liquefaction effects intensified and more widespread, with large lateral spreading and flow sliding adjacent to streams, canals, and lakes etc.	**MM9** Cracking on flat and sloping ground conspicuous. Landsliding widespread and damaging in susceptible terrain, particularly on slopes steeper than 20°. Extensive areas of shallow regolith failures and many rock falls and disrupted rock and soil slides on moderate and steep slopes (20°-35° or greater), cliffs, escarpments, gorges, and man-made cuts. Many small to large (10^3-10^6 m^3) failures of regolith and bedrock, and some very large landslides (10^6 m^3 or greater) on steep susceptible slopes. Very large failures on coastal cliffs and low-angle bedding planes in Tertiary rocks. Large rock/debris avalanches on steep mountain slopes in well-jointed greywacke and granitic rocks. Landslide-dammed lakes formed by large landslides in narrow valleys. Damage to road and rail infrastructure widespread with moderate to large failures of road cuts slumping of road-edge fills. Small to large cut slope failures and rock falls in open mines and quarries. Liquefaction effects widespread with numerous sand boils and water ejections on alluvial plains, and extensive, potentially damaging lateral spreading (fissuring and sand ejections) along banks of rivers, lakes, canals etc). Spreading and settlements of river stop banks likely.
MM10 Landsliding very widespread in susceptible terrain, with very large rock masses displaced on steep slopes. Landslide dammed lakes may be formed Liquefaction effects widespread and severe.	**MM10** Landsliding very widespread in susceptible terrain. [3] Similar effects to MM9, but more intensive and severe, with very large rock masses displaced on steep mountain slopes and coastal cliffs. Landslide-dammed lakes formed. Many moderate to large failures of road and rail cuts and slumping of road-edge fills and embankments may cause great damage and closure of roads and railway lines. Liquefaction effects (as for MM9) widespread and severe. Lateral spreading and slumping may cause rents over large areas, causing extensive damage, particularly along river banks, and affecting bridges, wharfs, port facilities, and road and rail embankments on swampy, alluvial or estuarine areas.

NOTES:

(1) "Some or "a few" indicates that the threshold for a particular effect or response has just been reached at that intensity.

(2) Intensity is principally a measure of damage. Environmental damage (response criteria) occurs mainly on susceptible slopes and in certain materials, hence the effects described above may not occur in all places, but can be used to reflect the average or predominant level of damage (or MM intensity) in a given area.

(3) Environmental response criteria have not been suggested for MM11 and MM12, as those levels of shaking have not been reported in New Zealand. However, earlier versions of the MM intensity scale suggest that environmental effects at MM11 and MM12 are similar to the new criteria proposed for MM9 and 10 above, but are possibly more widespread and severe.

[Page 2 of 2]

2.0 Table 9 — Comparison of earthquake intensity scales *(after Krinitzsky and Chang, 1988)*

Modified Mercalli (MM)	Japanese Metrological Agency (JMA)	Peoples Republic of China	Rossi - Forel (RF)	Medvedev, Sponheuer, Karnik (MSK)
1		I	I	I
2	I	II	II	II
3		III	III	III
4	II	IV	IV	IV
5	III	V	V	V
6	IV	VI	VI	VI
7	V	VII	VII	VII
8		VIII	VIII	VIII
9	VI	IX	IX	IX
10		X	X	X
11	VII	XI		XI
12		XII		XII

Environmental criteria are quite well defined within the MSK scale (summarised below), being broadly similar to those in the revised MM scale (Table 8). However, the proposed new environmental criteria are more detailed and complete, and are expected to be better for assigning MM felt intensities from landsliding in New Zealand.

3.0 Environmental criteria in the MSK Scale

MSK VI: *Narrow cracks (up to 10 cm) in wet ground, occasional landslides in mountains.*

MSK VII: *Isolated falls from sandy and gravelly banks.*

MSK VIII: *Small landslips in hollows and embank-ments; cracks several cm in ground*

MSK IX: *On flat land overflow of water, sand, and mud often observed (liquefaction effects); ground cracks to widths of up to 10 cm; falls of rock, many landslides and earth flows.*

MSK X: *Cracks in ground up to several decimeters and sometimes 1 m wide. Broad fissures occur parallel to water courses. Loose ground slides from steep slopes. Considerable landslides are possible from river banks and steep coasts. In coastal areas, displacements of sand and mud; new (landslide-dammed) lakes formed.*

MSK XI+: *Ground fractured considerably by broad cracks and fissures, slumps and spreads; numerous landslides and falls of rock. Other effects similar to MMX, but more severe.*

Institute of Geological & Nuclear Sciences Limited

Gracefield Research Centre
69 Gracefield Road
PO Box 30 368
Lower Hutt
New Zealand
Phone +64-4-570 1444
Fax +64-4-570 4600

Rafter Research Centre
30 Gracefield Road
PO Box 31 312
Lower Hutt
New Zealand
Phone +64-4-570 4637
Fax +64-4-570 4657

Dunedin Research Centre
764 Cumberland Street
Private Bag 1930
Dunedin
New Zealand
Phone +64-3-477 4050
Fax +64-3-477 5232

Wairakei Research Centre
State Highway 1, Wairakei
Private Bag 2000
Taupo
New Zealand
Phone +64-7-374 8211
Fax +64-7-374 8199

For more information visit the GNS website
http://www.gns.cri.nz